University of Kentucky

UKnowledge

Theses and Dissertations--Biology   Biology

2022

The Role of Sox4 in Ocular Morphogenesis and Retinal Differentiation

Rebecca Petersen
University of Kentucky, rpe230@uky.edu
Author ORCID Identifier:
https://orcid.org/0000-0001-6960-2948
Digital Object Identifier: https://doi.org/10.13023/etd.2022.409

Right click to open a feedback form in a new tab to let us know how this document benefits you.

STUDENT AGREEMENT:

I represent that my thesis or dissertation and abstract are my original work. Proper attribution has been given to all outside sources. I understand that I am solely responsible for obtaining any needed copyright permissions. I have obtained needed written permission statement(s) from the owner(s) of each third-party copyrighted matter to be included in my work, allowing electronic distribution (if such use is not permitted by the fair use doctrine) which will be submitted to UKnowledge as Additional File.

I hereby grant to The University of Kentucky and its agents the irrevocable, non-exclusive, and royalty-free license to archive and make accessible my work in whole or in part in all forms of media, now or hereafter known. I agree that the document mentioned above may be made available immediately for worldwide access unless an embargo applies.

I retain all other ownership rights to the copyright of my work. I also retain the right to use in future works (such as articles or books) all or part of my work. I understand that I am free to register the copyright to my work.

REVIEW, APPROVAL AND ACCEPTANCE

The document mentioned above has been reviewed and accepted by the student's advisor, on behalf of the advisory committee, and by the Director of Graduate Studies (DGS), on behalf of the program; we verify that this is the final, approved version of the student's thesis including all changes required by the advisory committee. The undersigned agree to abide by the statements above.

<div align="right">

Rebecca Petersen, Student

Dr. Ann C. Morris, Major Professor

Dr. Jessica Santollo, Director of Graduate Studies

</div>

The Role of Sox4 in Ocular Morphogenesis and Retinal Differentiation

_____

DISSERTATION
_____
A dissertation submitted in partial fulfillment of the
requirements for the degree of Doctor of Philosophy in the
College of Art & Sciences
at the University of Kentucky

By
Rebecca A. Petersen
Lexington, Kentucky
Director: Dr. Ann C. Morris, Professor of Biology
Lexington, Kentucky
2022

ABSTRACT OF DISSERTATION

The Role of Sox4 in Ocular Morphogenesis and Retinal Differentiation

Visual impairment ranges from mild forms that can be corrected with glasses to more severe cases that result in permanent loss of vision. Microphthalmia, anophthalmia, and coloboma (collectively referred to as MAC) account for 11% of cases of pediatric blindness and are a result of improper ocular morphogenesis. Retinitis Pigmentosa (RP) is a retinal degenerative disease that affects 1 in 3000 people worldwide. It is a progressive disorder that initially begins with loss of vision in low light settings due to rod photoreceptor degeneration but progresses to complete blindness upon loss of cone photoreceptors. Currently, there is no cure for either MAC or RP. Further insight into the essential components of ocular morphogenesis and the generation of retinal neurons could provide the base of knowledge needed for better patient screening and treatments like cell therapies.

The transcription factor Sox4 has previously been implicated as an important factor in both ocular morphogenesis and retinal development. Studies in humans, mice, zebrafish, and Xenopus have all linked Sox4 to microphthalmia and coloboma. Additional studies suggest a role for Sox4 in the generation of specific retinal neurons. Interestingly, in zebrafish, the absence of maternal *sox4* transcripts in the developing embryo results in both microphthalmia and a reduction of rod photoreceptors. This suggests that Sox4 has a critical role early in specification of the eyefield that influences later retinal differentiation, however the precise functions of Sox4 during vertebrate ocular morphogenesis and retinal cell type differentiation remain unclear.

The studies presented in this Dissertation provide new insights into the role of Sox4 in eye development. Chapter 1 of this dissertation presents a review of ocular morphogenesis, retinal development, and what is currently known about the function of SoxC transcription factors and particularly Sox4 in embryonic and ocular development. In Chapter 2, a method to visualize ocular morphogenesis in living zebrafish embryos with high spatial and temporal resolution is demonstrated. Chapter 3 describes a detailed characterization of the ocular phenotypes of zebrafish *sox4* mutants, and an in-depth analysis into the role

Sox4 plays in both ocular morphogenesis and retinal differentiation. *In vivo* time lapse imaging, assays to assess cell proliferation and cell death, and immunohistochemistry to detect retinal cell types were used to characterize the phenotypes of microphthalmia and a reduction of rod photoreceptors in the *sox4* mutants. Furthermore, scRNA-seq was used to address if there is any heterogeneity prior to ocular morphogenesis that may affect later retinal differentiation. Chapter 4 will address the impact of findings in the *sox4* mutants, and the suggested future directions for this project. Finally, an appendix chapter will include additional data about a possible role for Sox4 in neural crest cells.

KEYWORDS: Sox4, SoxC, zebrafish, eye development, ocular morphogenesis, retina

Rebecca A. Petersen
_____
(Name of Student)

08/10/2022
_____
Date

The Role of Sox4 in Ocular Morphogenesis and Retinal Differentiation

By
Rebecca A. Petersen

<div align="center">

Dr. Ann C. Morris
_____
Director of Dissertation

Dr. Jessica Santollo
_____
Director of Graduate Studies

08/10/2022
_____
Date

</div>

ACKNOWLEDGMENTS

Ellen Scott. Without all of their encouragement and support, I would not be the scientist I am today. Finally, I am so incredibly grateful for my fiancé, Dan Autore. He was there every step of the way with me, always the first to celebrate my successes and there to comfort me during the more challenging times. I could not have done this without his support.

TABLE OF CONTENTS

LIST OF TABLES

LIST OF FIGURES

LIST OF ADDITIONAL FILES

CHAPTER 1. INTRODUCTION

1.1 Importance of Vision

Vision, our ability to perceive the world around us, is arguably one of the most important senses we humans possess. Vision plays a key role in one's ability to observe and interpret our environment and is integral to learning, social development, self-awareness, and balance (Aki et al., 2007; Burmedi et al., 2009; Daugherty & Moran, 1982; Patla, 1997; Rainey et al., 2016). When asked which of the five basic senses people feared losing the most, an overwhelming majority (~73%) of the participants indicated vision loss (Thill et al., 2019). Another study found that 47% percent of people viewed vision loss among the worst health conditions that might occur to them (Flaxman et al., 2017; Scott et al., 2016). Vision is invaluable and vison loss can have an immeasurable impact on quality of life. Given the importance of vision, the study of ocular development is paramount for better understanding of various conditions that may result in visual impairment or loss. Improved understanding will lead to possible prevention or treatment of these conditions.

There are numerous conditions that can lead to visual impairment or loss. For example, if ocular morphogenesis does not occur correctly, it can lead to conditions such as microphthalmia (a small eye), anophthalmia (the absence of an eye), and coloboma (part of the eye tissue is missing, giving the pupil a keyhole shaped appearance). These conditions are collectively known as MAC. MAC is a leading cause of pediatric blindness, accounting for 11% of cases (Fahnehjelm et al., 2022). Problems can also arise if the neural retina is not properly differentiated during development or maintained later in life. An example of this would be Retinitis Pigmentosa (RP), a condition affecting approximately 1 in 3000 people worldwide. With RP the rod photoreceptors, one of the neurons responsible for vision in low light settings, are unable to survive and degenerate. This results in the initial symptom of RP, loss of night vision. The loss of these rods leads to gaps in the retina, compromising its structure. This compromised structure will then lead to the atrophy of the rest of the retina,

resulting in complete blindness (Kalloniatis & Fletcher, 2021; Newton & Megaw, 2020).

Better understanding of the genetic contributions to development of various conditions resulting in visual impairment will hopefully lead to better screening and early intervention for patients. Additionally, further insight into the components required for the genesis of specific retinal neurons may provide a foundation on which cell therapies can be derived and used to treat conditions like RP (Mount et al., 2015; Riham Mohamed Aly, 2020; Wang et al., 2021). In this chapter, I will describe the process of ocular morphogenesis, retinal development and regeneration, the influence of SoxC transcription factors in this process, how zebrafish are an excellent model to study eye development, and the rationale for my dissertation research. I will conclude with an overview of the research aims presented in this Dissertation.

1.2   Ocular Morphogenesis

The development of the vertebrate eye begins in a process called ocular morphogenesis. In ocular morphogenesis, the neural portion of the eye arises from the anterior neural plate, part of the developing forebrain. The part of the anterior neural plate that will give rise to the retina and RPE is the eyefield. The eyefield is specified by retinal homeodomain transcription factor (Rx/RAX). Loss of Rx/RAX leads to anophthalmia, indicating its essential role in eye development. Rx/RAX is responsible for the cell movements that lead to the evagination of the optic vesicle (Chow & Lang, 2001; Chuang et al., 1999; Fuhrmann, 2010; Katherine E Brown et al., 2010; Loosli et al., 2003; Rojas-Muñoz et al., 2005; Stigloher et al., 2006). Specification of the eyefield is also influenced by other transcription factors like Pax6, Six3, Otx2, and Hesx1/Rpx (Chow & Lang, 2001; Fuhrmann, 2010). These eyefield cells, evaginate away from the brain, toward the surface ectoderm to form two bilateral optic vesicles. In order for bifurcation of the eyefield to occur so the optic vesicles can evaginate, the expression of eyefield genes needs to be downregulated along the

midline of the embryo. Nodal and Hh signaling from the ventral midline promote Pax2 expression along the midline restricting the expression of Pax6 and triggering the anterior migration of the ventral diencephalon. This movement splits and displaces the optic tissue laterally (Chow & Lang, 2001; Choy & Cheng, 2012; England et al., 2006; Sampath et al., 1998; Schier & Talbot, 2003; Varga et al., 1999).

The optic vesicles invaginate to form a bilayered optic cup as they make contact with the surface ectoderm. The inner most layer will give rise to the neural retina while the outer layer will give rise to the retinal pigmented epithelium (RPE). The gradient of Pax2/Pax6 expression that was previously established contributes to the patterning of the optic vesicle and Bmp signaling in the dorsal forebrain help establish a signaling gradient along the dorsal/ventral axis. This dorsal/ventral gradient contributes to the patterning and differentiation of the neural retina and the RPE) (Chow & Lang, 2001; Fuhrmann, 2010; Z. Li et al., 2000; Pillai-Kastoori et al., 2014; S. W. Wilson & Houart, 2004). The surface ectoderm, neuroectoderm, and periocular mesenchyme, including contributions from the mesoderm and neural crest, will give rise to the anterior structures of the eye, including the lens, cornea, ciliary body, and iris (Chow & Lang, 2001; Cvekl & Tamm, 2004; Sowden, 2007). At the beginning of the formation of the optic cup, a channel, the choroid fissure, remains open on the ventral side for the choroid vasculature to enter the eye and the optic nerve to exit the eye. This opening eventually fuses to complete the optic cup; failure of the choroid fissure to properly fuse results in coloboma. The fusion of the choroid fissure is last change in ocular morphology and completes the process of ocular morphogenesis (Chow & Lang, 2001; Cvekl & Tamm, 2004; Fuhrmann, 2010; James et al., 2016; Pillai-Kastoori et al., 2014).

1.3   Retinal Differentiation

After the bilayered optic cup has been established, the two layers will differentiate into the RPE and neural retinal (Chow & Lang, 2001; Fuhrmann,

2010; Z. Li et al., 2000; Pillai-Kastoori et al., 2014; S. W. Wilson & Houart, 2004). The developing RPE and neural retina are distinguished by the expression of different transcription factors, *Mitf* and *Otx2* in the RPE and *Pax2*, *Pax6*, *Rx*, *Lhx2*, *Chx10*, *Optx2* in the neural retina (Chow & Lang, 2001; Pillai-Kastoori et al., 2015). The RPE forms a border between the choroid and the photoreceptor outer segments (POS) in the retina. The RPE has several critical roles in supporting the retina: it forms the blood-retinal barrier, regulating the transport of ions, amino acids, and glucose between the choroid and photoreceptors; it transports and stores retinoids that are vital for the visual cycle; it phagocytosis and recycles the old photoreceptor outer segments; and it reduces reactive oxygen species generated by its phagocytic activities and exposure to light (Boulton & Dayhaw-Barker, 2001; Yang et al., 2021). The function of the retina is to detect light and convert it to a neuronal signal that can be transmitted to the brain. A fully differentiated retina is comprised of three nuclear layers, two plexiform layers, and the optic nerve (Agathocleous & Harris, 2009; Demb & Singer, 2015; Masland, 2012; Pillai-Kastoori et al., 2014; Weysse & Burgess, 1906). The outer nuclear layer is comprised of the rod and cone photoreceptors, the neurons responsible for detecting light and converting it to a transmissible signal. Rod photoreceptors are responsible for the detection of low light levels, contributing to night vision (Baylor, 1996; Swaroop et al., 2010). Cone photoreceptors are responsible for the detection of specific wavelengths of light, contributing to color vision and visual acuity (Nathans et al., 1986; Swaroop et al., 2010). These photoreceptors synapse in the outer plexiform layer to horizonal and bipolar cells in the inner nuclear layer. Horizontal cells help modulate the signal from photoreceptors to adapt for bright and dim light conditions (Demb & Singer, 2015; Dyer et al., 2003; Masland, 2012). Bipolar cells coordinate the signals from different photoreceptors (Masland, 2012). The signal from the bipolar cells is passed through the inner plexiform layer to the retinal ganglion cells (RGCs) (Masland, 2012; Tomita et al., 2000). The RGCs provide feedback to the bipolar cells by way of the amacrine cells. The axons of retinal ganglion

cells bundle together to form the optic nerve which transmits the visual signal to the optic tectum in the brain (Masland, 2012; Niell & Smith, 2005).
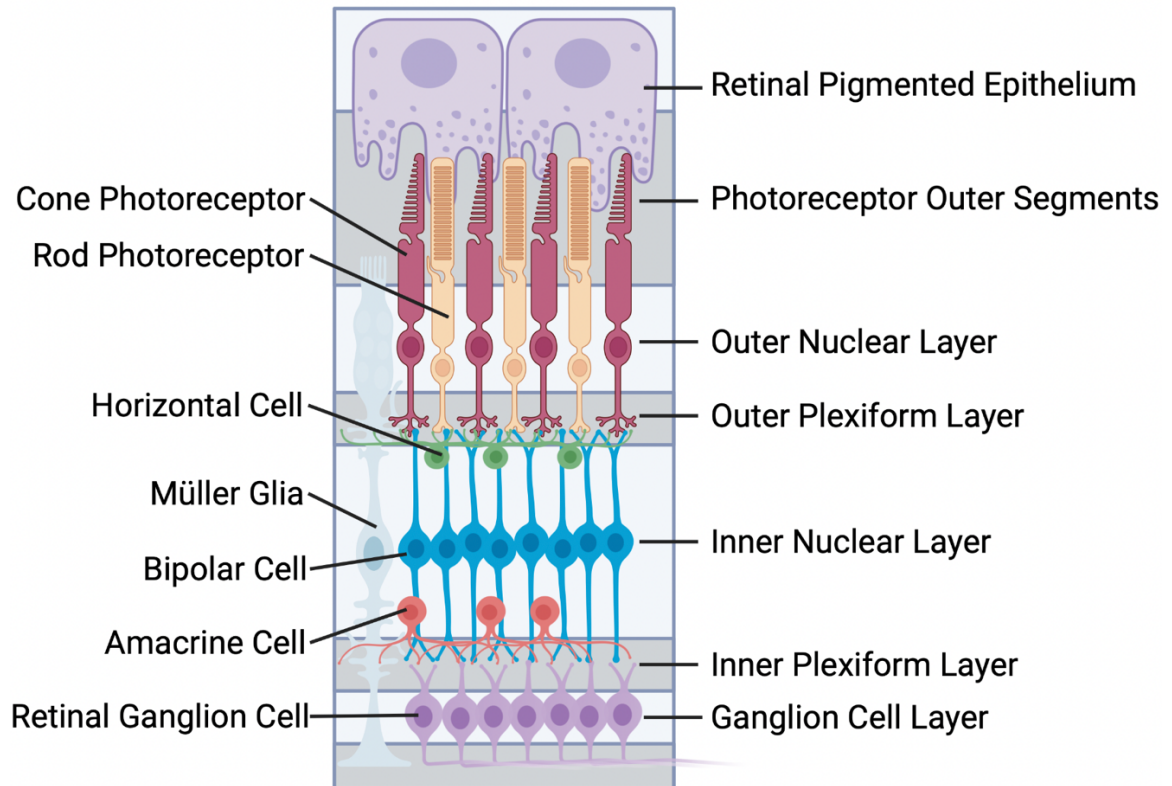
Figure 1.1 Layers and cell types found within the retina.

The process of the neural retina differentiation is highly conserved across vertebrate species and starts with a pool of multipotent progenitor cells (RPCs) (Livesey & Cepko, 2001). These RPCs will give rise to all the retinal neurons and the Müller glia (Holt et al., 1988; Turner et al., 1990; Turner & Cepko, 1987; Wetts & Fraser, 1988). The order in which the retinal neurons and glia differentiate follows a relatively conserved pattern with some overlap between the different cell types (Livesey & Cepko, 2001). The retinal ganglion cells are born first, followed by the cells of the inner nuclear layer, then the cone photoreceptors, and concluding with the Müller glia and rod photoreceptors (Livesey & Cepko, 2001; Pillai-Kastoori et al., 2014; Stenkamp, 2007). In

zebrafish (*Danio rerio)* specifically, neurogenesis begins in the ventral patch of the retina and progresses dorso-nasally in a fan-like gradient. A small pool of progenitors is maintained at the periphery of the retina known as the ciliary marginal zone (CMZ). The CMZ continues to populate the zebrafish retina with neurons as it continues to grow throughout the life of the fish (Livesey & Cepko, 2001; Pillai-Kastoori et al., 2014; Stenkamp, 2007). The initial differentiation of rod photoreceptors occurs in a distinct pattern from the rest of the retinal neurons. Rods can first be detected in the ventral patch of the retina, prior to cone differentiation unlike in the remainder of the retina. The ventral patch is densely populated with rods, and the temporal retina slowly and sporadically adds in rods rather than following a fan-like wave across the retina (A. C. Morris & Fadool, 2005; Schmitt & Dowling, 1996, 1999). The rod lineage begins with the inhibition of *pax6* expression in proliferating cells located in the ONL and the induction of *neuroD* expression. These *neuroD* positive precursors have the potential to differentiate into either cone or rod photoreceptors (Stenkamp, 2007). *crx* is the next transcription factor to turn on; it further specifies the progenitors towards a photoreceptor fate (Chen et al., 1997). The rod progenitors are committed to the rod fate with the expression of *nrl* and *nr2e3* and express *rhodopsin* (*rho*) upon terminal differentiation (Mears et al., 2001). Cone progenitors also express *crx* but are committed to the cone fate with the expression of *thyroid hormone receptor β2* (*trβ2*) or *retinoid x receptor γ* (*rxrγ*) and express either *short wavelength-opsin* (*opn1sw*), *medium wavelength-opsin* (*opn1mw*), or *long wavelength-opsin* (*opn1lw*) upon terminal differentiation (Chen et al., 1997; Jia et al., 2009; Ng et al., 2001).

There are competing ideas for how the retinal progenitors know what type of neuron or glial cell to become. Does the progenitor intrinsically know what it is going to become, does it rely on extrinsic signals, or is it some combination of intrinsic and extrinsic cues? The research currently supports a combination of intrinsic and extrinsic cues. The prevailing model for how retinal cell type differentiation occurs is called the competence model (Cepko et al., 1996; Livesey & Cepko, 2001). In this model, the RPC is competent to give rise to only

a specific subset of retinal neurons at different timepoints throughout development, losing and gaining the ability to give rise to certain neuronal precursors as its intrinsic gene expression program changes over time (Turner et al., 1990). Prior to neurogenesis, the pool of RPCs is established through a series of symmetric cell divisions that give rise to more RPCs. After the onset of neurogenesis, RPCs are more likely to divide asymmetrically. Out of the two daughter cells, one gives rise to another RPC and the other becomes a post mitotic neuronal precursor (Chenn & McConnell, 1995). This intrinsic cuing is thought to be sufficient to restrict a neural progenitor to a subset of fates, but it does not fully determine the fate of neural progenitors. It has been suggested that the number of cell divisions a RPC undergoes may be linked to its competency state, while other extrinsic factors may influence further specification of neuronal fate choice (Edlund & Jessell, 1999; Livesey & Cepko, 2001).

The idea of a neurogenic timer that controls progenitor competency is intriguing. However, it may be more complex than previously suggested. Neurogenesis and differentiation have been assumed to follow a linear order of events starting with neurogenesis, migration of post-mitotic precursors to their final location, and terminal differentiation into the mature neuron. However, in zebrafish retinas, bipolar and horizontal cells do not follow this order of events, but instead cell-cycle exit, migration, and differentiation are independently timed (Engerer et al., 2017; Godinho et al., 2007). Taken together, these data suggest the number of cell divisions does not solely determine the competency state of the RPCs. If the number of cell divisions is not responsible for setting the differentiation clock, then what is mechanism for the neurogenic timer? A way to address this question would to be to assess the individual states of gene expression in RPCs and how that differs across the population as well as how that shifts temporally. A recent advancement in transcriptomics, single cell RNA-seq (scRNA-seq) provides the ability to achieve this.

To perform scRNA-Seq, a tissue of interest is first dissociated into individual cells. Those cells are then isolated into individual droplets from which

their RNA is extracted and barcoded. Each cell has a unique barcode, so the RNA can be identified as belonging to a specific cell bioinformatically. This technique has provided the opportunity to ascertain the transcriptome of individual cells across a tissue of interest (Trapnell, 2015). scRNA-seq results in a highly dimensional dataset since every cell is potentially expressing thousands of genes. Computation methods are used to prioritize which genes are compared to determine similarities between cells. A popular algorithm for reducing the dimensionality of the data is the principal component analysis (PCA). PCA compares cells across 2 dimensions at a time. The vast proportion of the variance in the dataset will be encompassed by the first several principal components. In terms of visualizing the data, dimensionality can be reduced by a UMAP plot. UMAP plots allow the data to be visualized in 2D or 3D. Cells can be clustered based on similarity of gene expression to help characterize distinct populations. Graph-based clustering takes the PCA output and categorizes the cells into groups based on their similarity in gene expression. Trajectory analysis can help to organize the cells by temporal or developmental state. Monocle is a software tool that uses pseudotime as a measure of where a cell lies in comparison to other cells along a developmental trajectory. Pseudotime is a trajectory inference that is determined by the change in mean gene expression by individual cells. This shift in gene expression suggests a that there may be an underlying biological mechanism. Taken together, these scRNA-Seq and the associated bioinformatic analyses can elucidate previously unknown heterogeneity across a tissue or cell type, the trajectory a cell type transitions through during differentiation, and can identify novel genes previously unassociated with a particular cell type or state (Luecken & Theis, 2019; Trapnell, 2015).

ScRNA-Seq technology has been applied to study the developing eye and retina of humans, mice, and zebrafish in several studies, some of which are described in more detail below. ScRNA-seq was performed on human fetuses from 5-24 weeks of gestation. The gene expression profiles of the neural retina and RPE are distinct in these samples. Known markers of human retinal cells

were used to tease out the order of retinal neuron differentiation in humans. Retinal ganglion cells differentiated first followed by horizontal cells, amacrine cells, photoreceptors, bipolar cells, and Müller Glia in that respective order with some overlap between cell types (Hu et al., 2019).

ScRNA-seq was used to compare the developing human retina to developing human retinal organoids, which are 3D structures of retinal tissue that have been derived from stem cells (X. Li et al., 2021). The retinal organoids and developing human retina shared a similar cellular composition at the equivalent timepoints. Additionally, post-mitotic retinal progenitors were able to be transcriptomically detected at various time-points (Sridhar et al., 2020). It was demonstrated that retinal organoids are transcriptomically more similar to the peripheral retina than the fovea, the cone-rich central region of the human retina. As the ability to create retinal organoids advances, scRNA-seq can be used to assess their transcriptomic fidelity to the human retina. Additionally, these datasets can be used to link genes that have known roles in retinal disease, with the specific cell types they may be impacting, especially if an animal model for that disease does not currently exist (Cowan et al., 2020).

In mice, scRNA-seq was completed across the full course of retinal development. Evidence for molecularly distinct RPCs was not found at individual timepoints. However, the competence state between early and late RPCs was molecularly detectable. Cells in these two states clustered distinctly from one another in response to both graph-based clustering and pseudotime analyses (Clark et al., 2019). The developing mouse retina was compared to the developing human retina and developing human retinal organoids to the developing mouse retina by scRNA-seq. The lack of a region comparable to the fovea was again noted in the retinal organoids in comparison to the human retina. Mice also lack this region of the retina, as it is specific to primates. Shared and divergent gene roles were identified between species across retinal development. One such gene with divergent expression was *LOXL1* (Lu et al., 2020). Mutations in *LOXL1* are associated with exfoliation glaucoma in humans

(Thorleifsson et al., 2007). However, expression in scRNA-seq suggests that it may also be involved in photoreceptor development in humans but not in mice. This is a reminder that that not all studies of genes involved in human retinal development can be recapitulated in mice (Lu et al., 2020). Another study used scRNA-seq to look even earlier at the developing optic vesicles in mouse retinas. RPCs in the optic vesicles were primarily distinguished by developmental stage rather than subgroups within each timepoint (Yamada et al., 2021).

In zebrafish, RNA-seq in conjunction with ATAC-seq was performed on cells from developing optic vesicles at 16,18, and 24 hpf to elucidate the gene regulatory networks that give rise to retinal neurons and the RPE. Distinct transcriptomic changes were noted between the neural retina (NR) and RPE that could be identified prior to actual structural changes *in vivo* (Buono et al., 2021). RPCs were compared to the retinal stem cells (RSC) of adult zebrafish CMZ. The RPCs and RSCs appear to share a similar gene expression program for differentiation, supporting previous in situ data. Zebrafish RPCs also share traits with the RPCs identified in human and mouse studies. Interestingly, postembryonic RSCs are transcriptomically more similar to the early RPCs. Some caveats to the scRNA-seq approach were also identified. Discrepancies between lineage determined by psudeotime analysis versus lineage tracing were noted. This suggests that similarities in transcriptomic state at a certain point in time do not necessarily mean they share a close origin in lineage (B. Xu et al., 2020).

scRNA-seq has shed some light on important aspects of retinal development. It has expanded the number of genes associated with specific cell types or states. This includes assessing the heterogeneity of RPCs as retinal differentiation progresses, categorizing RPCs into early and late states. However, there is yet to be transcriptomic evidence that points to distinct competence states beyond the broad categories of early and late RPCs. Additionally, it is important to remember that scRNA-seq only provides partial information on the intrinsic states of cells at a given point in time. It does not

inform on epigenetic changes, post-transcriptional and post-translational modifications, or extrinsic influences like spatial positioning and non-autonomous signaling (Shiau et al., 2021). Overall, scRNA-seq will be a useful tool going forward to provide further information regarding the transcriptomic trajectory progenitors undergo on their way to becoming a differentiated neuron and to reveal previously unrecognized heterogeneity across specific cell types in the developing retina.

1.4 Retinal Regeneration in Zebrafish

In addition to the initial neurogenesis that populates the retina, some organisms possess the ability to generate new neurons in response to damage as adults. Zebrafish are one of these organisms. In addition to the retinal neurons, the zebrafish retina contains one intrinsic glial cell type, the Müller glia. The Müller glia has several important roles in the retina, providing structure, monitoring the retinal environment, and responding to injury. When responding to an injury, the Müller glia undergo a gliotic response that is followed by a reprograming to mimic some stem cell attributes (Powell et al., 2013; Ramachandran, Fausett, et al., 2010; Wan & Goldman, 2016). The nuclei of the Müller glia will then dedifferentiate and divide asymmetrically. One daughter cell will remain a Müller glia and the other will give rise to a progenitor capable of replacing any of the retinal neurons (Fausett & Goldman, 2006; Ramachandran, Reifler, et al., 2010; Wan & Goldman, 2016). This regenerative capability provides an additional lens to study how neurogenesis occurs in the retina.

1.5 Complexity of Gene Expression and Regulation

At each step of ocular morphogenesis and retinal differentiation, precise timing, and control of various signaling pathways are essential. Alteration in the expression of a single gene can lead to a cascade of events that drastically impact eye development. For example loss of *rx3* expression in zebrafish leads to anophthalmia (Loosli et al., 2003), loss of *pax2a* expression leads to coloboma

(Lusk & Kwan, 2022), and loss of *nr2e3* prevents differentiation of rod photoreceptors (Xie et al., 2019). To better understand how a single gene can have such a large impact, we need to consider the protein that gene creates and the role it has in the network of elements that impact the functionality and identity of a cell.

The central dogma of biology states that DNA is transcribed into mRNA which is then translated into protein (Crick, 1970). This is a simplified overview of how the information encoded in DNA results in the production of functional proteins. In reality, this process is much more complex. The control of signaling pathways occurs at several different levels within this process. The first level of control is with chromatin remodelers, which are able to change which parts of DNA are accessible to be transcribed into mRNA (Fry & Peterson, 2001). The DNA itself also contains intrinsic cis-regulatory sequences called enhancers and silencers that respectively promote or prevent transcription of nearby genes (Kolovos et al., 2012). Then, there are transcription factors that either activate or repress gene expression by recognition of specific DNA binding sequences (Latchman, 1997). Once mRNA has been transcribed, it undergoes quality control. mRNA that does not meet certain standards, for example if it contains a premature termination codon or an unusually long 3'UTR, undergoes nonsense mediated decay and is not made into protein (Kurosaki et al., 2019). mRNA from multiple exon genes can also undergo splicing to form different variations of protein that potentially have different functions (Shin & Manley, 2004). miRNAs are a class of noncoding RNAs that post-transcriptionally regulate the stability of mRNA and influence alternative splicing (Catalanotto et al., 2016). At the level of translation, the ribosome is the unit responsible for translating mRNA into protein. It consists of 2 subunits that are made up of many ribosomal proteins and rRNAs. Recent research suggests that there may be heterogeneity in these ribosomal subunits that influences the efficiency at which certain mRNAs are translated (Caron et al., 2021; Genuth & Barna, 2018; Zhou et al., 2015). And finally posttranslational protein modifications can lead to changes in protein location, function, signaling, and stability or degradation (Millar et al., 2019). Taken

12

together, all of these components form a complex web that controls gene expression and it is important to consider how they might contribute to dynamic processes like ocular morphogenesis and retinal differentiation.

For example, SoxC transcription factors have been shown to play a role in ocular morphogenesis and retinal differentiation (Bhattaram et al., 2010; Jiang et al., 2013; Lakshmi Pillai-Kastoori, 2015; Pillai-Kastoori et al., 2014; Schilham et al., 1996; Usui, Iwagawa, et al., 2013; Usui, Mochizuki, et al., 2013; Wen, 2016; Wen et al., 2015; Wurm et al., 2008; Ya et al., 1998). To fully understand how they are involved in this process, it is important to consider the different ways their own expression is regulated. Additionally, as transcription factors themselves, they directly target other genes to affect their transcription. Their direct targets and how they each function in this process also needs to be considered. All of these components combined will further elucidate the details of the regulatory network that controls eye development.

1.6   Sry-box (Sox) Transcription Factors

The Sry-box (Sox) transcription factors are grouped together by their shared homology of a high mobility group (HMG) DNA binding domain. The HMG domain binds to the minor groove of its target DNA sequence, known as the Sox motif, and sharply bends the DNA. Between all the Sox proteins, the HMG domain is at least 50% identical (Bowles et al., 2000). However, the remainder of the protein is more variable. There are 8 subfamilies of the Sox proteins, A-H, that are grouped based on homology within the HMG domain, and additional homology in other functional domains (M. Angelozzi & Lefebvre, 2019; Bowles et al., 2000; Stevanovic et al., 2021). The Sox proteins are also highly conserved across vertebrate species and have been studied in human, mouse, Xenopus, and zebrafish models, among others (M. Angelozzi & Lefebvre, 2019; Bowles et al., 2000; Dy et al., 2008; Goslik E. Schepers et al., 2002; Stevanovic et al., 2021).

The SoxC subfamily is comprised of Sox4, Sox11, and Sox12. In addition to containing the conserved HMG domain, the SoxC proteins also contain a second functional domain known as the transactivation domain located near the C-terminus. The transactivation domain is responsible for partnering with other proteins to activate transcription. Sox4 and Sox11 target overlapping sets of genes but have differing efficiencies in binding DNA and activating transcription *in vitro* (Van De Wetering et al., 1993). Sox4 is more efficient at binding DNA than Sox11 and Sox11 is more efficient at activating transcription than Sox4 *in vitro*. (Dy et al., 2008; Hoser et al., 2008; Penzo-Méndez, 2010; Van De Wetering et al., 1993; Wiebe et al., 2003). Transcriptional activation is the primary role of the SoxC proteins; however, one instance of repressor activity has been shown in male germ cell differentiation *in vitro* (Zhao et al., 2017).

SoxC proteins work in partnership with other proteins to bind to DNA (Table 1.1). To better understand how exactly they function, their partner proteins and direct DNA targets must be elucidated. So far it has been shown that partnering with Brn-1 and Brn-2 increases transcription activity of both Sox4 and Sox11 in rat oligodendrocytes and *in vitro* studies (Kuhlbrodt et al., 1998; Wiebe et al., 2003). Additionally, some direct DNA targets of SoxC proteins have been identified. Tead2 is a direct target of Sox4 and Sox11, to promote cell survival in the mesoderm (Bhattaram et al., 2010). Neurog3 is a direct target in pancreatic endocrine cells (E. E. Xu et al., 2015); Tubb3, Prox-1, and DCS are direct targets in neurons (Bergsland et al., 2006; Jacob et al., 2018; Mu et al., 2012); Brn3b is a direct target in RGCs (Jiang et al., 2013); and Plexan1 and Nrcam are direct targets for RGC axon guidance (Kuwajima et al., 2017). However, these discoveries are not an exhaustive list of partner proteins and DNA targets, as these can differ by both developmental time and by cell type.

Table 1.1 Binding Partners and Direct Targets of SoxC Proteins

System	Organism	Binding Partner	Target Gene	Reference
Oligodendrocytes	Rat	Brn-1	Nestin	(Kuhlbrodt et al., 1998; Wiebe et al., 2003)
		Brn-2		
Mesoderm	Mouse		Tead2	(Bhattaram et al., 2010)
Pancreatic Endocrine Cells	Mouse		Neurog3	(E. E. Xu et al., 2015)
Neurons	Mouse		Tubb3	(Bergsland et al., 2006)
	Chicken		Prox-1	(Jacob et al., 2018)
	Human		DCS	(Mu et al., 2012)
Retinal Ganglion Cells	Mouse		Brn3b	(Jiang et al., 2013)
Retinal Ganglion Cell Axon Guidance	Mouse		Plexan1	(Kuwajima et al., 2017)
			Nrcam	

SOX4 has previously been implicated to have redundant roles with SOX11 as a necessary transcription factor for cell survival and in the development of pancreatic cells, the kidney, the urinary tract, the heart outflow tract, germ cells, osteoblasts, lymphocytes, and neurons (Bergsland et al., 2006, 2011; Bhattaram et al., 2010; Dy et al., 2008; Hoser et al., 2008; Huang et al., 2013; Ling et al., 2009; Mavropoulos et al., 2005; Neirijnck et al., 2018; M. Paul, 2014; M. H. Paul

et al., 2014; Potzner et al., 2010; Sock et al., 2004; Tanaka et al., 2004; Thein et al., 2010; Von Wittgenstein et al., 2020; M. E. Wilson et al., 2005) In addition to their overlapping roles, SOX4 and SOX11 also have distinct functions. In mice, a *Sox4* knockout is embryonic lethal due to heart defects in the form of a common trunk at E14; in contrast, *Sox11* knockout is perinatal lethal due to heart defects in the form of a common trunk or ventricular separation at birth resulting in congenital cyanosis (Wurm et al., 2008; Ya et al., 1998). These differences in phenotypes suggest similar yet independent roles in development exist between SOX4 and SOX11 (Bergsland et al., 2006, 2011; Bhattaram et al., 2010; Dy et al., 2008; Huang et al., 2013; Ling et al., 2009; Mavropoulos et al., 2005; Neirijnck et al., 2018; M. Paul, 2014; M. H. Paul et al., 2014; Potzner et al., 2010; Sock et al., 2004; Thein et al., 2010; Von Wittgenstein et al., 2020; M. E. Wilson et al., 2005). Additionally, there is a growing body of evidence that SOX4 and SOX11 have a vital role in eye development.

1.7   Eye Development Requires SoxC Transcription Factors

SOX4 and SOX11 have been shown to play a critical role in eye development in *Mus musculus* (Bhattaram et al., 2010; Jiang et al., 2013; Usui, Iwagawa, et al., 2013; Usui, Mochizuki, et al., 2013). In mice a *Sox4* knockout is embryonic lethal prior to the completion of eye development, however, the *Sox11* null mice do survive long enough to exhibit microphthalmia and anterior coloboma. (Bhattaram et al., 2010; Jiang et al., 2013; Schilham et al., 1996; Usui, Mochizuki, et al., 2013; Wurm et al., 2008; Ya et al., 1998). In *Sox11* null mice there is a reduction of *Bmp7*, which may explain the microphthalmia and anterior coloboma phenotypes (Wurm et al., 2008). *Sox11* is robustly expressed in the retina at E12. This expression then gradually decreases until P5, when it is no longer expressed. *Sox4* is also strongly expressed in the retina at E12 and increases in expression until P1 where it then decreases in expression. The expression of *Sox4* and *Sox11* in the retina are controlled by Notch signaling and histone modifications. Forced activation of Notch signaling inhibited both *Sox4* and *Sox11* expression but does not account for the temporal differences in

expression since it equally affected *Sox4* and *Sox11* expression. Histone modifications were detected at the *Sox4* and *Sox11* loci. Histone 3 (AcH3) was found at the *Sox11* transcriptional start site and Anti-histone H3 tri-methyl Lys27 (H3K27) was found at transcriptional start sites of *Sox4* and *Sox11*. The timing of these histone modifications, acetylation of AcH3 and methylation of H3K27, matched the different temporal expressions of *Sox4* and *Sox11* in the developing retina.(Usui, Iwagawa, et al., 2013). In eye specific knockouts, there was a modest but significant loss of RGCs, amacrine, and bipolar cells in both *Sox4* and *Sox11* mutants. The loss of RGCs, amacrine, and bipolar cells was compounded in dual *Sox4* and Sox11 knockouts. Dual *Sox4* and Sox11 knockouts also had a single thin layer of neural retina and the loss of the optic nerve, resulting in a striking phenotype (Jiang et al., 2013). In *Xenopus laevis*, knockdown of *sox4* and *sox11* by translation blocking morpholinos led to microphthalmia and deformed eyes. Additionally, they also showed a reduction in retinal ganglion cells similar to mouse eye specific knockouts of *Sox4* and *Sox11* (Cizelsky et al., 2013).

In zebrafish, knockdown of *sox4* by translation blocking morpholinos leads to a reduction in *bmp7b* expression which increases *ihhb* signaling, resulting in ocular coloboma (Wen et al., 2015). Knockdown of *sox11* by morpholinos showed more severe but similar phenotypes to the loss of *sox4* (Pillai-Kastoori et al., 2014). This is similar to the reduction of *Bmp7* seen in *Sox11* null mice and suggests a conserved role for how Sox4 is involved in ocular morphogenesis.

Sox4 and Sox11 have also been impacted in having a role in the zebrafish retina. The zebrafish XOPS:mCFP transgenic line carries a rod-targeted transgene that is toxic to the rod photoreceptors. This line undergoes a continual cycle of rod degeneration and regeneration (A. C. Morris & Fadool, 2005). A microarray analysis was performed to compare the gene expression between Wildtype (WT) and the XOPS:mCFP transgenic zebrafish retinas and it was found that several transcription factors were upregulated. Included in these were the zebrafish orthologues of *sox4* and *sox11*, suggesting a role in rod

differentiation (Ann C. Morris et al., 2011). In *sox11* and *sox4* morphants, there was a decrease in the number of rod photoreceptors present at larval stages. (Lakshmi Pillai-Kastoori, 2015; Wen, 2016). Taken together, these data suggest that SoxC transcription factors are important for the genesis of rod photoreceptors, both during embryonic development and in adult retinal regeneration.

1.8 SOXC Transcription Factors Are Critical for Human Development

SOXC genes have been shown to play a vital role in development in animal models across may development systems (Bergsland et al., 2006, 2011; Bhattaram et al., 2010; Dy et al., 2008; Huang et al., 2013; Jiang et al., 2013; Ling et al., 2009; Mavropoulos et al., 2005; Neirijnck et al., 2018; M. Paul, 2014; M. H. Paul et al., 2014; Potzner et al., 2010; Sock et al., 2004; Thein et al., 2010; Usui, Iwagawa, et al., 2013; Usui, Mochizuki, et al., 2013; Von Wittgenstein et al., 2020; M. E. Wilson et al., 2005; Wurm et al., 2008; Ya et al., 1998). They have also been implicated in causing various developmental disorders in humans like MAC, Coffin-Siris Syndrome (CSS), CHARGE Syndrome, and SOX4-Related Neurodevelopmental Syndrome, all of which include issues with visual impairment (Al-Jawahiri et al., 2022; M. Angelozzi & Lefebvre, 2019; Marco Angelozzi et al., 2022; Feng et al., 2013; Ghaffar et al., 2021; Pillai-Kastoori et al., 2014; Schrier et al., 2012; Sperry et al., 2016; Tsurusaki et al., 2014; Zawerton et al., 2019). The phenotypes *SOXC* mutations are associated with affect a wide but consistent range of developmental systems, including the eye. Two patients from a screen of 79 individuals with MAC were identified to have mutations in *SOX11*, one of which also had a reduction in rod photoreceptor function determined by an electroretinogram (Pillai-Kastoori et al., 2014).

The first developmental disorder that has been associated with SOX11 is CSS. CSS is characterized by the presence of either aplasia or hypoplasia of the distal phalanx or absence of the fingernail, primarily involving the fifth finger, developmental or cognitive delay, characteristic facial features, hypotonia, hair

growth in atypical areas, and sparse scalp hair (Schrier et al., 2012). CSS has predominately been associated with mutations in *SMARCB1*, *SMARCA4*, *SMARCE1*, *ARID1A* and *ARID1B*. However, two *de novo* *SOX11* mutations were found in two unrelated patients diagnosed with CCS (Tsurusaki et al., 2014). A later study identified an additional 38 patients with mutations in *SOX11* (Al-Jawahiri et al., 2022). The clinical presentation of these patients was compared to previous patients identified with *SOX11* mutations and the clinical phenotype of CSS. SOX11 Syndrome was determined to be distinct from CSS, due the inclusion of differentiating features. These features included oculo-motor apraxia, ocular malformations, and idiopathic hypo-gonadotrophic hypogonadism (Al-Jawahiri et al., 2022).

Another developmental disorder that is associated with *SOXC* genes is CHARGE Syndrome. CHARGE is an acronym for the symptoms that can occur in the syndrome: coloboma, heart defects, choanal atresia, retardation of development and growth, genital abnormalities, and ear defects. Today CHARGE is primarily characterized by the presence of choanal atresia, coloboma, characteristic ears and cranial nerve anomalies (George et al., 2020). Additional phenotypes of cardiovascular malformation, genital hypoplasia, cleft lip/palate, tracheoesophageal fistula, distinctive CHARGE facies, and delayed growth and development occur with varying frequencies across patients. CHARGE Syndrome is due to mutations in *CHD7* in 60-80% of patients (Blake & Prasad, 2006; George et al., 2020; Lalani et al., 2006; Patten et al., 2012). A CHARGE patient has been identified that has a duplication of *SOX11* and not a mutation of *CHD7* (Sperry et al., 2016). Additionally, CHD7 is a chromatin remodeler and has been shown to directly target *SOX4* and *SOX11* (Feng et al., 2013). Taken together, these data suggest that many of the overlapping symptoms of patients with *CHD7* or *SOXC* mutations may be due to this relationship.

SOX4 has also been associated with a developmental disorder. Patients identified with mutations in *SOX4* were classified as having SOX4-Related

Neurodevelopmental Syndrome. All patients exhibited a combination of some of the following features: dysmorphic features, palatal anomalies, retrognathia, cardiac defects, visual impairment, hearing impairment, and intellectual disability. Visual impairments were frequently observed, mainly in the form of myopia, strabismus, and keratoconus (Marco Angelozzi et al., 2022; Ghaffar et al., 2021; Zawerton et al., 2019).

Taken together, the various ocular abnormalities associated with mutations in both *SOX11* and *SOX4* indicate that SOXC factors play a critical role in the development of the visual system. However, more research needs to be done on SOXC proteins in development to better understand how they impact vision in these relevant disorders. More specifically, a detailed understanding of how of SoxC factors regulate each stage of eye development, from early ocular morphogenesis through terminal differentiation of the various retinal cell types, is needed.
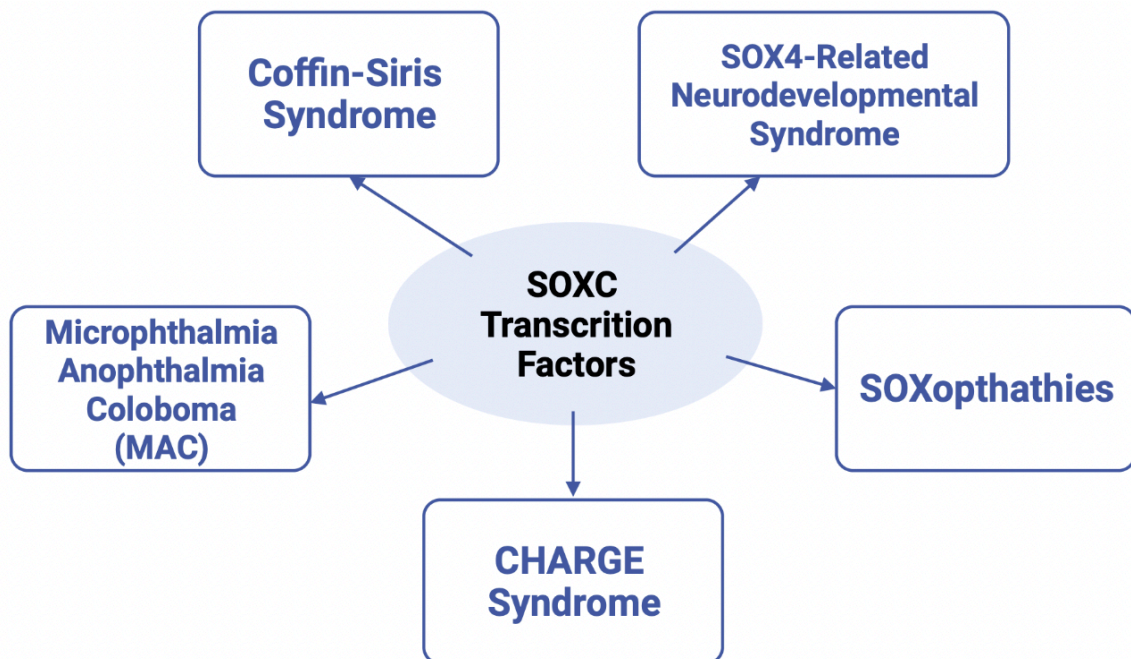
Figure 1.2 Developmental syndromes associated with SOXC transcription factors.

1.9   Zebrafish, an Excellent Model for Vision Research

Zebrafish are an excellent model for researching the role of Sox4 in eye development in multiple facets. They have a short generation time, high fecundity, external fertilization, rapid development, and a plethora of genetic tools available to investigate gene function (Stenkamp, 2007). Some examples of the genetic tools available for zebrafish are a fully sequenced genome, various transgenic lines, gene knock down by morpholinos, and gene editing by CRISPR/Cas9.

Due to a genome duplication that occurred at the base of the teleost lineage, zebrafish have duplicates of many genes. This includes *sox4*, resulting in *sox4a* and *sox4b* co-orthologues. Sox4a shares 64% protein sequence homology with Sox4b, 68% homology with mouse SOX4, and 40% homology with human SOX4. Sox4b shares 65% homology with mouse SOX4 and 38% homology with human SOX4. However, all share a very high conservation of sequence (greater than 95%) in the high mobility group (HMG) and transactivation domains (TAD) (Mavropoulos et al., 2005).

Figure 1.3 Comparison of human and zebrafish Sox4 proteins.

(A) Protein domains for Human SOX4. (B) Protein domains for Zebrafish Sox4a and Sox4b.

Genetic mutants and morpholinos are useful tools for loss of function studies but induce loss of function through different methods. Morpholinos are small oligonucleotides that either block translation or splicing of a specific gene, allowing for temporary knock-down of gene expression (Bill et al., 2009). CRISPR/Cas9 allows for targeted gene editing, which is useful for inducing

mutations in a gene of choice (Charpentier & Doudna, 2013; Doudna & Charpentier, 2014; Sampson & Weiss, 2014). For loss of function studies, the goal is to create a mutation that would result in an early stop codon or a large deletion of the functional domains within the gene. These types of mutations would result in no functional protein being made.

It is important to compare the phenotypes between mutants and morphants. An interesting phenomenon has been observed in numerous zebrafish mutants. The mutants either completely lack a phenotype or the phenotype is much less severe compared to that of the morphant. For example, *egfl7* mutants did not show a morphant phenotype when injected with morpholinos that target *egfl7.* This indicates that the morphant phenotype is not due to off target effects but rather that the mutant is somehow compensating for the loss of Egfl7 (Rossi et al., 2015). This is not the case for all genetic mutants. It appears to be specific to mutant mRNA transcripts that are flagged for non-sense mediated decay, that genetic compensation is triggered (El-Brolosy et al., 2018).

Previous studies have shown the role of Sox4 in early zebrafish eye development using translation blocking morpholinos to knock down gene expression. These studies revealed that Sox4 is upstream of Hedgehog signaling and is required for choroid fissure closure. Evidence suggests that *bmp7* may be a target of Sox4 in regulating Hedgehog signaling (Wen et al., 2015). Additionally, a novel role for Sox4 in terminal rod photoreceptor differentiation was demonstrated (Wen, 2016). However, it remains unclear what the targets of Sox4 are in ocular morphogenesis, how Sox4 influences terminal rod photoreceptor differentiation, and if Sox4 has a role later in retina development. To that end, the goal of the research described in this dissertation is to investigate the function of Sox4 in early and late retinal development using genetic mutants and transcriptomic analyses.

1.10 Rationale and Specific Aims

As described above, Sox4 plays an important role in ocular morphogenesis and in the neurogenesis of rod photoreceptors in zebrafish (Wen et al., 2015), however details of how Sox4 regulates these processes are lacking. A better understanding of the role of Sox4 in ocular morphogenesis will contribute to the network of genes that result in conditions like MAC. Additionally, elucidating how Sox4 influences the terminal differentiation of rod photoreceptors will further our understanding of the components required to make fully differentiated and function rod photoreceptors.

Previous studies on the role of Sox4 in the developing zebrafish have relied on the use of translation blocking morpholinos to knockdown *sox4* expression (Wen et al., 2015). This was a useful approach to start determining the role of Sox4 in ocular morphogenesis and in the neurogenesis of rod photoreceptors. However, morpholinos knockdown gene expression for a limited period of time. Genetic mutants are required for long term loss-of-function studies. Zebrafish mutant lines for *sox4a* and *sox4b* were generated by CRISPR/Cas9 and are predicted to produce no functional protein (Wen, 2016). This will allow us to determine if the mutant phenotype recapitulates the morphant phenotypes. The *sox4* mutants will also allow us to determine how the loss of Sox4 affects the retinal later in zebrafish development.

Additionally, there are transgenic lines available that are of relevance to this project. Sox4 has previously been implicated in having a role in ocular morphogenesis (Wen et al., 2015). The rx3:eGFP transgenic line expresses eGFP under the Medaka Rx3 promoter. This labels cells in the developing forebrain that are specified to become the retina; this allows us to track them through the process of ocular morphogenesis (Katherine E Brown et al., 2010). Additionally, Sox4 has been implicated in having a role in rod photoreceptor neurogenesis (Wen, 2016). The XOPS:GFP transgenic line expresses GFP under the *Xenopus* Rhodopsin promoter (Fadool, 2003). This labels rod photoreceptors with GFP in the zebrafish retina, allowing them to easily be

23

visualized. Combining the *sox4* mutants with each of these transgenic lines will provide useful insights into how the loss of Sox4 impacts ocular morphogenesis and rod photoreceptor neurogenesis.

In this dissertation I address the following questions: how does Sox4 contribute to ocular morphogenesis, how does Sox4 influence retinal differentiation, particularly of rod photoreceptors, and what are the targets of Sox4 in both ocular morphogenesis and rod photoreceptor differentiation?

To address these questions, I characterized the ocular phenotypes of zebrafish mutant lines for *sox4a* and *sox4b*, as well as *sox4a/b* double mutants. Supporting previous research in zebrafish *sox4* morphants, I demonstrate that Sox4 is involved in both the process of ocular morphogenesis and the differentiation of rod photoreceptors (Wen, 2016; Wen et al., 2015). To elucidate the role of Sox4 in in ocular morphogenesis in further detail, I used the zebrafish transgenic line rx3:eGFP in combination with live imaging by Lightsheet Microscopy. This technique is described in detail in Chapter 2. Using this method, I discovered that the rx3:eGFP population of cells is smaller in *sox4* mutants from the earliest stages of the eye field.
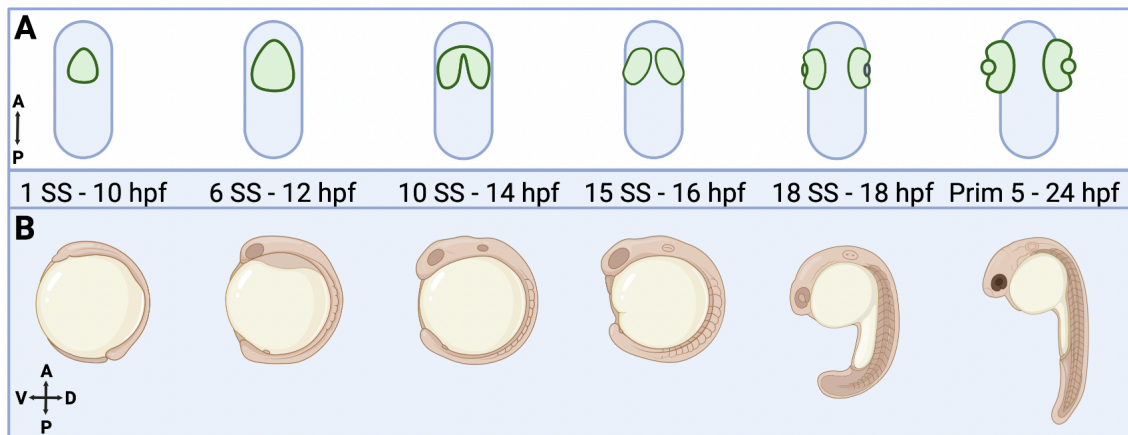
Figure 1.4 Ocular Morphogenesis in the Developing Zebrafish.

(A) Dorsal vantage of ocular morphogenesis from specification of the eyefield at 1 SS to the formation of the optic up at prim-5 as would be labeled by the zebrafish transgenic line rx3:eGFP. (B) Lateral vantage of a developing zebrafish embryo at the corresponding stages of ocular morphogenesis.

A role for Sox4 in zebrafish rod photoreceptor development has been suggested by previous research (Morris et al., 2011; Wen, 2016). This led me to use the XOPS:GFP transgenic line to compare the differences between wildtype and *sox4* mutants. In Chapter 3, I show that the *sox4* mutants display a reduction of rod photoreceptors.

Interestingly, both ocular morphogenesis and rod photoreceptor differentiation are dependent on the presence or absence of maternal *sox4* transcripts in the developing embryo. This indicates that events occurring early in specification of the eyefield (when maternally derived Sox4 is still present) influence later retinal differentiation. To investigate this hypothesis, I used scRNA-seq to analyze the developing eyefield prior to evagination into bilateral optic vesicles for the first time. These data, presented in Chapter 3, provide a foundation for further investigations into whether transcriptional signatures of eye field cells can be linked to later developmental outcomes in the retina. Finally, I characterized additional phenotypes throughout the *sox4* mutants which implicate a potential role for Sox4 in neural crest development.

Taken together, these studies contribute to our understanding of the regulatory networks influencing ocular morphogenesis and rod photoreceptor differentiation by implicating a role for Sox4 in the specification of the eyefield and in rod photoreceptor neurogenesis and maturation. This information will be useful in furthering our understanding of how ocular complications arise in human patients with mutations in *SOX4*.

This research will be addressed by the following aims:

Specific Aims

I. Visualize Ocular Morphogenesis by Lightsheet Microscopy

    a. Demonstrate a method for live imaging of ocular morphogenesis with high spatial and temporal resolution

    b. Provide a method of analysis of the live imaging dataset of ocular morphogenesis

II. Determine the role of Sox4 in eye development

    a. Characterize the process of ocular morphogenesis in *sox4* zebrafish mutants

    b. Characterize retinal cell types of *sox4* zebrafish mutants

III. Establish if signaling in the eyefield impacts later retinal differentiation

    a. Determine the cell type composition of the developing eyefield

    b. Establish the transcriptomic impact of the loss of *sox4* on the early developing eye

IV. Investigate a role for Sox4 in neural crest development

    a. Characterize additional phenotypes of *sox4* zebrafish mutants

    b. Propose a mechanism by which the additional phenotypes may be linked

Aim I is presented in Chapter 2

Aims II and III are presented in Chapter 3

Aim IV is presented in the Appendix

CHAPTER 2. VISUALIZING OCULAR MORPHOGENESIS BY LIGHTSHEET MICROSCOPY USING RX3:GFP TRANSGENIC ZEBRAFISH

Rebecca A. Petersen, Ann C. Morris

Department of Biology, University of Kentucky, Lexington KY 40506

N.B. For this dissertation, figure numbers, headings, and text were modified to match

dissertation style.

2.1 Abstract

Vertebrate eye development is a complex process that begins near the end of embryo gastrulation and requires the precise coordination of cell migration, proliferation, and differentiation. Time-lapse imagining offers unique insight to the behavior of cells during eye development because it allows us to visualize oculogenesis in vivo. Zebrafish are an excellent model to visualize this process due to their highly conserved vertebrate eye and their ability to develop rapidly and externally while remaining optically transparent. Time-lapse imaging studies of zebrafish eye development are greatly facilitated by use of the transgenic zebrafish line Tg(rx3:GFP). In the developing forebrain, rx3:GFP

expression marks the cells of the single eye field, and GFP continues to be expressed as the eye field evaginates to form an optic vesicle which then invaginates to form an optic cup. High-resolution time-lapse imaging of rx3:GFP expression therefore allows us to track the eye primordium through time as it develops into the retina. Lightsheet microscopy is an ideal method to image ocular morphogenesis over time due to its ability to penetrate thicker samples for fluorescent imaging, minimize photobleaching and phototoxicity, and image at a high speed. Here, the study provides a protocol for time-lapse imagining of ocular morphogenesis using a commercially available lightsheet microscope and an image processing workstation to analyze the resulting data. This protocol details the procedures for embryo anesthesia, embedding in low melting temperature agarose, suspension in the imaging chamber, setting up the imaging parameters, and finally analyzing the imaging data using image analysis software. The resulting dataset can provide valuable insights into the process of ocular morphogenesis, as well as perturbations to this process as a result of genetic mutation, exposure to pharmacological agents, or other experimental manipulations.

2.2   Introduction

Embryonic development is a complex process that requires the precise coordination of many different events. The formation of the vertebrate eye begins in the developing forebrain, where a portion of the cells are specified as the eye field. These cells will evaginate towards the surface ectoderm, giving rise to two bilateral optic vesicles(Chow & Lang, 2001; Eckert et al., 2019; Fuhrmann, 2010; Heermann et al., 2015; Kimmel et al., 1995; Kwan et al., 2012; Z. Li et al., 2000; Picker et al., 2009; S. W. Wilson & Houart, 2004; Yoon et al., 2020). Contact with the surface ectoderm then induces an invagination of the optic vesicle into an optic cup. The surface ectoderm will give rise to the anterior structures of the eye, such as the lens and cornea, while the optic cup will give rise to the neural retina and retinal pigmented epithelium(Chow & Lang, 2001; Eckert et al., 2019; Fuhrmann, 2010; Heermann et al., 2015; Kimmel et al., 1995; Kwan et al., 2012;

Z. Li et al., 2000; Picker et al., 2009; Pillai-Kastoori et al., 2015; Sidhaye & Norden, 2017; Yoon et al., 2020). Disruptions in this process can lead to congenital defects like microphthalmia, anophthalmia, and coloboma (MAC). At this time, there are no options to correct these defects(Chow & Lang, 2001; Eckert et al., 2019; Fuhrmann, 2010; Kwan et al., 2012; Picker et al., 2009; Pillai-Kastoori et al., 2015; Sidhaye & Norden, 2017; Yoon et al., 2020). Further studies of the mechanisms of ocular morphogenesis and the problems that can lead to MAC will provide a foundation of knowledge that will potentially lead to treatments. One powerful tool to investigate the dynamic behaviors of cells during eye development is time-lapse imagining, which allows this process to be visualized and characterized in vivo and in real time.

Zebrafish (*Danio rerio*) are an excellent model to visualize early ocular development using time-lapse imaging. They have a highly conserved vertebrate eye and possess the ability to develop rapidly and externally while remaining optically transparent(Kimmel et al., 1995). Zebrafish provide a great resource for time-lapse imaging due to these characteristics that mammalian models lack. Time-lapse imaging studies of zebrafish eye development are greatly facilitated by use of the transgenic zebrafish line Tg(rx3:GFP). RX3 (Retinal homeobox protein 3) is a transcription factor essential for eye development(Loosli et al., 2003). Rx3 is the first of the three 'rx' genes in the zebrafish to be expressed, starting its expression mid-gastrulation, approximately 8 hours post fertilization (hpf)(Cavodeassi et al., 2005; Chuang et al., 1999). The rx3:GFP transgene can be visualized in the developing forebrain starting at the 1 somite stage (ss), approximately 10 hpf(Chuang et al., 1999; Ebert et al., 2014; Emerson et al., 2017; Hehr et al., 2018; Ivanovitch et al., 2013; Jemielita et al., 2013). In the developing forebrain, rx3:GFP expression marks the cells of the single eye field, and GFP (green fluorescent protein) continues to be expressed through the remainder of ocular morphogenesis. High resolution time lapse imaging of rx3:GFP expression therefore allows us to track the single eye field through time as it develops into the retina(Ebert et al., 2014; Hehr et al., 2018; Ivanovitch et al., 2013; Jemielita et al., 2013).

Time-lapse imaging studies of zebrafish development have primarily been performed using confocal or Lightsheet microscopy. Confocal microscopy is advantageous in that it allows for the precise imaging of samples along the z axis and reduces fluorescent background signal. However, it is limited by the amount of time it takes to acquire an image, sample position rigidity, and its propensity towards photobleaching and phototoxicity of live samples. Lightsheet microscopy is an ideal method to image ocular morphogenesis over time due to its ability to penetrate thicker samples for fluorescent imaging, increased flexibility in sample orientation, minimized photobleaching and phototoxicity, and imaging at a high speed(Huisken et al., 2004; Icha et al., 2016; Jemielita et al., 2013; Keller et al., 2008, 2010; Keller & Dodt, 2012; Pampaloni et al., 2015; Pantazis & Supatto, 2014; Park et al., 2015; Reynaud et al., 2008; Royer et al., 2016). The spatial resolution achievable with current light sheet microcopy systems is approximately 250-500 nanometers (nm). Although this is not significantly different from what can be obtained with confocal microscopy, the sample can be freely rotated and imaged from multiple angles, improving both imaging depth and resolution, and offering much greater flexibility for in vivo time lapse imaging experiments than the confocal platform(Pantazis & Supatto, 2014; Santi, 2011). For these reasons, Lightsheet microscopy is quickly becoming the favored method for time-lapse imaging studies of zebrafish development. This protocol describes the steps of quantifying oculogenesis through the imaging of Rx3:GFP transgenic zebrafish using a commercially available Lightsheet microscope(Reynaud et al., 2014) and details a pipeline for image analysis using the arivis software platform.

2.3   Protocol

All experiments involving the use of zebrafish were carried out in accordance with protocols established by the University of Kentucky Institutional Animal Care and Use Committee (IACUC).

2.3.1 Sample Preparation

A.   Set up a mating pair of Tg(Rx3:GFP) zebrafish in a gated cross tank the night before imaging is planned. The mating pair of fish selected should be between 4 months to 2 years in age and are easily distinguished as male or female based on body shape and coloration[34]. The following morning pull the gate as the lights come on in the fish facility(Avdesh et al., 2012)[,34].

B.   Check the crosses every half hour for embryos and note what time embryos are first visualized in the bottom of the cross tank. Transfer the embryos to a petri dish and maintain the embryos at 28.5 °C for approximately 10 hours to develop to the 1-2 somite stage (ss). Begin to image at the 1-2 somite stage (ss).

C.   To screen for the presence of somites, observe the embryos under a stereoscope at 10 hpf and count the number of somites[1].

    NOTE: Any embryos that are beyond the single somite stage should not be used for this experiment.

D.   Out of the embryos that are at the single somite stage, screen for GFP expression using a fluorescence adapter in combination with a stereomicroscope to confirm the presence of the Rx3:GFP transgene. Once 3-5 GFP positive individuals have been identified, use fine forceps to dechorionate the embryos and transfer them into a small petri dish containing E3 embryo buffer with a glass pipette[34].

E.   Anesthetize the embryos by transferring them into 0.5 mL E3 embryo buffer (pH 7) containing 0.168 mg/mL Tricaine (MS222) in an micro centrifuge tube(Hirsinger & Steventon, 2017; Westerfield, 2007). Spontaneous muscle movements begin as early as 17 hpf(Saint-Amant & Drapeau, 1998). Ensure that embryos are anesthetized to image beyond this timepoint.

F. Embed the embryos in 1% low melting temperature agarose in 0.168 mg/mL Tricaine and E3.

NOTE: This is the optimal concentration of low melting temperature agarose to allow for the embryo to be held in place but remain pliable enough to permit the growth of the embryo over the imaging time-course(Keller et al., 2008, 2010).

G. Prepare a 10 mL solution of 2% low melting temperature agarose in E3 buffer. Heat it in a microwave oven to dissolve agarose using 15 s intervals, to prevent the solution from boiling over. Allow the solution to cool enough to hold without discomfort but not so much that it solidifies, and not cause harm to the embryos. Once the agarose is sufficiently cool, add 0.5 mL to the embryos in the tube of Tricaine in E3 and gently pipet the solution and embryos to mix.

H. Using a 1 mm glass capillary and Teflon plunger, pull up the embryos in the agarose solution into the capillary. Make sure to pull multiple embryos into the capillary. Aim to pull a total of 3-5 embryos to increase the likelihood of having a well-positioned embryo.

NOTE: Due to the round nature of the embryos at this timepoint, it is challenging to guarantee a specific orientation in the capillary. Ideally, the body of the embryo will be positioned laterally in the capillary, allowing for the greatest ease of positioning within the microscope.

I. Let the agarose solidify over a period of 30-60 s at room temperature. Place the capillary in a beaker of 0.168 mg/mL Tricaine in E3 buffer until ready to image (Figure 1A).

NOTE: The excess 2% low melting temperature agarose solution can be allowed to solidify and subsequently reheated in future experiments.

J.   Place the capillary into the sample holder (Figure 1B–F) as described step 3.

2.3.2 Zeiss Lightsheet Z.1 set up

A.   Switch on each component of the microscope and the computer in the following order: 1) System, 2) PC, then 3) Incubation (Figure 2A).

B.   Place the 20x imaging objective and the 10x illumination objective into the microscope chamber. Match the objective settings in the Zen Software interface under the Maintain tab.

C.   Slide the chamber (Figure 2C) into the housing on the track (Figure 2B) with the tubing facing out. The tubing connects to the appropriate ports on the right as shown in Figure 2E.

D.   Attach the extension line to the syringe with the luer-lock mechanism (Figure 2D), fill it with Tricaine in E3, and place it in the holder attached to the right of the microscope(Westerfield, 2007). Connect the extension attached to the syringe filled with Tricaine in E3 to the bottom right of the chamber with the Luer-Lock mechanism. Push the plunger to fill the chamber with the Tricaine/E3 buffer. Close the door to the chamber.

E.   Place the capillary with the sample into the capillary sample holder. The capillary sample holder is comprised of two rubber sleeves, a metal sample holder disc, a metal stem, and a metal cap (Figure 1B). Click the metal sheath into the center of the metal disc (Figure 1C). Place the two rubber stoppers into the sheath, with the slits facing the ends of the sheath

followed by the capillary. Slide the capillary through the middle of the rubber stoppers. Fasten it in place with the metal cap once the marker is at the base of the metal sheath (Figure 1D).

F.   Place the capillary sample holder onto the top of the microscope, with the white marks aligning (Figure 1E,1F). Close the lid.

G.   Click the Locate Capillary button on the software interface (Figure 3A). Use the ErgoDrive control panel, a manual device that controls the capillary orientation (Figure 3E), to move the capillary and position it just above the objective (Figure 3B).

H.   Open the lid, and gently push on the plunger until the section of agarose containing the embryo is hanging below the capillary bottom and is in front of the objective (Figure 3C).

I.   Turn off Locate Capillary and click on the Locate Sample button (Figure 3A). This switches the view from the sample chamber's web cam to the microscope objective (Figure 3D). Use this view to adjust the position of the sample more precisely. Turn off Locate Sample (Figure 3A).

J.   Switch over to the Acquisition tab. Check the boxes for Z-Stack and Time Series.

K.   In the Acquisition Mode parameters window, choose the Dual Side Lightsheet setting and check the boxes for Online Dual Side Fusion and Pivot Scanning.

L.   In the Channels window, choose the 488 channel, set the laser power to 1, and the exposure time to 7.5 ms.

M.   Next, click the Continuous button to get a live view of the embryo. Use the ErgoDrive control panel to adjust the position of the embryo until the eye field is directly facing the camera. Continue adjusting the left and right lightsheets in the Channels parameters until the eye field is sufficiently in focus.

N.   Set the Z-Stack parameters by using the ErgoDrive control panel to move through the Z-plane. Set the first and the last Z-Positions around 500 µm beyond the last detectable fluorescent signal. This leaves room for the eye field to remain in frame as the embryo grows throughout the time-lapse imaging session. After setting the range of the Z-Stack click on the Optimal button to set the step size to 0.477 µm, the optimal setting.

O.   Set the Incubation parameters by checking the box for the Peltier Unit to keep the temperature at 28 °C. In the Time Series window, choose the frequency and time interval to acquire images. In this protocol, the parameters were set to image every 5 min, for a total of 166 intervals.

P.   Click the Start Experiment button. Choose the folder to save the image set. Set the image prefix and hit Save to start the imaging.

NOTE: The microscope will now run through each image set at the interval specified.

Q.   After the time-lapse imaging session has been completed, send the stage to the load position and remove the capillary sample holder. Take apart the capillary sample holder in the reverse order that it was put together and use the plunger to remove the sample and excess agarose from the capillary. Open the chamber door. Use the syringe to remove the chamber liquid from the chamber, disconnect and remove the chamber, then rinse with water and air dry.
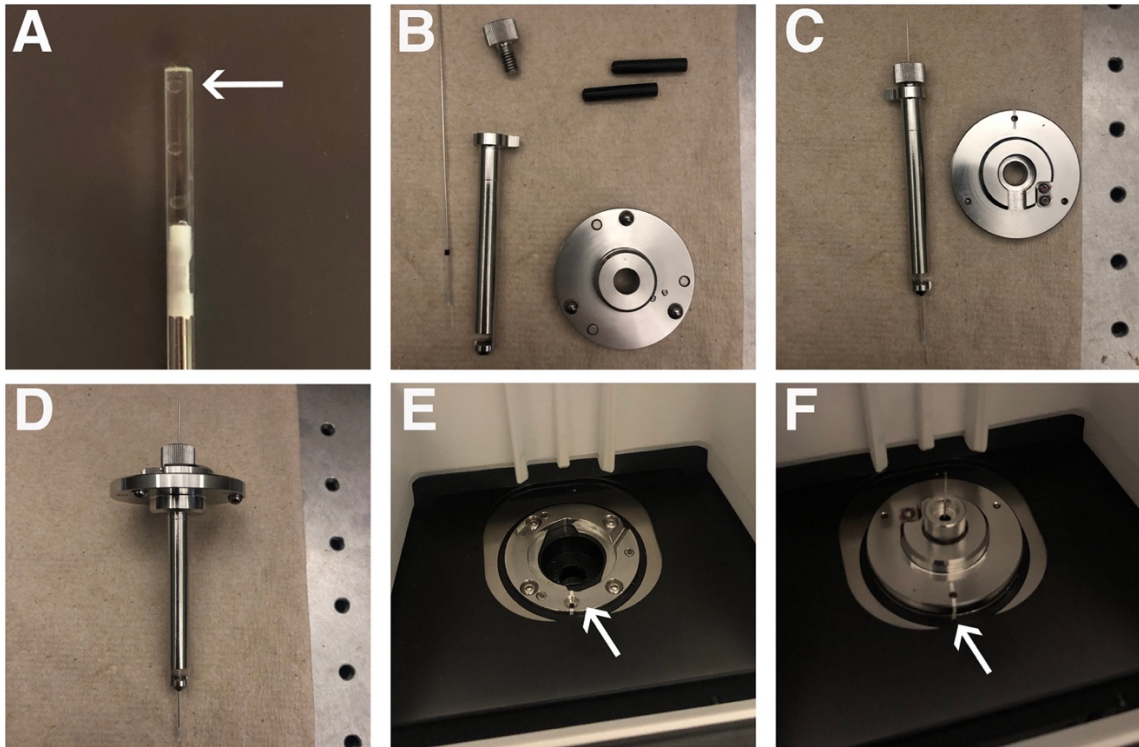
Figure 2.1 Sample preparation.

(A) Positioning of embryos in a glass capillary. The arrow points to an embryo in the capillary. (B) Glass capillary and capillary holder parts. (C) Partially assembled capillary holder. (D) Fully assembled capillary holder. (E) Lightsheet mounting chamber. The arrow indicated the white line used to orient the capillary holder. (F) Capillary holder properly mounted in the Lightsheet. The arrow shows the matching white lines, indicating proper orientation of the capillary holder.
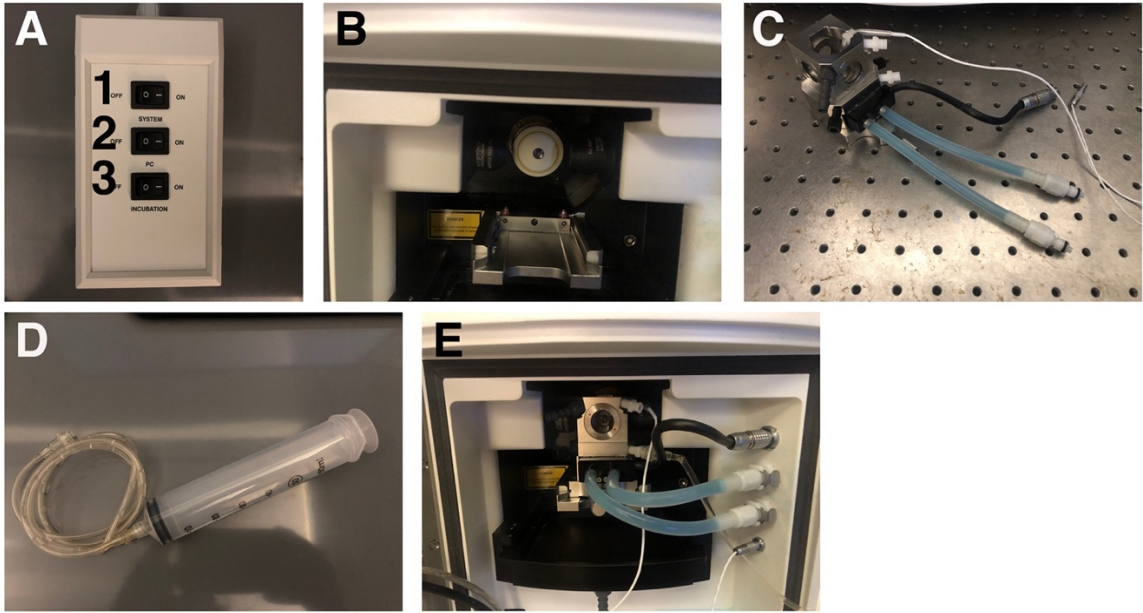
Figure 2.2 Lightsheet imaging set-up.

(A) Switchboard to turn on the Lightsheet, computer, and incubation unit. The numbers indicate the order of operations. (B) Lightsheet objective chamber. (C) Imaging chamber. (D) Syringe and tubing that will be connected to the imaging chamber. (E) The imaging chamber properly positioned within the objective chamber with all of the tubes connected to the appropriate ports to the right
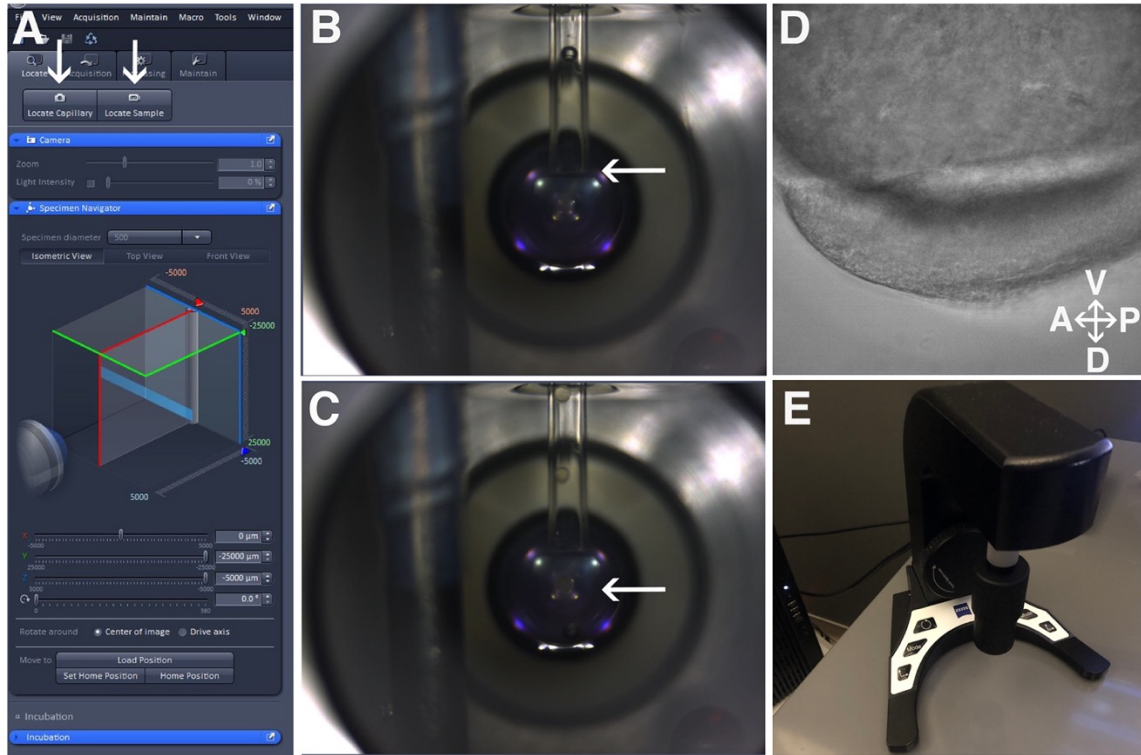
Figure 2.3 Sample positioning.

(A) Locate Capillary and Locate Sample buttons in Zen Software as indicated by the arrows. (B) The positioning on the glass capillary. The arrow indicates the edge of the glass capillary positioned just above the lens of the objective. (C) The embryo suspension beyond the glass capillary. The arrow indicated the embryo suspended in agarose beneath the glass capillary in front of the objective's lens. (D) View of the embryo through the objective. (E) The ErgoDrive control panel.

2.3.3   Image Analysis

A.   Open the arivis Vision4D software program.

B.   Click File, then choose Import file. Select all .czi files from the time-lapse imaging session and open. The next window opens with the options on how to import the files; select Z-stacks as frames to order the z-stacks in the order obtained. Once the files have been imported, the software saves as a single .sis file. To specify the location for the file to be saved, select

the folder prior to clicking Import.

C.   After the file is imported, arivis is now ready to render a video of the time-lapse images. Click on the 4D Viewer Cube in the bottom left corner and the Scale Bar icon (Figure 4D–E). Click the Video icon to bring the Storyboard taskbar to the bottom of the screen (Figure 4C).

D.   In the Storyboard taskbar, choose Add Keyframe Sequence (Figure 4F). Specify the duration of the video in seconds, uncheck the Create Rotation box, and check the Use Time Progression to include the specific timepoints in the video. The software displays these parameters to the right of the Storyboard taskbar for any adjustments at any time. Save the Storyboard to apply the same parameters to multiple image sets (Figure 4F).

E.   Click Export Movie to save a video of the time-lapse imaging (Figure 4F). Specify the movie export settings, including the File name and location, video format (.mp4), video resolution (1080p), framerate (60 FPS), and data resolution (1297x1297x784). Add timestamps here, if desired. Once these parameters are set, choose Record (Figure 4F).

F.   Steps 4 and 5 can be repeated with modification to Step 4 to create rotation videos at specific timepoints. When adding a keyframe sequence to the storyboard, check the Create Rotation box, and uncheck the Use Time Progression. Then follow the same instructions as in Step 5.

G.   To render a high-resolution image at any orientation at any individual time point, select the camera icon in the 4D Viewer to obtain a high-resolution image (Figure 4C).

H. To build a pipeline for analysis, choose the flask icon to access the Analysis panel (Figure 4B). In the analysis panel, click on the analysis operations dropdown menu. As an example, the protocol demonstrates below the sequence of operations for a volume analysis pipeline. Run or undo individually each step of the pipeline to fine tune each parameter (Table 1).

I. Click on the blue triangle at the top of the pipeline to allow the pipeline to run.

NOTE: This will take some time depending on the speed of the computer. Once the pipeline has been optimized, the pipeline can be exported and imported to arivis with ease and applied to multiple datasets in a batch analysis.

J. To access batch analysis, click Batch Analysis under the Analysis tab.

K. After the pipeline runs, a window pulls up with all of the objects found. Access this manually through the table icon (Figure 4B). At the top of this window, click on the box labeled Feature Columns to pull up a list of features that can provide information about the object of interest. For the eye field volume analysis, these features include Surface Area, Volume (Volume, VoxelCount), Intensities #1 (Mean), Attributes (Id, Type), and Time Point (First). Click Export to export the data to a spreadsheet.
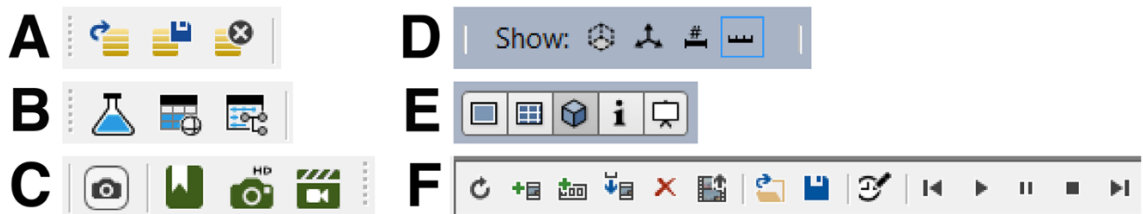
Figure 2.4 Important icons for navigating arivis Vison4D.

Each panel has the icon function identified from left to right. (A) Open, Save, Close. (B) Analysis Panel, Show Objects Table, Open Track Editor. (C) Copy current viewer content as an image into clipboard, Toggle Bookmarks, Create a high-resolution image for the current view, Toggle Storyboard. (D) Show Measure Box, Show Orientation Cross, Show Legend, Show Scale Bar. (E) Show as 2D Viewer, Show as Gallery Viewer, Show as 4D Viewer, Show as Info Viewer, Show as Projection Viewer. F) Refresh all Keyframes, Add Keyframe, Add Keyframe sequence, Insert Keyframe, Remove all Keyframes, Export Movie, Load Storyboard, Save Storyboard, Adjust the target time of the entire movie, First Keyframe, Play, Pause, Stop, Last Keyframe.

2.4   Representative Results

The dataset displayed here was imaged using the protocol described above. A Tg(Rx3:GFP) embryo was imaged starting at the 1 somite stage (ss) through 24 hpf, a total time period of 14 h, with the images acquired at 5 min intervals. Time-lapse imaging allows for easy selection and comparison of any time-point that shows a phenotype of interest. Figure 5 demonstrates a set of high-resolution images that were rendered from the dorsal vantage point at select developmental time-points. The pipeline run in arivis Vision4D builds a mask that represents the developing eye as identified by fluorescent signal. In Figure 5 and Videos 1–6, the mask can be visualized in comparison to the fluorescent rendering of the developing eye. Additionally, Table 2 displays the volume data from the developing eye at every imaging point. This dataset includes the segment name, id, volume in both µm³ and voxel count, the mean fluorescence intensity of the object, the time point the object was identified, and the object's surface area in μm^2. It is important to note that when the eye field separates into two optic vesicles (starting at Timepoint 64), there remains a third region that is Rx3:GFP positive in the forebrain which will contribute to the hypothalamus (Cavodeassi et al., 2013; Muthu et al., 2016; Rojas-Muñoz et al., 2005) (Fig. 5D-M). This shows up in the volume data represented in Table 2 (highlighted in yellow starting at Timepoint 71) and can easily be separated out from the optic vesicles, since it is much smaller in volume than either optic vesicle.
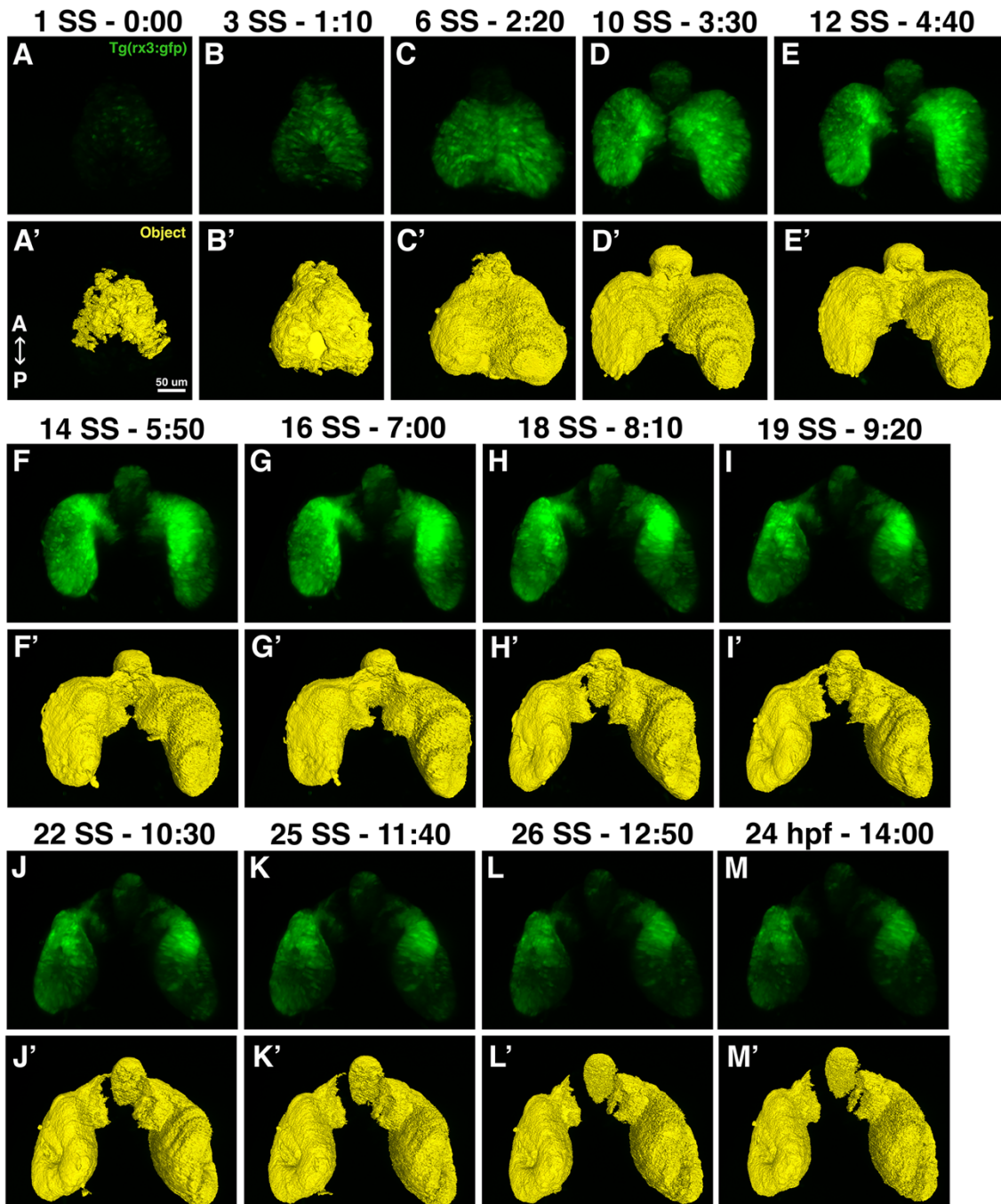
Figure 2.5 High-resolution images and eye field masks.

(A–M) A set of high-resolution images that were rendered from the dorsal vantage points, (A'–M') the eye field masks for each corresponding timepoint. Each image set is notated by the time it was acquired from the start of imaging and the corresponding developmental stage in either somite stage (ss) or hours post fertilization (hpf).

Video 2.1 Time-lapse video of Tg(rx3:GFP) zebrafish embryo from the 1ss – 24hpf.

Video 2.2 Time-lapse video of Tg(rx3:GFP) zebrafish embryo from the 1ss – 24hpf with the eyefield as identified by the arivis Vision4D pipeline.

Video 2.3 360° rotation of a Tg(rx3:GFP) zebrafish embryo at 1ss.

Video 2.4 360° rotation of a Tg(rx3:GFP) zebrafish embryo eye field mask at 1ss.

Video 2.5 360° rotation of a Tg(rx3:GFP) zebrafish embryo at 24hpf.

Video 2.6 360° rotation of a Tg(rx3:GFP) zebrafish embryo eye field mask at 24hpf.

Table 2.1 arivis Vision4D pipeline for volume analysis of the developing eye field.

Input ROI	Sets boundaries of the data set that will be included in the analysis.
Denoising Filter	Removes some autofluorescence or "noise" from data set.
Intensity Filter	Sets the min/max of what fluorescent signal is "real"
Segment Filter	Excludes objects that are not part of the eyefield based on object volume.
Export Objects Feature	Where to export the "object" information and in what format.
Store Objects	Which data to include in and save in "object" export.

Table 2.2 Volume and surface area of the developing eye field acquired by arivis Vision4D.
The rows pertaining to the presumptive hypothalamus are highlighted in yellow to distinguish them from the optic vesicles.

Table 2.3 Materials required for the protocol.

Name	Company	Catalog Number
60mL Syringe Luer-Lok Tip	BD	309653
Agarose, Low Melting Temperature	Promega	V2111
arivis Vision4D Software	arivis	https://www.arivis.com/en/imaging-science/arivis-vision4d
Dumoxel N3C Forceps	Dumont	0203-N3C-PO
E3 fish buffer (5 mM NaCl, 0.17 mM KCl, 0.33 mM CaCl$_2$, 0.33 mM MgSO$_4$)		
Glass Capillary – Size 2 (~1mm)	Zeiss	Black/701904
Heidelberger Extension Line 100cm	B. Braun	4097262
Light & Filter Set – Royal Blue	Night Sea	SFA-LFS-RB
Petri Dish (100 x 15 mm)	VWR	25384-302
Stereomicroscope Fluorescence Adapter	NightSea	
Teflon Tipped Plunger – Size 2	Zeiss	#701997
Tg(rx3:GFP) zebrafish		This line was established by Rembold et al.[13]
Tricaine (MS222)	Sigma	A-5040

Table 2.3 Continued.

Z.1 Lightsheet	Zeiss	
Zen Software	Zeiss	https://www.zeiss.com/microscopy/us/products/microscope-software/zen.html

2.5   Discussion

In this protocol, the Lightsheet microscope was used to perform time-lapse imaging of eye development and the resulting data were analyzed. The resulting dataset can provide valuable insights into the process of ocular morphogenesis, as well as perturbations to this process as a result of genetic mutation, exposure to pharmacological agents, or other experimental parameters. Here the protocol demonstrated how this dataset can be obtained and provided an example of how to analyze the volume of the eye field through early development. These data were found to be reproducible and consistent (less than 10% variation in volume) across biological replicates, bearing in mind that slight differences in embryo staging prior to the start of the run can lead to some variation in final volume measurements.

Care should be taken in the initial positioning of the embryo in the capillary and in positioning the embedded embryo in front of the objective. Orientation plays an important role in preventing the embryo from growing and moving out of the view of the objective. The embryos have a round shape at 10 hpf which makes it challenging to guarantee a specific orientation in the capillary. Ideally, the body of the embryo will be positioned laterally in the capillary. Loading multiple embryos in the capillary will increase the likelihood of having a well-positioned embryo.

In this procedure, the embryo is embedded in agarose in order to suspend it in front of the imaging and illumination objectives. Choosing the correct

concentration of the low melting temperature agarose is critical. Too high of a concentration will constrict the embryo and prevent it from properly developing; too low of a concentration will result in the agarose falling apart and not holding the embryo. The concentration optimal for this protocol is a final concentration of 1% low melting temperature agarose (Keller et al., 2008, 2010).

Another element that should be taken into consideration is the level of saturation. As the eyefield grows and differentiates, the strength of the Rx3:GFP signal intensifies. Therefore, when setting the initial imaging parameters, the exposure and laser power should be reduced to undersaturate the image. This will prevent the image from becoming oversaturated as the Rx3:GFP gets brighter over time. Modifications can be made to correct for undersaturation in image processing, but oversaturation cannot be corrected after the images have been acquired.

There are a few additional modifications that can be made to this protocol that may be advantageous to some projects that are not described in this paper. For example, it is possible to set up Multiview imaging in the image acquisition set up. This parameter would allow multiple embryos at different positions along the y-axis to be sequentially imaged at each time interval. While adding complexity to the data set, it would increase the rate of data collection. Additionally, in terms of image processing, it is possible to quantify the eye field by other parameters. Here we described how to quantify the data in terms of the eye field volume. Alternatively, a pipeline could be made to quantify and track individual cells or determine the rate of optic vesicle evagination.

As previously mentioned, both confocal and Lightsheet microscopy have been used to perform time-lapse imaging studies of zebrafish. Lightsheet was specifically chosen for this project due to its superior ability to image through a thick (>1 mm) sample, because it is equipped with an incubation unit to maintain an ideal temperature environment for the zebrafish embryo, and because its ability to image at a faster rate than confocal microscopy allows for image acquisition at the numerous time intervals required for this protocol no

accompanying damage or photobleaching of the embryo (Huisken et al., 2004; Icha et al., 2016; Jemielita et al., 2013; Keller et al., 2008, 2010; Keller & Dodt, 2012; Pampaloni et al., 2015; Pantazis & Supatto, 2014; Park et al., 2015; Reynaud et al., 2008; Royer et al., 2016). It is also important to note that the Lightsheet microscope is equipped to image the signal from multiple fluorophores. The Lightsheet microscope used in this study has solid state laser excitation lines at 405, 445, 488, 515, 561, and 638nm, which could be useful for imaging transgenic embryos expressing more than one fluorescent reporter transgene.

While this protocol details instructions for image acquisition analysis specifically using the Lightsheet Z.1 Dual Illumination Microscope System and arivis Vision4D analysis software, there are other commercially available Lightsheet microscopes made by Leica, Olympus, and Luxendo, as well as image analysis software by Imaris, that could be used to achieve similar results. The selection of equipment and software for this protocol was determined by availability at our institution.

In summary, it is anticipated this protocol will provide a solid starting point for conducting time-lapse imaging using Lightsheet microscopy, and for image quantification of early eye development in zebrafish.

2.6   Disclosures

The authors declare no competing financial interests.

2.7   Acknowledgements

CHAPTER 3. THE ROLE OF SOX4 IN OCULAR MORPHOGENESIS AND RETINAL DIFFERENTIATION

Rebecca A. Petersen, Wen Wen, Cameron Reinisch, Sumanth Manohar, Ann C. Morris

Department of Biology, University of Kentucky, Lexington KY 40506

Key words: Sox4, SoxC, zebrafish, eye development, ocular morphogenesis, retina

This chapter includes contributions from Dr. Wen who generated the zebrafish *sox4* genetic mutants, Cameron Reinisch who performed blind cell counts and assisted with statistical analyses, and Dr. Sumanth Manohar who detected *her9* expression by HCR.

3.1   Abstract

The SoxC transcription factors Sox4 and Sox11 have previously been implicated in playing a role in both ocular morphogenesis and retinal development. Sox4 in particular was linked to microphthalmia and/or coloboma in humans, mice, zebrafish, and Xenopus. An additional role for Sox4 in the generation of specific retinal neurons has also been suggested. I show that in zebrafish, *sox4* mutants only show the phenotypes of microphthalmia and a reduction of rod photoreceptors in the absence of both maternal and zygotic *sox4* transcripts. This suggests that Sox4 has a critical role at the earliest stages of eye development that influences later retinal differentiation. However, the precise functions of Sox4 during vertebrate ocular morphogenesis and retinal cell type differentiation remain unclear.

In this chapter, I describe a detailed characterization of the ocular phenotypes of zebrafish *sox4* mutants, and an in-depth analysis into the role Sox4 plays in both ocular morphogenesis and retinal differentiation, using in vivo time lapse imaging, assays to assess cell proliferation and cell death, and immunohistochemistry to detect retinal cell types. Furthermore, I used scRNA-seq to address if cell type heterogeneity exists in the eye field and optic vesicles that could explain the maternal effects of loss of Sox4 on later retinal differentiation.

3.2   Introduction

Visual impairment can greatly impact quality of life. 11% of cases of pediatric blindness are accounted for by microphthalmia, anophthalmia, and coloboma (collectively referred to as MAC). Cases of MAC result from improper ocular morphogenesis (Fahnehjelm et al., 2022). Retinitis Pigmentosa (RP) is a retinal degenerative disease that affects 1 in 3000 people worldwide. It initially begins with loss of rod photoreceptors which manifests as loss of vision in low light settings but eventually progresses to complete blindness (Kalloniatis & Fletcher, 2021; Newton & Megaw, 2020). Currently, there is no cure for either MAC or RP. Further insight into the essential components of ocular morphogenesis and the generation of retinal neurons could provide the base of knowledge needed for better patient screening and treatments like cell therapies.

Ocular morphogenesis initiates vertebrate eye development. In ocular morphogenesis, the anterior neural plate, part of the developing forebrain, gives rise to the neural portion of the eye known as the eyefield (Chow & Lang, 2001; Chuang et al., 1999; Fuhrmann, 2010; Katherine E Brown et al., 2010; Loosli et al., 2003; Rojas-Muñoz et al., 2005; Stigloher et al., 2006). The eyefield evaginates toward the surface ectoderm to form two bilateral optic vesicles (Chow & Lang, 2001; Choy & Cheng, 2012; England et al., 2006; Sampath et al., 1998; Schier & Talbot, 2003; Varga et al., 1999). Upon contact with surface ectoderm, the optic vesicles invaginate to form a bilayered optic cup. The inner

most layer will give rise to the neural retina while the outer layer will give rise to the retinal pigmented epithelium (RPE) (Chow & Lang, 2001; Fuhrmann, 2010; Z. Li et al., 2000; Pillai-Kastoori et al., 2014; S. W. Wilson & Houart, 2004). The anterior structures of the eye form from the surface ectoderm, neuroectoderm, periocular mesenchyme, and periocular neural crest (Chow & Lang, 2001; Cvekl & Tamm, 2004; Sowden, 2007). During the formation of the optic cup, a channel remains open on the ventral side for the choroid vasculature to enter the eye and the optic nerve to exit the eye. This opening is referred to as the choroid fissure, which eventually fuses as retinal development progresses. Failure of choroid fissure closure results in coloboma (Chow & Lang, 2001; Cvekl & Tamm, 2004; Fuhrmann, 2010; James et al., 2016; Pillai-Kastoori et al., 2014).

A fully differentiated retina is comprised of three nuclear layers, two plexiform layers, and the optic nerve (Agathocleous & Harris, 2009; Demb & Singer, 2015; Masland, 2012; Pillai-Kastoori et al., 2014; Weysse & Burgess, 1906). The retina consists of six different cell types: five classes of retinal neurons and one intrinsic glial cell. In the zebrafish, these cells are generated sequentially from a single pool of progenitor cells. The rod photoreceptors are one of the last retinal neurons born (Pillai-Kastoori et al., 2015; Stenkamp, 2007).

The SoxC subfamily is comprised of Sox4, Sox11, and Sox12. All contain a highly conserved HMG domain, and a transactivation domain located near the C-terminus. The HMG domain binds to the minor groove of its target DNA sequence, known as the Sox motif. The transactivation domain is responsible for partnering with other proteins to activate transcription (M. Angelozzi & Lefebvre, 2019; Bowles et al., 2000; Dy et al., 2008; Hoser et al., 2008; Penzo-Méndez, 2010; Stevanovic et al., 2021; Van De Wetering et al., 1993; Wiebe et al., 2003). The transcription factor Sox4 has previously been implicated as an important factor in both ocular morphogenesis and retinal development by studies in mice, zebrafish, and Xenopus (Bhattaram et al., 2010; Cizelsky et al., 2013; Jiang et al., 2013; Usui, Iwagawa, et al., 2013; Usui, Mochizuki, et al., 2013; Wen, 2016; Wen et al., 2015) and is associated with visual impairment in humans (Marco

Angelozzi et al., 2022; Ghaffar et al., 2021; Zawerton et al., 2019). Due to a genome duplication that occurred at the base of the teleost lineage, zebrafish have duplicates of many genes, including *sox4*, resulting in *sox4a* and *sox4b* co-orthologues (Mavropoulos et al., 2005).

In zebrafish, *sox4a* and *sox4b* are expressed in the embryo prior to zygotic genome activation due to the presence of maternally deposited mRNA transcripts (data not shown). Because *sox4a/b* are single exon genes, morpholinos targeting *sox4a/b* were designed to block the translation start site, preventing expression of both zygotic and maternal *sox4* transcripts. In the *sox4* morphants, ocular phenotypes included microphthalmia, coloboma, and a reduction of rod photoreceptors (Wen, 2016; Wen et al., 2015). However, it was not clear whether these phenotypes were due to loss of zygotic or maternal Sox4, or both. To further investigate the function of Sox4 in eye development, germline *sox4a* and *sox4b* mutants were generated using CRISPR-Cas9 genome editing. Characterization of the ocular phenotypes in single and double zygotic and maternal zygotic (MZ) mutants suggests that maternal Sox4 is required for proper eye development, and that Sox4 has a critical role in specification of the early eyefield that influences later retinal differentiation.

3.3 Results

3.3.1 Zebrafish Mutants Were Identified for *sox4a* and *sox4b*

To further explore the role of Sox4 in ocular morphogenesis and retinal differentiation, zebrafish mutants were generated using CRISPR/Cas9 genome editing. Two single strand guide RNAs (sgRNA) were designed for each co-orthologue of Sox4, targeting before and after the HMG domain. Both sgRNAs were injected with Cas9 mRNA to generate a large deletion in both *sox4a* and *sox4b.* Founder fish were identified for mutations in both *sox4a* and *sox4b.* The *sox4a* mutation consisted of a 427bp deletion and a 297bp inversion. The predicted protein would be 68 amino acids long with only the first 5 sharing homology to wildtype Sox4a*,* which consists of 363 amino acids*.* The *sox4b*

mutation consisted of a 407bp deletion. The predicted protein would be 128 amino acids long with only the first 51 sharing homology to wildtype Sox4b, which consists of 342 amino acids (Fig. 3.1) (Wen, 2016). qPCR was performed to detect the mutant copy of *sox4* in each mutant. This revealed a 9-fold downregulation of *sox4a* expression in *sox4a* mutants, and a 5-fold downregulation of *sox4b* expression in *sox4b* mutants (Fig. 3.5), indicating that both mutant transcripts are subject to nonsense-mediated decay.
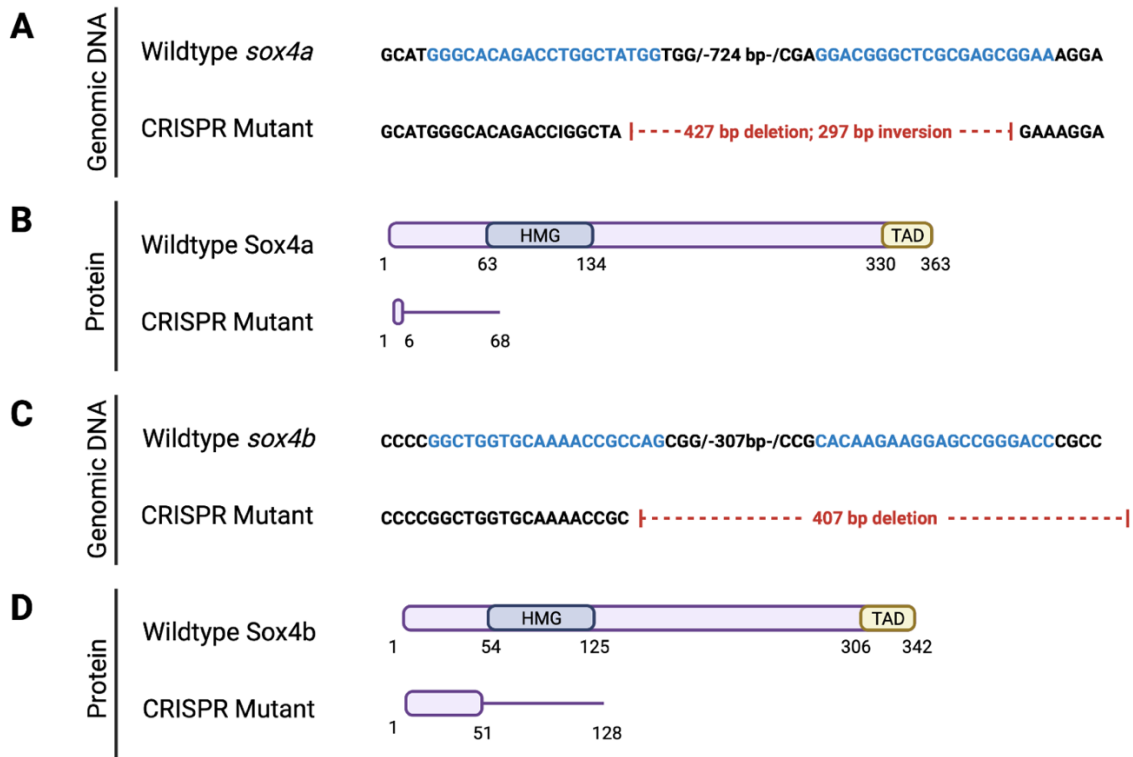
Figure 3.1 CRISPR mutagenesis produces large deletions in *sox4a* and *sox4b*.

(A) *sox4a* mutant genomic DNA sequence. (C) *sox4b* mutant genomic DNA sequence.) and their predicted proteins (B) Sox4a mutant gDNA sequence. (D) Sox4b mutant gDNA sequence.) to Wildtype. (A & C) CRISPR target sites are notated on the wildtype strand in blue (Wen, 2016).

3.3.2 *Sox4* maternal zygotic (MZ) Mutants Display Microphthalmia

The *sox4* mutants were initially characterized using stereo microscopy to visualize general morphology. *Sox4a -/-*, *sox4b -/-*, and *sox4ab -/-* embryos from *sox4ab +/-* incrosses displayed no detectable phenotype (Figure 3.2). During oogenesis, some maternal mRNAs are deposited into the egg to initiate development upon fertilization until the embryo undergoes the maternal-to-zygotic transition and is able to start making transcripts of its own during the mid-blastula transition (MBT) (Aanes et al., 2011; Newport & Kirschner, 1982; Yasuda & Schubiger, 1992). *sox4* is one of these maternally expressed transcripts (data not shown). To remove the maternal contribution of *sox4*, homozygous *sox4* mutants were incrossed with one another to generate maternal zygotic (MZ) homozygous mutants. The *sox4a* MZ, *sox4b* MZ, and *sox4ab* MZ mutants were characterized using stereo microscopy (Fig. 3.3). 27.7% of *sox4a* MZ, 38.5% of *sox4b* MZ, and 100% of *sox4ab* MZ embryos displayed microphthalmia. To quantify the microphthalmia, the area of the eye was measured and then normalized to the length of the embryo to account for any eye size differences that may be due to an overall reduction in body size. The *sox4a* MZ had a 18%, *sox4b* MZ had a 12%, and *sox4ab* MZ mutants had a 13% average reduction in normalized eye size at 48 hpf and the *sox4a* MZ had a 15%, *sox4b* MZ had a 20%, and *sox4ab* MZ mutants had a 25% average reduction in normalized eye size at 72 hpf (Fig. 3.3 D-D'). The mutants also displayed delayed closure of the choroid fissure. 35% of *sox4a* MZ, 40% of *sox4b* MZ, and 43% of *sox4ab* MZ mutants had delayed choroid fissure closure at 48 hpf; however, choroid fissure closure did occur by 72 hpf across all mutant genotypes. Another phenotype that was observed in the Sox4 MZ mutants was opacity of the developing brain at 24 hpf, which was detected in 4% of *sox4a* MZ, 9% of *sox4b* MZ, and 18% of *sox4ab* MZ embryos; brain opacity suggests that those cells may be undergoing apoptosis. An acridine orange staining, which labels apoptotic cells, confirmed that a similar percentage of embryos had an increase in apoptosis in the brain region at 24 hpf (Fig. 3.4). These results suggest that loss of maternal and

zygotic Sox4 results in microphthalmia, delayed fusion of the choroid fissure, and increased cell death in the head.
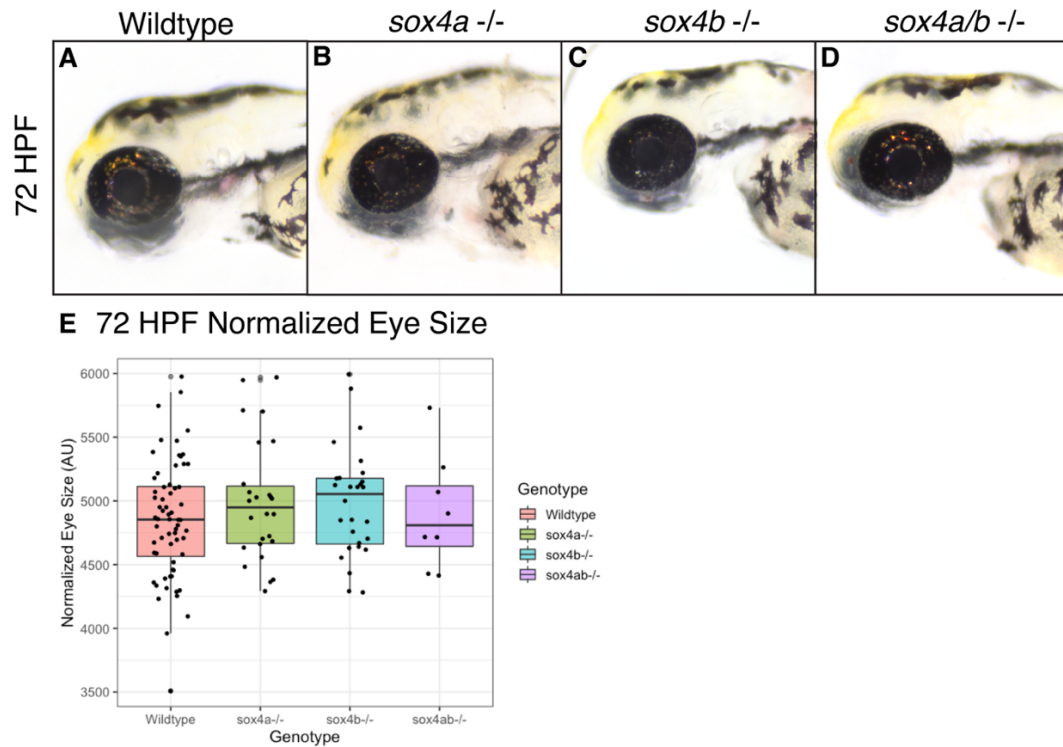
Figure 3.2 Zygotic *sox4* mutants have no discernible ocular phenotypes.

(A-D) 72 hpf zebrafish (A) WT (B) *sox4a* -/- mutant (C) *sox4b* -/- mutant (D) *sox4ab* -/- mutant (E) Boxplot of normalized eye size.
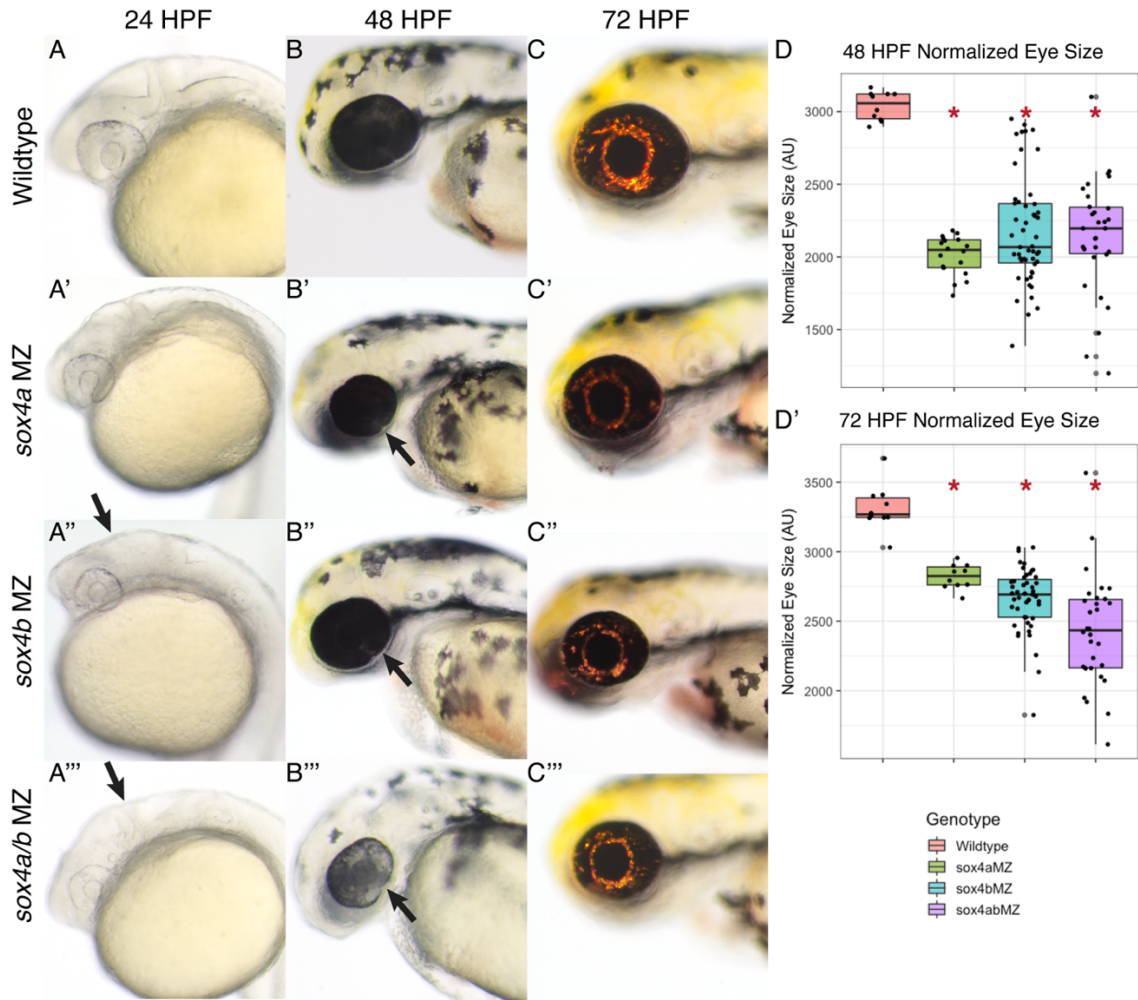
Figure 3.3 Maternal zygotic *sox4* mutants display microphthalmia, delayed choroid fissure closure, and opaque brains.

(A) 24, (B) 48, and (C)72 hpf *sox4* maternal zygotic (MZ) mutants. (A-C) WT, (A'-C') *sox4a* MZ, (A"-C") *sox4b* MZ, (A"'-C"') *sox4ab* MZ. (A"-A"') Arrow points to cloudy brain. (B'-B"') Arrow points to unclosed choroid fissure. (D) Boxplot of normalized eye size at 48 hpf. (D') Boxplot of normalized eye size at 72 hpf. Significance at p ≤ 0.05 notated with *.
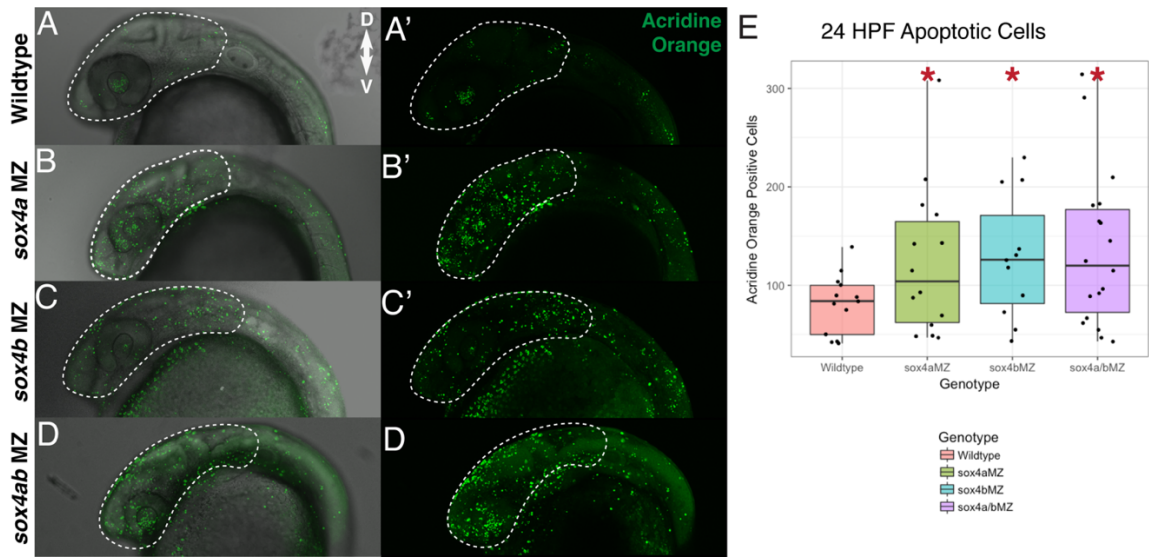
Figure 3.4 Maternal zygotic *sox4* mutants have increased apoptosis in the head.

Acridine orange stain of 24 hpf *sox4* MZ mutants (A) WT (B) *sox4a* -/- mutant (C) *sox4b* -/- mutant (D) *sox4ab* -/- mutant (E) Boxplot of acridine positive cells, counted in the head between the anterior edge of the nose to the anterior edge of the otic placode. Significance at $p \leq 0.05$ notated with *.

3.3.3 Loss of Sox4 Leads to Transcriptional Adaptation

In previous studies, *sox4* morphants were shown to have microphthalmia and ocular coloboma (Wen et al., 2015). In contrast, the *sox4* MZ mutants display microphthalmia but do not have ocular coloboma. This phenomenon of less severe phenotypes in mutants vs. morphants has been observed in numerous zebrafish studies and may be due to non-sense mediated decay of the mutant transcript triggering transcriptional adaptation by other related genes (El-Brolosy et al., 2018; Rossi et al., 2015). The SoxC family members share a high degree of sequence homology and partially overlapping function (Dy et al., 2008; Hoser et al., 2008; Penzo-Méndez, 2010; Van De Wetering et al., 1993; Wiebe et al., 2003). Sox11 mRNA was able to partially rescue the *sox4* morphant phenotype (Wen 2015) indicating that compensation could be a possible explanation for the reduced penetrance and severity of the *sox4* MZ mutant

phenotype. To assess potential compensation from other SoxC members, qPCR was performed to compare transcript levels of *sox4a*, *sox4b*, *sox11a*, and *sox11b* in wild type and *sox4* MZ mutant embryos at 48 hpf. In the *sox4a* MZ mutants, *sox4b* is upregulated by 2.7-fold; in the *sox4b* MZ mutants, *sox11b* is upregulated by 2.6-fold; and in the *sox4ab* MZ mutants, *sox11b* is upregulated by 2-fold (Fig. 3.5). Taken together, these results suggest upregulation of other SoxC members may compensate for the loss of *sox4* through transcriptional adaptation.

An alternative explanation for the discrepancy between the more severe phenotypes observed in previous *sox4* morpholino studies and the milder *sox4a/b* MZ mutant phenotypes is that the morphant phenotypes were due to off-target effects. To test this hypothesis, the *sox4a* morpholino was microinjected into the *sox4a* mutant, and similarly the *sox4b* morpholino was microinjected into *sox4b* mutant. If the morpholinos had off-target effects, this should result in a more severe phenotype in the *sox4* mutants. However, no exacerbation of the mutant phenotype was observed (data not shown). This result indicates that the less severe phenotype in *sox4a/b* MZ mutants is due to transcriptional adaptation in the mutants and not off-target effects from the morpholino.
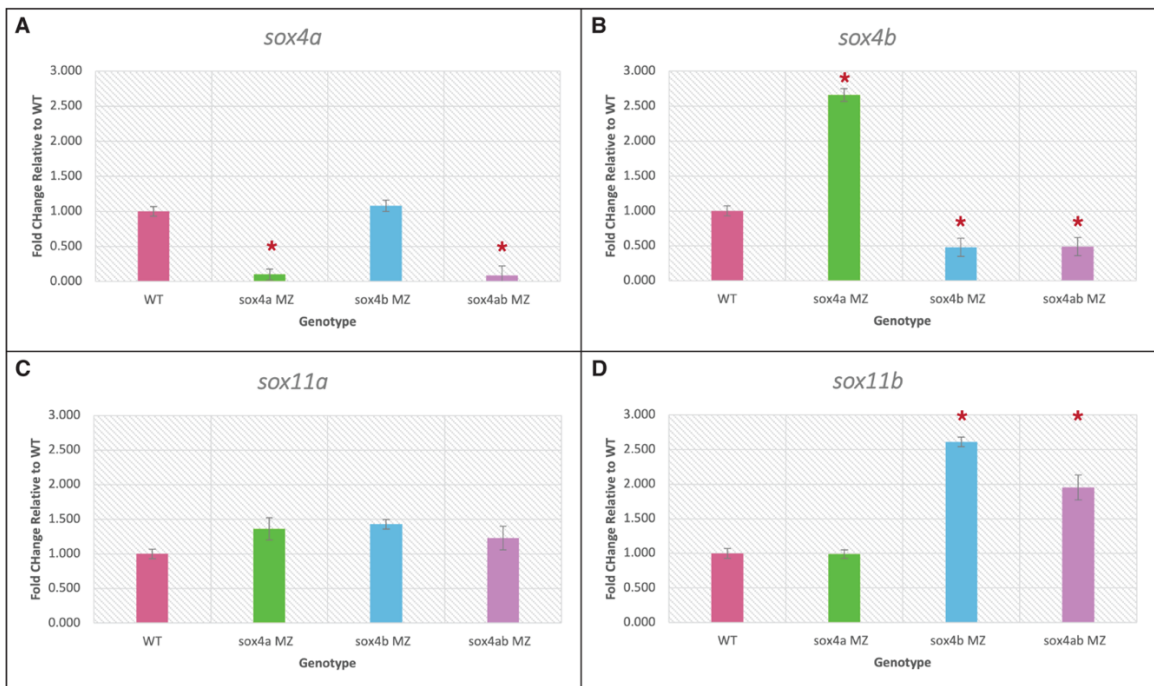
Figure 3.5 Maternal zygotic *sox4* mutants display upregulation of other *soxC* family members.

qPCR of soxC transcription factors in 48 hpf *sox4* MZ mutants (A) *sox4a* expression (B) *sox4b* expression (C) *sox11a* expression (D) *sox11b* expression. Significance at p ≤ 0.05 notated with *.

3.3.4   Eyefield Volume is Reduced in Maternal Zygotic *sox4* Mutants

To get a clearer image of why the *sox4* MZ mutants have microphthalmia, the mutants were crossed onto the RX3:eGFP transgenic background, which expresses GFP in cells specified to become the eyefield and continues to express GFP in the optic vesicle and optic cup. Wildtype and *sox4* MZ mutant, RX3:eGFP positive embryos were collected at the following timepoints: 1 somite stage (ss) (10 hpf), 6ss (12 hpf), 10 ss (14 hpf), 15 ss (16 hpf), and 18 ss (18 hpf); the GFP+ cells were imaged in whole fixed embryos using lightsheet microscopy. When comparing wildtype and mutant embryos, imaging revealed that *sox4* MZ mutants have a reduction of the eyefield volume starting at 1 ss. This reduction persists through 18 ss. The phenotype is both increased in penetrance and severity in the *sox4a/b* MZ mutants compared to the induvial *sox4a* MZ and *sox4b* MZ mutants (Fig. 3.6 A-E""). This reduction in volume remains steady over time (Fig. 3.6 G). Additionally, the expression of the RX3:eGFP transgene is also reduced, suggesting that *rx3* expression is downregulated in the *sox4* MZ mutants (Fig. 3.6 A-D"",F-F"""). Live imaging was performed on wildtype and *sox4b* MZ mutants from 10 to 18 hpf (Videos 2.1, 3.1) and no difference was noted between the timing of the separation between the optic vesicles and pre-thalamus (Fig. 3.6 G'). Taken together, these results suggest that the microphthalmia observed in *sox4* MZ mutants is a consequence of fewer cells in the eyefield and not delayed or altered cell migration during ocular morphogenesis.
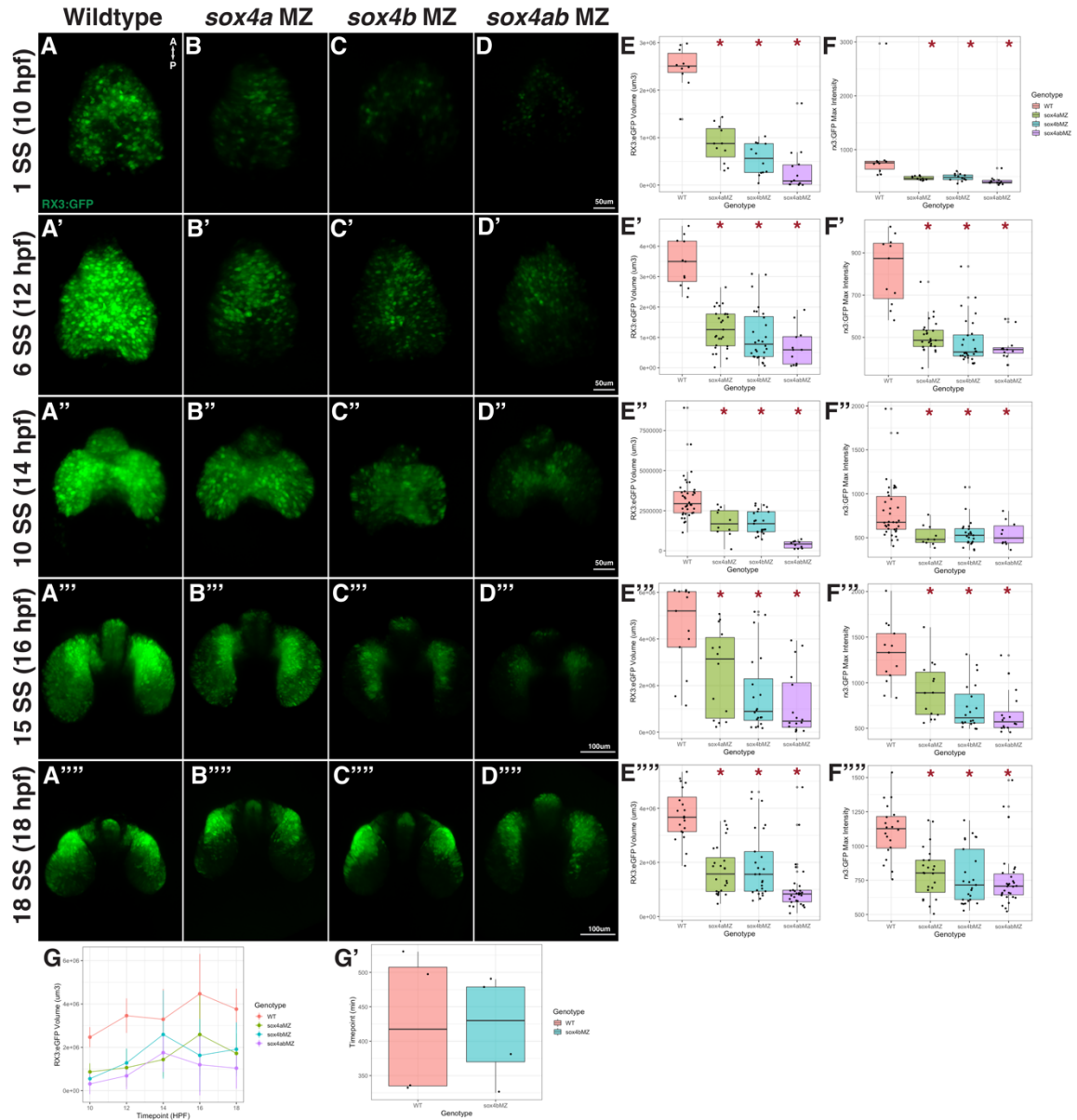
Figure 3.6 Eyefield is reduced in maternal zygotic *sox4* mutants starting at 10 HPF.

RX3:eGPF positive *sox4* MZ mutants (A-A"") WT, (B-B"") *sox4a* MZ mutant, (C-C"") *sox4b* MZ mutant, (D-D"") *sox4ab* MZ mutant, (E-E"") Boxplot of the volume of RX3:eGFP cells, (F-F"") Boxplot of the max intensity of RX3:eGFP expression. (A-E) 1 SS (10 HPF), (A'-E') 6 SS (12 HPF), (A"-E") 10 SS (14 HPF), (A'"-E'") 15 SS (16 HPF), (A""-E"") 18 SS (18 HPF). (G) Line graph of the change of the volume of RX3:eGFP cells at each timepoint by genotype. (G') Boxplot of the time of separation between the optic vesicles and prethalamus during live image analysis. Significance at p ≤ 0.05 notated with *.

3.3.5 Reduced Eyefield in the Maternal Zygotic *sox4* Mutants is Not Due to Changes in Apoptosis or Cellular Proliferation

Why are *sox4* MZ mutant eye fields abnormally small? One possibility is that the eyefield cells could be undergoing apoptosis. Another possibility is that *sox4* MZ mutant retinal progenitor cells (RPCs) do not proliferate at the normal rate. Alternatively, it is possible that fewer cells become specified to the eye field at the earliest stages of regionalization of the forebrain. To investigate these possibilities, TUNEL labeling was performed on RX3:eGFP positive embryos at the 1 ss; no apoptotic cells were detected in the eyefield at this stage in either wild type or mutant embryos (Fig. 3.7 A-E). Cell proliferation was observed by collecting 1 ss RX3:eGFP positive embryos and performing IHC for the mitosis marker PH3+; again, no significant difference was detected in the number of proliferating cells in the eyefield between wild type and *sox4* MZ mutant embryos (Fig. 3.7 A'-E'). This suggests that the differences in eye size are likely due to fewer cells being specified to become the eyefield.
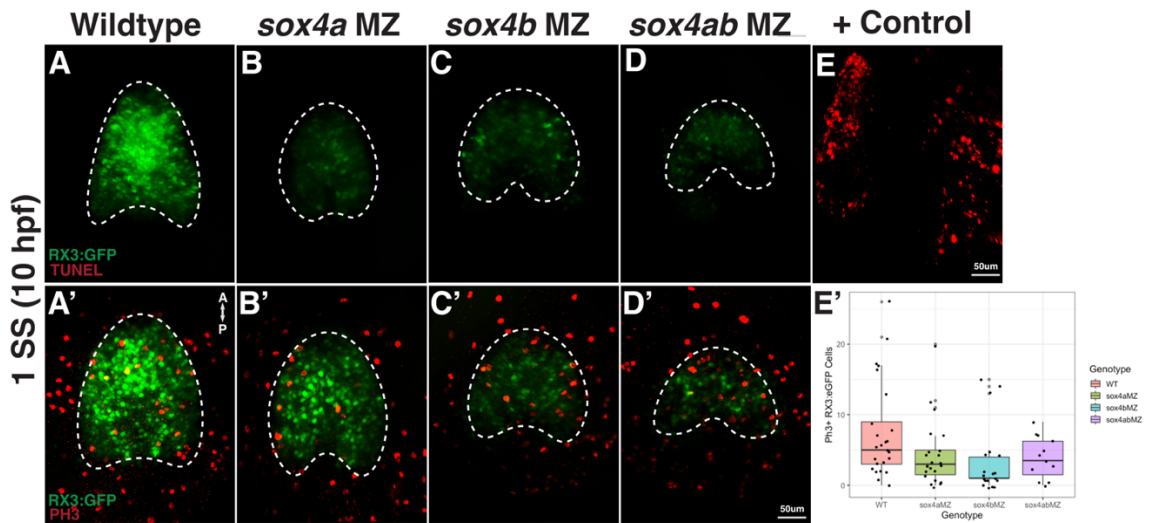
Figure 3.7 No significant difference in apoptosis and cell proliferation in maternal zygotic *sox4* mutant eyefields.

(A-E) TUNEL stain for apoptosis, (A'-D') PH3 IHC for proliferating cells. (A-A') WT, (B-B') *sox4a* -/- mutant, (C-C') *sox4b* -/- mutant (D-D') *sox4ab* -/- mutant, (E) TUNEL positive control. (E') Boxplot of PH3 and RX3:eGFP positive cells. No significant differences were observed between genotypes.

3.3.6 *sox4* MZ Mutants Have a Reduction in Rod Photoreceptors

The *sox4* MZ mutants show defects in ocular morphogenesis, but is retinal differentiation affected? Immunohistochemistry was performed on retinal sections at 5 dpf with antibodies that recognize the different retinal cell types. Since the *sox4* MZ mutants have microphthalmia, all cell counts were normalized to the perimeter of the retina to account for differences in eye size. No significant differences were observed in the density of any retinal cell type, with the exception of a reduction in rod photoreceptors in all *sox4* MZ mutants and a modest reduction of retinal ganglion cells in the *sox4b* MZ mutants (Fig. 3.8 A, A", G and 3.10). The reduction of rod photoreceptors is specific to the MZ mutants and was not present in the zygotic mutants (Fig. 3.9). This result aligns with data from the *sox4* morphants, which also showed a reduction of rod photoreceptors but not in other retinal neurons (Wen 2016). This reduction of rod photoreceptors in the *sox4* MZ mutants persisted through development, and remained significant at 3, 5, 7, and 14 dpf (Fig. 3.10 A-D"'). While rod density initially seemed to start catching up at 5 dpf in the *sox4* mutants, it failed to increase at the same rate as the wildtype retinas and *sox4ab* MZ rod density remained 31% less than wild type at 14 dpf (Fig. 3.10 H). Moreover, the rods that were produced in mutant retinas had a "wispy" appearance compared to their wildtype counterparts due to being significantly smaller in size (Fig. 3.10 F-F', G-G'). After differentiation, rod photoreceptors still need to mature prior to being able to contribute to the visual abilities of the retina. Maturation of the rod photoreceptors is complete in zebrafish larvae by 20 dpf when their outer segments reach their full adult length (Branchek & Bremiller, 1984). At 14 dpf, in addition to a reduction in the density of rod photoreceptors in the retina, the rod photoreceptors that were present appeared to be less mature due to the shortened and wispy morphology at this timepoint (Fig. 3.10 A"'-D"').
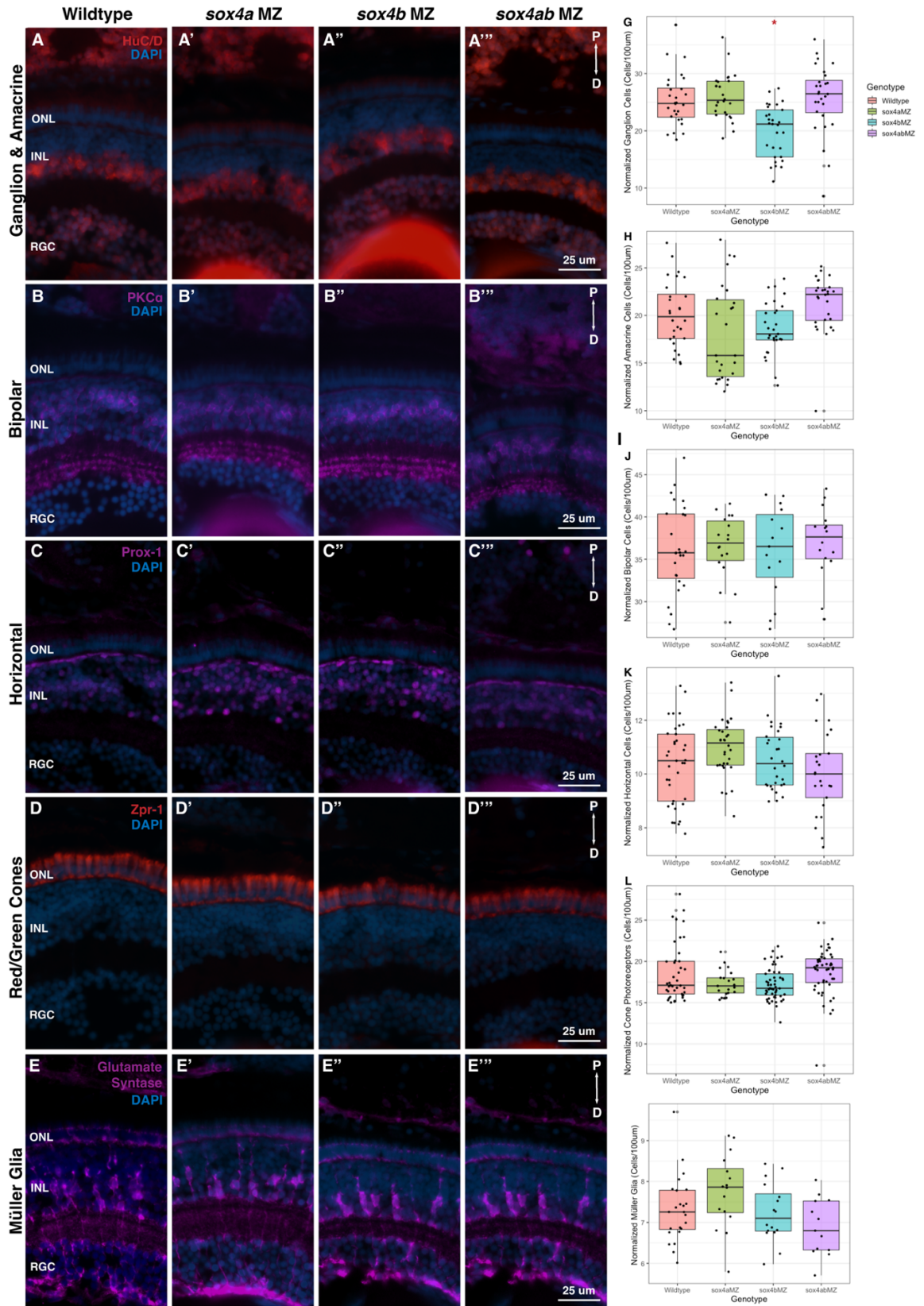
Figure 3.8 Maternal zygotic *sox4* mutants display no difference in the majority of retinal neurons.

Retinal cell type in 5 dpf *sox4* MZ mutants (A) WT (B) *sox4a* MZ mutant (C) *sox4b* MZ mutant (D) *sox4ab* MZ mutant (E) Boxplots of retinal cell counts normalized to retina size. Significance at p ≤ 0.05 notated with *.

The reduction of rod photoreceptors in *sox4* MZ mutants could be explained by lack of rod progenitors due to lower RPC proliferation, apoptosis of rods or their progenitors, or a delay or arrest of terminal differentiation in rods. A TUNEL assay revealed no differences in apoptosis in the differentiating retina at 48 or 72 hpf in the *sox4* MZ mutants (Fig. 3.11). This suggests that the reduction of rod photoreceptors is not due to the rod photoreceptors or their progenitors dying. Cell proliferation was assessed by EdU staining and PH3 IHC at 72 hpf. There was a significant reduction in EdU-positive cells the CMZ, but the reduction in PH3 positive cells did not meet the threshold for significance (Fig. 3.12). PH3 labels cells only in late G2/M phase whereas EdU labels cells in S phase (Flomerfelt & Gress, 2016; Kim et al., 2017). This suggests that fewer cells are entering the cell cycle at 72 hpf. However, rod photoreceptors are not derived from the CMZ but from proliferating progenitors in the ONL. To fully assess whether differences in proliferation are contributing the reduction of rod photoreceptors, this experiment needs to be repeated at 48 hpf. Data from *sox4* morphants showed no reduction in the number of *nr2e3* positive rod progenitors through fluorescent *in situ* hybridization, suggesting the reduction in rod photoreceptors in the morphants is not due to problems with cell fate specification (Wen, 2016). Although this experiment needs to be repeated for the *sox4* mutants, taken together these results suggest that the reduced number of rods in upon loss of Sox4 is not due to changes in cell death, cell proliferation, or lineage specification, but rather to effects on their terminal differentiation.
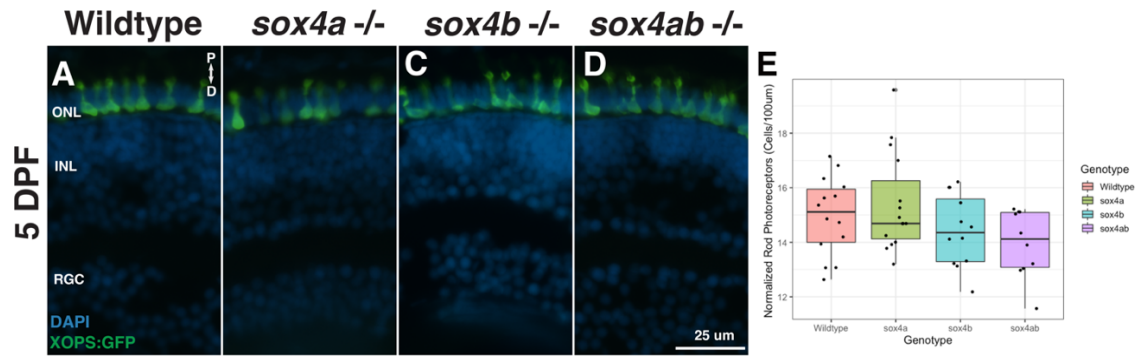
Figure 3.9 Zygotic *sox4* mutants have no discernible change in rod photoreceptors.

Rod photoreceptors in *sox4* zygotic mutants (A) WT (B) *sox4a* -/- mutant (C) *sox4b* -/- mutant (D) *sox4ab* -/- mutant (E) Boxplot of rod photoreceptor counts normalized to retina size.

Wildtype   *sox4a* MZ   *sox4b* MZ   *sox4ab* MZ

3 DPF

ONL
INL
RGC

DAPI
XOPS:GFP

25 um

5 DPF

25 um

7 DPF

25 um

14 DPF

50 um

Wildtype   ***sox4ab* MZ**

5 DPF

XOPS:GFP

0   µm   75

67
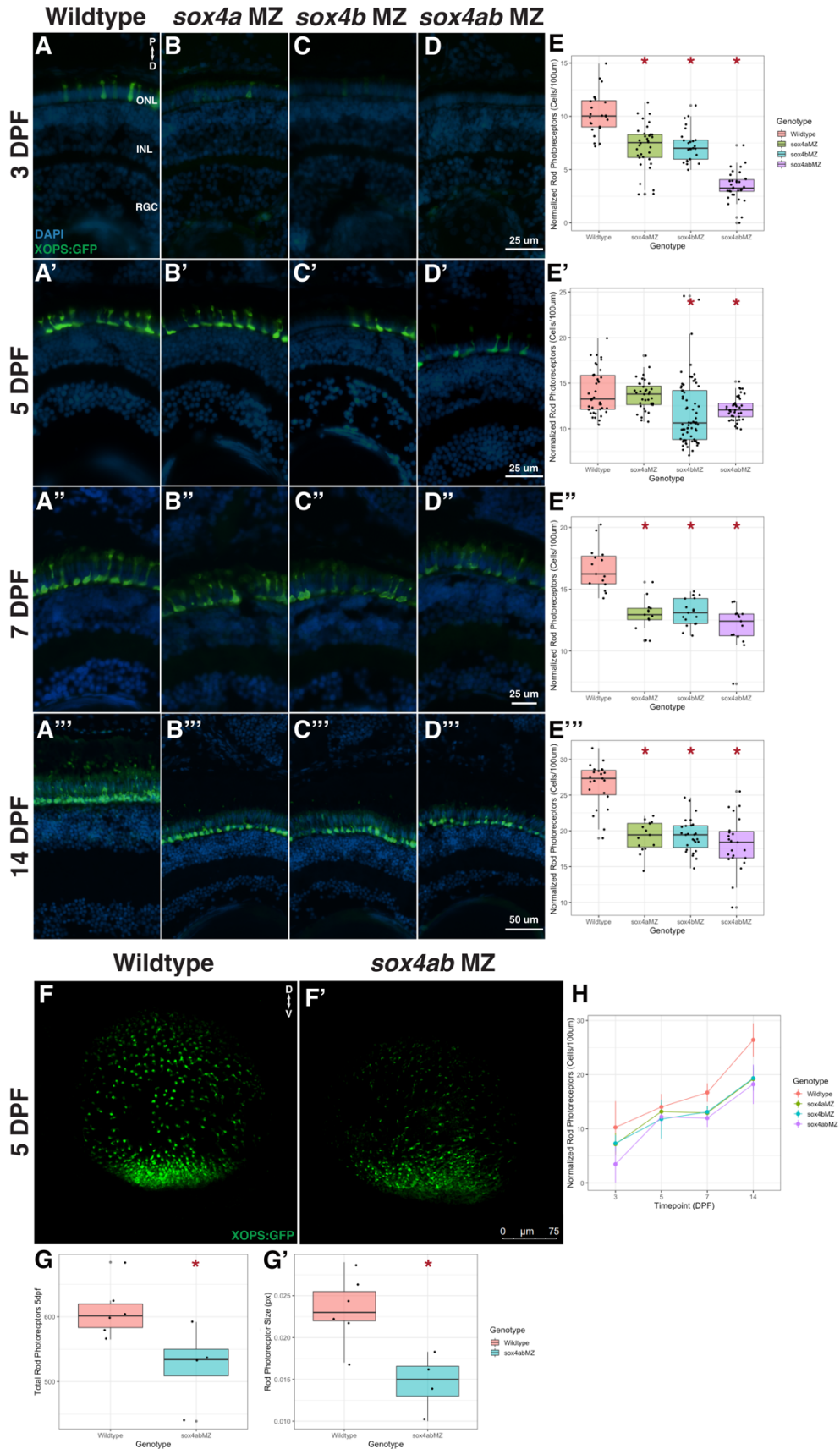
Figure 3.10 Maternal zygotic *sox4* mutants have a notable reduction of rod photoreceptors

Rod photoreceptors are reduced in *sox4* MZ mutants (A-A''', F) Wildtype (B-B''') *sox4a* MZ mutant (C-C''') *sox4b* MZ mutant (D-D''', F') *sox4ab* MZ mutant. (A-D) 3 dpf retinas (A-D) 5 dpf retinas (A-D) 7 dpf retinas (A-D) 14 dpf retinas. (E-E''') Boxplots of rod photoreceptor counts normalized to retina size. (F-F') 5 dpf retina whole mounts. (G) Boxplot of rod photoreceptor counts from retina whole mounts.(G) Boxplot of rod photoreceptor average size from retina whole mounts. (H) Line graph of the change of the rod photoreceptors per 100 mm at each timepoint by genotype. Significance at p ≤ 0.05 notated with *.
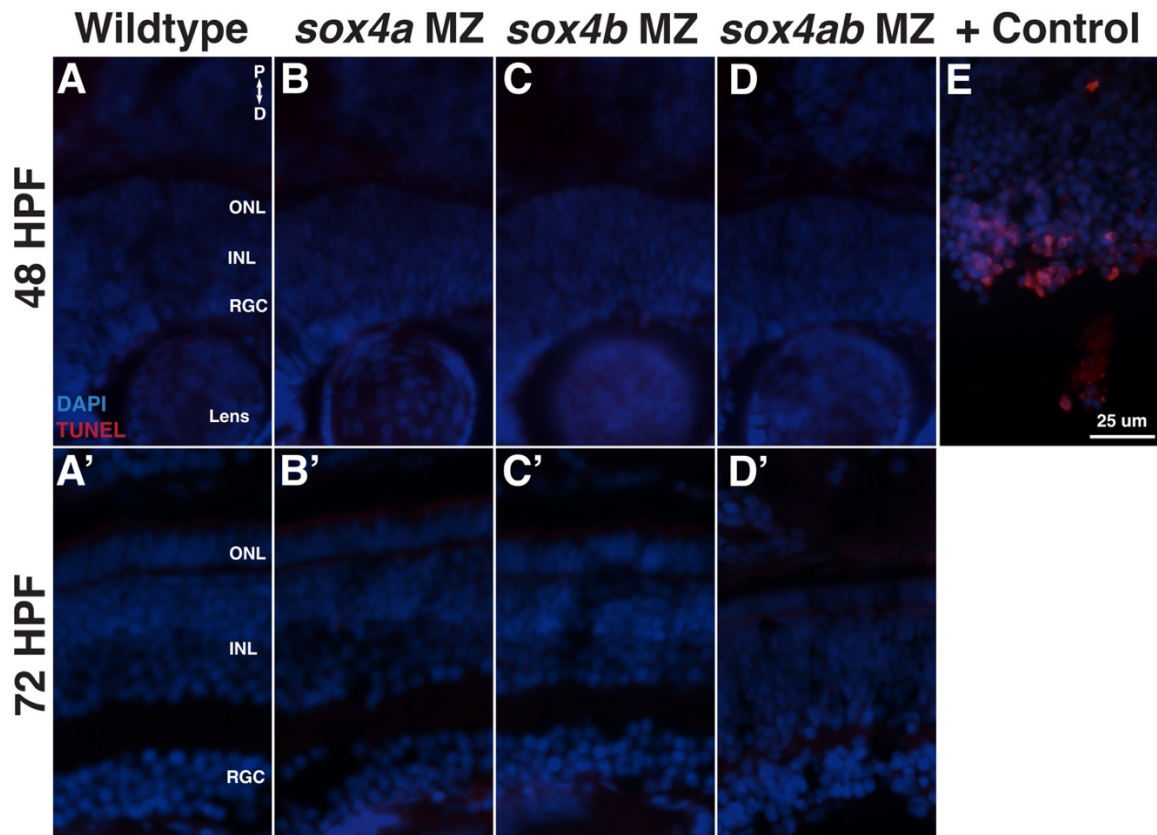
Figure 3.11 Maternal zygotic *sox4* mutants display no apparent difference in levels of apoptosis in the retina.

Apoptosis in 48 and 72 hpf *sox4* MZ mutant retinas (A-D) 48 hpf (A'-D') 72 hpf (A-A') WT (B-B') *sox4a* MZ mutant (C-C') *sox4b* MZ mutant (D-D') *sox4ab* MZ mutant. (E) TUNEL positive control.
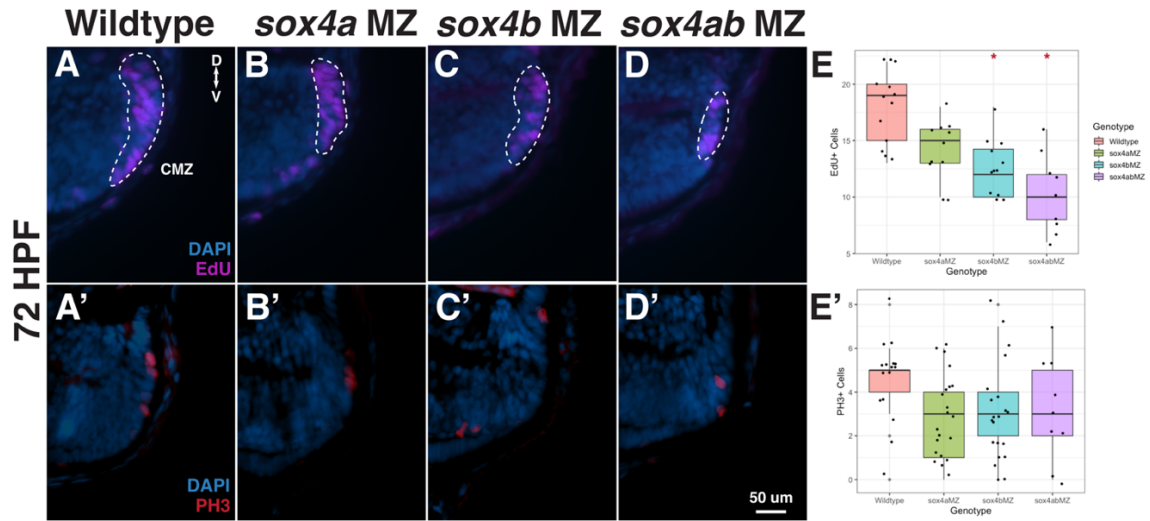
Figure 3.12 Maternal zygotic *sox4* mutants have a smaller CMZ at 72 hpf.

Cell Proliferation in 72 hpf *sox4* MZ mutant retinas. (A-D) EdU stain, (A'-D') PH3 IHC. (A-A') WT (B-B') *sox4a* MZ mutant (C-C') *sox4b* MZ mutant (D-D') *sox4ab* MZ mutant. (E) Boxplot of EdU positive cells (E') Boxplot of PH3 positive cells. Significance at $p \leq 0.05$ notated with *.

3.3.7 Cell heterogeneity can be detected in the early eye field by scRNA-Seq

This interesting phenotype of reduced rod photoreceptors is present in the *sox4* MZ mutants but not in the *sox4* zygotic mutants. This indicates that the lack of maternal *sox4* is influencing specific cell type differentiation later in retinal development. Differences in the developing eye are apparent as early as the eyefield stage in the *sox4* MZ mutants. Therefore, it is possible that loss of Sox4 at the eyefield stage influences development of rod photoreceptors later in development by altering RPC specification or some intrinsic neurogenic timer in the eyefield RPC population. For this to be the case, the RPCs of the eyefield must be more transcriptomically distinct than has been previously appreciated. Some previous lineage tracing studies in Xenopus have suggested that the eyefield is in fact a heterogeneous population of cells. The expression patterns of transcription factors like *rx1, pax6*, *six3*, and *otx2* are known to partially overlap but also be expressed in distinct regions of the eyefield (Zaghloul & Moody, 2007). Individual loss of signaling of *rx1* or *pax6,* starting in the eyefield

69

stage rather than later in ocular morphogenesis leads to the alteration of specific cell fates in retinal development (Zaghloul & Moody, 2007). This suggests that there are different populations within the developing eyefield that are already skewed towards a particular neuronal fate. With the advent of single cell transcriptomics, this hypothesis can now be tested.
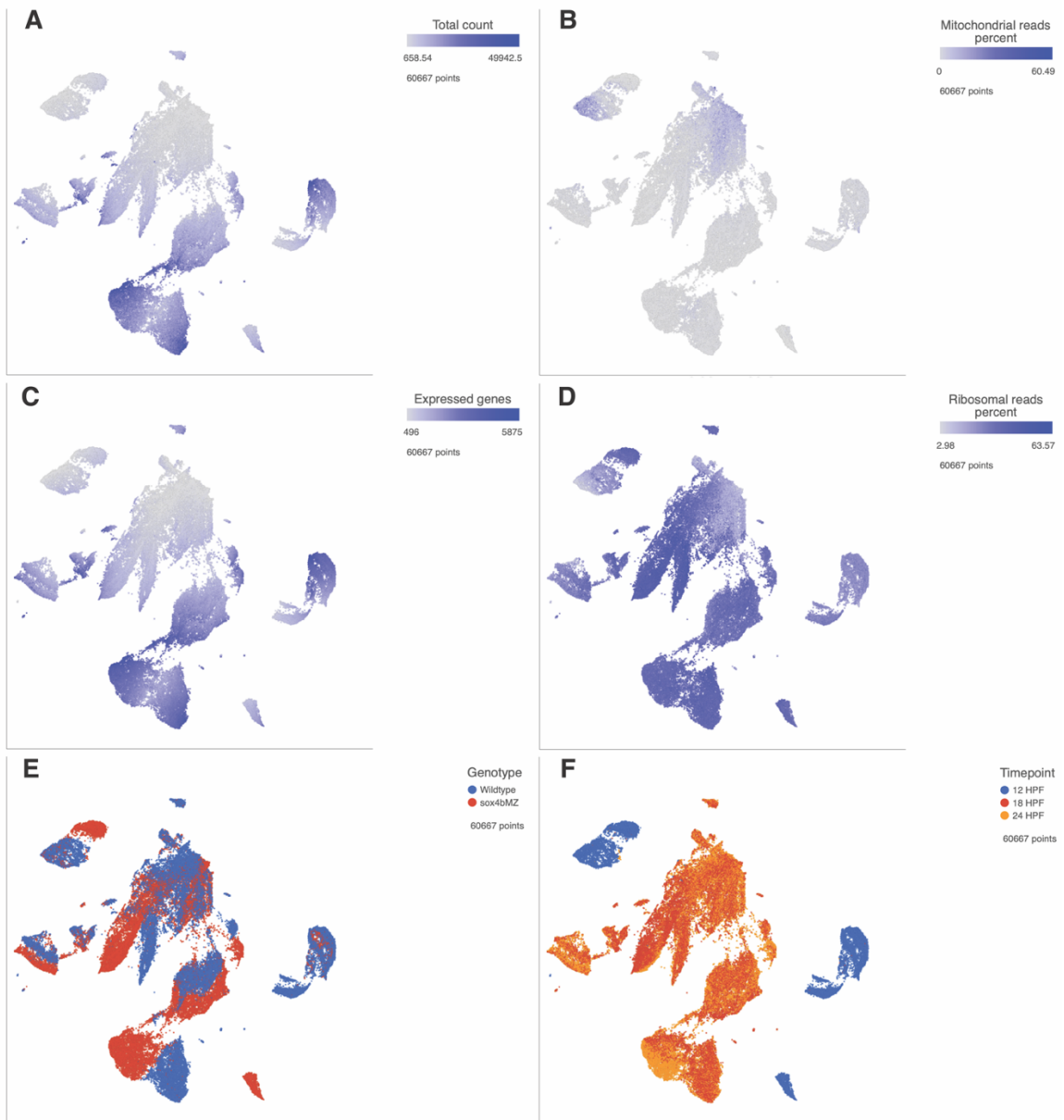
Figure 3.13 Assessment of scRNA-seq parameters for quality control.

(A-F) UMAP of FACS sorted GFP positive cells from wildtype and *sox4b* MZ, RX3:eGFP transgenic fish at 12,18, & 24 HPF (6 SS, 18 SS, 5-prim). (A) UMAP of cells labeled by total count of reads. (B) UMAP of cells labeled by percentage of mitochondrial reads. (C) UMAP of cells labeled by expressed genes. (D) UMAP of cells labeled by percentage of ribosomal reads. (E) UMAP of cells labeled by genotype. (F) UMAP of cells labeled by timepoint.

To that end, scRNA-seq was performed on FACs sorted GFP positive cells from wild type Rx3:eGFP transgenic fish at 12 hpf (6 ss, eyefield), 18 hpf (18ss, optic vesicle), and 24 hpf (prim-5, optic cup) stages. Quality of the data collected was assessed by comparing the following parameters: total count of reads per cell, number of expressed genes per cell, percentage of mitochondrial reads per cell, and the percentage of ribosomal reads per cell. Cells that exceeded 50,000 total counts were filtered out as duplicates. A portion of the cells overlapped with low number of expressed genes, high percentage of mitochondrial reads, and low percentage of ribosomal reads per cell. Taken together, these combined parameters suggest that these cells were 'unhealthy' and were removed from the dataset (Fig. 3.13 A-D). Percentages of 'unhealthy' cells did not vary between genotypes and timepoints, suggesting they are likely an artifact of sample preparation (data not shown).

Cells from 12 hpf clustered distinctly from those at 18 and 24 hpf which strongly overlapped with one another (Fig. 3.13 F) suggesting that even though the timepoints represented are equally spaced out from one another, cells from 18 and 24 hpf optic vesicle and cup are highly similar to one another transcriptomically. This makes sense in that at 12 hpf, the cells are part of a single contiguous eye field whereas by 18 hpf they are 2 optic vesicles and a prethalamus, or 2 optic cups and a prethalamus at 24 hpf. These results indicate that cells that make up the optic vesicle/cup and prethalamus at 18 and 24 hpf are structurally and transcriptomically similar to one another.

At 12 hpf the eyefield is still one contiguous population and has not started yet to evaginate into two optic vesicles (Fig. 3.6 A'). Graph-based clustering across a UMAP categorized the cells into 10 clusters. 3 of these clusters were

enriched with overlapping canonical eyefield genes such as *lhx2b*, *otx2*, *pax6*, *rx3*, and *six3.* The other 7 clusters were not enriched with genes distinct to their clusters alone. The top differentially expressed genes were expressed broadly across the dataset, suggesting the defining factor of these clusters was the reduction of expression in the canonical eyefield genes (data not shown). To determine if this was an artifact of the cells existing in different states of differentiation within the eyefield, a trajectory analysis to calculate the cells position in pseudotime was performed on the dataset. The cells separated out into two distinct trajectories suggesting there are two different populations of RPCs at this stage, rather than one population spanning different differential states. The cells in these two trajectories which will be referred to as superclusters 1 and 2 (Fig. 3.14 B). Supercluster 1 is transcriptomically distinguished by the strong expression of the canonical eyefield genes *lhx2b*, *otx2*, *pax6*, *rx3*, and *six3*. These genes are also expressed in supercluster 2 but they are downregulated with respect to supercluster 1 and are expressed in fewer cells throughout the cluster (Fig. 3.14 K). Therefore, Supercluster 2 is primarily distinguished by a weaker canonical eyefield signature.

Interestingly, one gene that is differentially expressed between the two superclusters is *her9,* which our lab has shown is involved in photoreceptor fate specification and rod and red/green cone photoreceptor survival (Coomer et al., 2020). In the wildtype eyefield, 68.87% of 6 SS Rx3:eGFP positive cells express *her9*. *her9* expression accounts for 92.78% of the cells in supercluster 1 but only 43.25% of cells in supercluster 2. To determine whether this difference in expression could be detected in the eyefield in vivo, *in situ* hybridization chain reaction (HCR) was performed on Rx3:eGFP transgenic fish at the 6 SS to detect *her9* RNA expression. This experiment showed that *her9* expression is restricted the lateral and posterior edges of the eyefield, colocalizing with 69.05% of eyefield cells (Fig. 3.14 E,G-I). Since *her9* is most strongly expressed on the borders of the eyefield, this domain may correspond to the supercluster 1 cells observed in the scRNA-Seq dataset. Moreover, given its location, *her9* and other supercluster 1 cell genes may represent a transcriptomic signature for cells that

are preparing to evaginate out to become the optic vesicles. This would need to be followed up by tracking cells expressing *her9* within the eyefield and observing their fate throughout ocular morphogenesis.

A pathway analysis was performed to identify the top pathways differentially regulated between superclusters 1 and 2. Some of the most differentially enriched pathways were Notch signaling, FoxO signaling, TGF-beta signaling, and Wnt signaling, all of which were downregulated in supercluster 2 (Table 3.4) relative to supercluster 1. However, no genes or pathways related to neurogenesis or cell lineage specification were differentially expressed between the two superclusters. Thus, there is no current evidence of individual eyefield subpopulations being skewed towards a later neuronal fate. Rather, the evidence points towards the source of eyefield heterogeneity being the strength of canonical eyefield identity.

Given that scRNA-Seq indicates the wildtype eyefield is a heterogeneous population of cells, we next asked whether loss of Sox4 alters the transcriptional signature of any or all of the eyefield cells. scRNA-seq was repeated under the same conditions on *sox4b* MZ mutants to compare to the wildtype dataset. The *sox4b* MZ mutants were selected over the *sox4a* MZ and *sox4a/b* MZ for this experiment because they had the highest fecundity out of the *sox4* mutant lines and were able to produce enough embryos at a single time for the scRNA-seq experiment. At the eyefield stage (12 hpf), the majority of *sox4b* MZ mutant cells clustered independently from their wildtype counterparts. This separate cluster of *sox4b* MZ cells was distinct from the wildtype superclusters 1 and 2 and was therefore designated supercluster 3 (Fig. 3.14 C-D). This suggests that the loss of *sox4b* transcriptomically alters the identity of cells within the eyefield at 12 hpf. A pseudo bulk RNA-seq analysis was performed to find the top differentially regulated genes (DRG). 227 genes were upregulated in the *sox4b* MZ mutants and 1626 were downregulated by a fold change of 2 or greater. A pathway analysis on the DRG revealed that the top enriched pathways were for ribosomal proteins in addition to other post-transcriptional modification pathways, Notch

signaling, Hh signaling, and Wnt signaling (Table 3.5). The enrichment of the Hh signaling pathway is of interest considering Hh expression was expanded in the *sox4* morphants at the midline at this timepoint (Wen et al., 2015). The role of the other pathways has not yet been explored in relation to the loss of Sox4 in zebrafish.

Similar to supercluster 2, the *sox4b* MZ cells that form supercluster 3 are distinguished by a downregulated expression of canonical eyefield genes such as *lhx2b*, *otx2*, *pax6*, *rx3*, and *six3* compared to supercluster 1 (Fig. 3.14 K). This suggests that the loss of sox4 reduces a strong eyefield identity in Rx3:eGFP positive cells. Also similar to supercluster 2, supercluster 3 also showed a downregulation in *her9* expression and the number of cells expressing *her9* was 19.22%, compared to 92.78% in supercluster 1 and 43.25% in supercluster 2 (Fig. 3.14 E). HCR of *her9* was repeated under the same conditions on *sox4b* MZ mutants to compare to the wildtype by measuring the amount of colocalization between Rx3:eGFP and *her9*. In contrast to the scRNA-Seq data, quantification of Rx3:GFP+ and *her9* positive cells indicated that *sox4b* MZ mutants had a higher percentage of their eyefield co-expressing *her9* compared to wildtype, with 97.8% colocalizing with Rx3:GFP-positive eyefield cells (Fig. 3.14 G-I). This result conflicts with the scRNA-seq dataset which is surprising given the reproducibility found in the wildtype dataset at this same timepoint. A plausible reason for this is that the scRNA-Seq was obtained from cells that were collected by FACS; therefore, cells must have a threshold level of GFP to be collected by this method. Given that expression of the Rx3:eGFP transgene is reduced in the *sox4b* MZ mutants, it is possible that a portion of low-expressing Rx3:GFP+ cells that also express *her9* were detected by the more sensitive imaging methods but did not meet the threshold of fluorescence for sorting, thus skewing the scRNA-Seq expression data. Interestingly, the HCR of *her9* does show a different expression pattern in the *sox4b* MZ mutants compared to the wildtype. Expression of *her9* is expanded along the lateral edges and reduced at the midline posterior to the eyefield (Fig. 3.14 H-I). Given that Her9 has a known role in photoreceptor differentiation and survival (Coomer et al., 2020), the

expanded *her9* expression in the *sox4b* MZ eyefield may connected in some way to the later retinal phenotypes.

Pathway analysis of the DEGs between wildtype and *sox4b* mutant eyefield cells revealed one of the top differentially expressed pathways was for ribosomal proteins (Table 3.5). A total of 40 ribosomal proteins were upregulated and 7 were downregulated by at least a 2-fold change in the *sox4b* MZ cells (Fig. 3.14J). In particular, *rpl26* (*60S ribosomal protein L26*) was strongly upregulated in the *sox4b* MZ cells and was differentially expressed across the two wildtype superclusters (Fig. 3.14 F,J). This result is intriguing because there is recent evidence suggesting heterogeneity among ribosomal subunits can influence translation of specific mRNA transcripts over an extended period of time (Caron et al., 2021; Dörrbaum et al., 2018; Genuth & Barna, 2018). The differences in *rpl26* expression (and other ribosomal subunit genes) between wildtype and *sox4b* mutants will need to be validated *in vivo*. If confirmed, it will be interesting to determine whether altered expression of ribosomal subunits leads to differences in translational capacity, or even altered translation of specific mRNAs, in *sox4* mutants, and whether these differences could account for the retinal differentiation phenotypes observed at later stages.
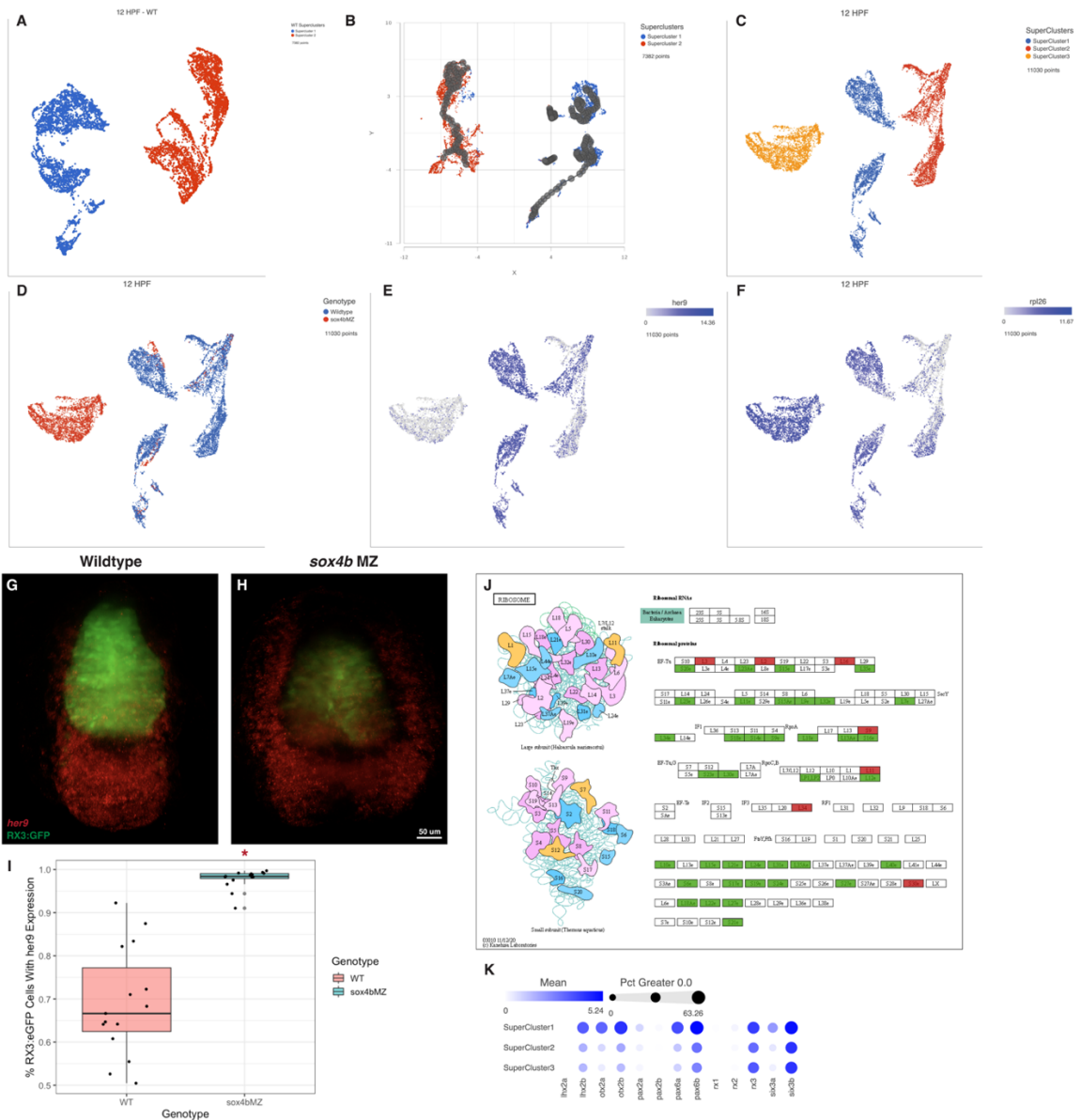
Figure 3.14 *her9* and *rpl26* show differential expression between WT and *sox4b* MZ cells at 12 hpf.

scRNA-seq 12 hpf WT vs. *sox4b* MZ. (A-B) 12 hpf WT Rx3:eGFP cells labeled by superclusters (A) UMAP, (B) Trajectory analysis, (C-F) UMAPs of 12 hpf WT and *sox4b* MZ, Rx3:eGFP cells, (C) Cells labeled by supercluster, (D) Cells labeled by genotype, (E) Cells labeled by *her9* expression, (F) Cells labeled by *rpl26* expression, (G-H) HCR of *her9*, (G) 12 hpf WT Rx3:eGFP, (H) 12 hpf *sox4b* MZ Rx3:eGFP, (I) Boxplot of *her9* expression that colocalizes with Rx3:eGFP cells. Significance at p ≤ 0.05 notated with *, (J) KEGG ribosome pathway, ribosomal genes upregulated in *sox4b* MZ cells are labeled in green and ribosomal genes downregulated in *sox4b* MZ cells are labeled in red, (K)

Bubble plot of expression of canonical eyefield transcription factors between superclusters.

3.3.8 Rod Photoreceptor Bias is Not Detectable by scRNA-seq

ScRNA-seq was also performed on FACS sorted GFP positive cells from Rx3:eGFP transgenic fish at 18 and 24 hpf in both wildtype and *sox4b* MZ fish. Interestingly, the cells at 18 and 24 hpf do not cluster independently from one another like the cells from 12 hpf do (Fig. 3.13 F). Prior to 18 and 24 hpf, the eyefield split into two optic vesicles and the prethalamus. Known markers were used to identify cells that belonged to the prethalamus versus the optic vesicle/cup (Fig 3.15 B-B', Table 3.3). Cells with a prethalamus versus optic identity did not strongly cluster out from one another. Some of the clusters identified by graph-based clustering were enriched with markers for a prethalamus versus optic identity but the majority shared expression of these markers (Fig. 3.15 A-A', B'). This is likely because neuronal progenitors in the retina and in the brain share some redundancy in the transcriptional networks they use to differentiate. The cells were examined for expression of known rod photoreceptor progenitor markers. No evidence was found of any progenitors being skewed towards a rod photoreceptor fate at these timepoints. Genes specific to the rod photoreceptor lineage, *nrl*, *nr2e3* and *rho* are not yet expressed. There are distinct clusters in this population at 18 and 24 hpf, which indicates heterogeneity among the progenitors (Fig. 3.15 A'). RNA-seq has previously been performed on cells from developing optic vesicles at 16,18, and 24 hpf where distinct transcriptomic changes were noted between the neural retina and RPE prior to actual structural changes (Buono et al., 2021). Cluster 18 from cells at 18 and 24 hpf (Fig. 3.15 A') shared a similar expression to the transcriptomic profile associated with the RPE (Buono et al., 2021). It would be worth following up on markers associated with these populations in addition to the others identified by graph-based clustering to see if they mark distinct

populations in vivo and if those populations are skewed towards giving rise to specific cell types later in retinal differentiation.

Additionally, the cells from wildtype vs. *sox4b* MZ fish share more similarity at these stages than at the 12 hpf timepoint but still show some distinct transcriptomic differences (Fig. 3.13 E). Previous work in zebrafish *sox4* morphants suggested that Sox4 downregulates Hh signaling at the midline through regulation of Bmp signaling (Wen et al., 2015). In the scRNA-seq dataset, *bmp2b*, *bmp4*, *shha*, and *shhb* are down-regulated at 6 SS in the *sox4b* MZ cells and *bmp2b*, *bmp4*, and *bmp7b* are down-regulated at 18 hpf (Fig. 3.15 C-C'). The *bmp* genes were also down-regulated in the *sox4* morphants at the same timepoints as detected by qPCR (Wen et al., 2015). In contrast, the scRNA-Seq dataset does not show a similar response of upregulation in *ihhb* expression as was observed in the *sox4* morphants. However, the expansion of Hh signaling in the *sox4* morphants was localized to the ventral midline adjacent to the eye, and therefore we would not expect to see differences in the Rx3:eGFP cells at 18 and 24 hpf. Additionally, transcriptional adaptation in the *sox4b* MZ mutants may reduce the transcriptomic effects from the loss of *sox4b*. Taken together, these results suggest that Bmp signaling is downregulated in response to the loss of *sox4*. However, it is not yet clear whether the loss of *sox4* leads to an upregulation of Hh signaling in the *sox4* mutants.
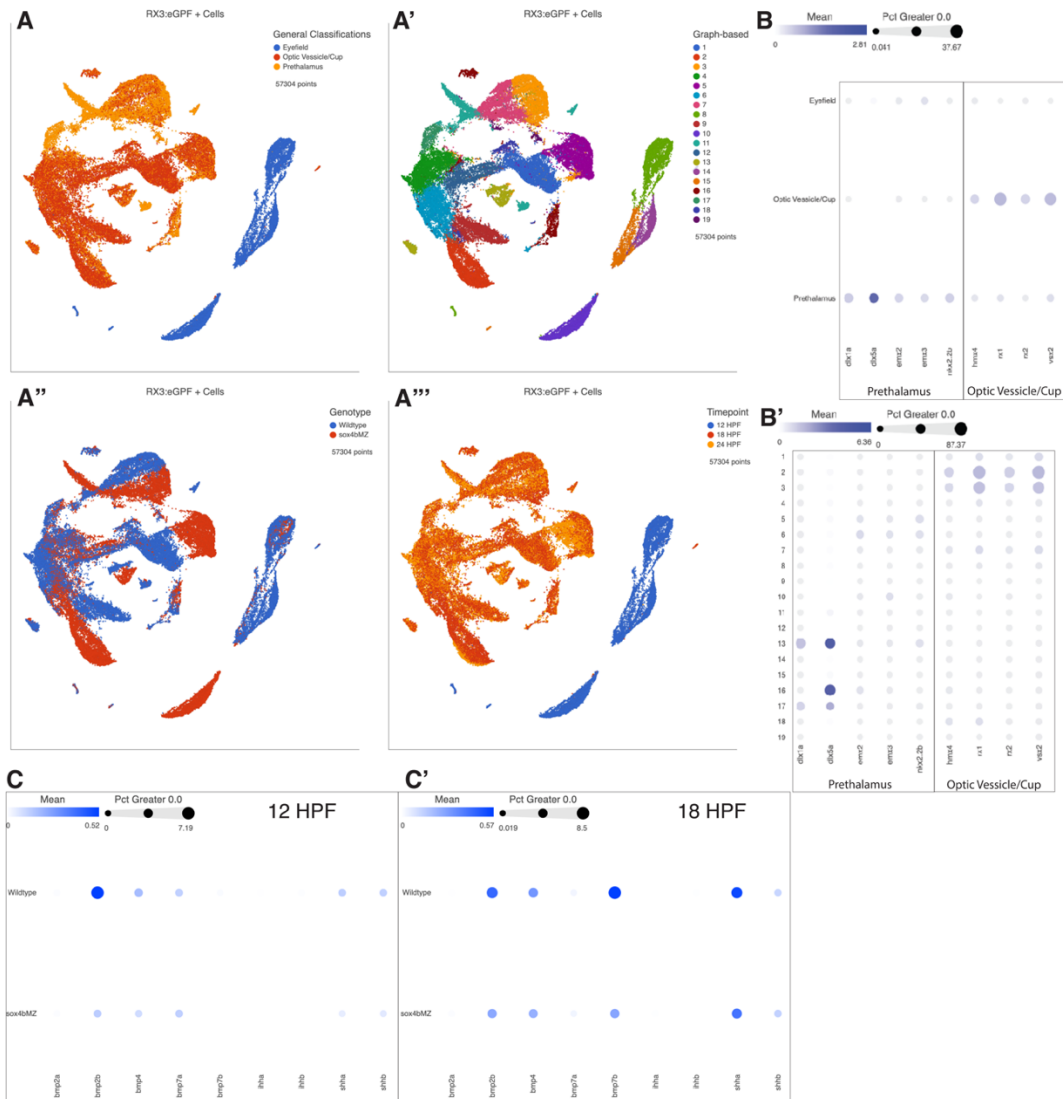
Figure 3.15 Bmp signaling is downregulated in *sox4b* MZ cells compared to WT at 12 and 18 hpf.

scRNA-seq (A-A''') UMAP of Rx3:eGFP Positive Cells at 12, 18, and 24 HPF, (A) Cells labeled by type, (A') Cells labeled by graph-based clusters, (A'') Cells labeled by genotype, (A''') Cells labeled by timepoint. (B) Expression profile of markers by classified cell type, (B') Expression profile of markers graph-based clusters, (C) *Bmp* and *Hh* gene expression by genotype at 12 HPF, (C') *Bmp* and *Hh* gene expression by genotype at 18 HPF.

3.4   Discussion

The vast network that regulates eye development is complex and our understanding of it is starting to expand. Several congenital disorders in humans

with ocular complications have been linked to mutations in *SOX4* or *SOX11*; examples are MAC, CSS, CHARGE syndrome, and SOX4-Related Neurodevelopmental Syndrome (Al-Jawahiri et al., 2022; Marco Angelozzi et al., 2022; Ghaffar et al., 2021; Pillai-Kastoori et al., 2014; Sperry et al., 2016; Tsurusaki et al., 2014; Zawerton et al., 2019). However, the specifics of how loss of SOXC transcription factors leads to those ocular complications are not fully understood. Previous work in zebrafish using morpholinos demonstrates a role for Sox4 and Sox11 in ocular morphogenesis (Pillai-Kastoori et al., 2014; Wen et al., 2015). Building off of this work we demonstrate a role for Sox4 in ocular morphogenesis and retinal differentiation in zebrafish *sox4* MZ mutants.

The *sox4* MZ mutants displayed microphthalmia and delayed choroid fissure closure, similar to the phenotype described in the *sox4* morphants, which displayed microphthalmia and coloboma (Wen, 2016; Wen et al., 2015). Additionally, both the *sox4* morphants and mutants showed a reduction in rod photoreceptors, which was similar in severity in the mutants when compared to the *sox4* morphants without coloboma. The *sox4* morphants with coloboma had a much more severe reduction in rods but this may have been secondary to the coloboma phenotype (Wen, 2016). Although the *sox4* mutants had microphthalmia, delayed choroid fissure closure and reduced rods, similar to the sox4 morphants, overall, the mutant phenotype was less severe than the *sox4* morphants. This phenomenon has previously been observed with morphant and mutant comparisons in zebrafish (Rossi et al., 2015). Evidence suggests it is due to non-sense mediated decay of the mutant transcript which triggers transcriptional adaptation from genes with similar sequence and function (El-Brolosy et al., 2018). Upregulation of other SoxC family members was detected in *sox4* mutants by qPCR. We were able to show that the severity and penetrance of the mutant phenotypes increased when zebrafish lacked both *sox4a* and *sox4b.* However, these double mutants showed an increase in *sox11b* expression. In order to fully appreciate the effect SoxC transcription factors have on zebrafish eye development, quadruple mutants for *sox4a*, *sox4b, sox11a*, and *sox11b* will need to be generated.

Observations of the eyefield using the Rx3:eGFP transgenic line were used to investigate the *sox4* MZ mutant phenotype of microphthalmia. This showed that the *sox4* MZ mutants have smaller volume of Rx3:eGFP+ cells from 1-18 SS. Moreover, the level of GFP expression was reduced in *sox4* mutant eyefield cells. Given that these differences are detectable at the earliest stage of eyefield formation, this suggests that loss of Sox4 alters eyefield formation prior to or concurrent with the onset of expression of *rx3*. Formation of the eyefield requires the expression of *rx3* which is regulated by Wnt and b-Catenin signaling (Cavodeassi et al., 2005). Therefore, it is possible that loss of Sox4 disrupts either or both of these signaling pathways, which would place *rx3* expression downstream of but not completely reliant on Sox4.

Our results show that there is an additional role for Sox4 in rod photoreceptor neurogenesis. The loss of Sox4 leads to a reduction of the number of rod photoreceptors and delays their maturation. There was a reduction in proliferating cells the CMZ of *sox4* mutants at 72 hpf, suggesting that abnormal rod progenitor proliferation might account for the rod phenotype of sox4 mutants. However, the rod photoreceptor progenitors are derived from proliferating cells in the ONL and not the CMZ. Therefore, cell proliferation in this region needs to be assessed at 48 hpf to determine if there are any alterations of proliferation in the ONL contributing to the phenotype.

It is particularly intriguing that the *sox4* mutant phenotypes are dependent on the presence or absence of wildtype maternal *sox4* transcripts. This indicates that aberrant expression of *sox4* very early in development continues to affect events occurring days later. One of the upregulated genes in the eyefield of *sox4b* MZ mutants compared to WT was *rpl26.* Mutations in RPL26 are associated with the disease Diamond-Blackfan anemia (DBA), which can also be caused by mutations in *RPL3, RPL7, RPL8, RPL10, RPL14, RPL17, RPL19, RPL23A, RPL26, RPL27,RPL35, RPL36A, RPL39, RPS4X, RPS4Y1,* and *RPS21* (Gazda et al., 2012). Out of these ribosomal proteins *rpl7, rpl10, rpl14, rpl23a, rpl26, rpl27, rpl35,* and *rpl36a* were upregulated in the *sox4b* MZ mutant

eyefield at 12 hpf. Interestingly, DBA is also associated with ocular complications such as cataracts and glaucoma (Tsilou et al., 2010), and ocular abnormalities are observed in other diseases cause by mutation of ribosomal protein subunits. Taken together, these data show that changes in ribosomal proteins result in tissue specific phenotypes, including in the eye, rather than causing global complications. This is interesting since translation is an essential process in all cells and sparks the consideration that there may be cell-type specific heterogeneity among ribosomes. Ribosomal heterogeneity has been proposed to influence ribosomal function and which transcripts are selected for translation (Genuth & Barna, 2018). For example, loss of Sox9 in chondrocytes early in chondrogenesis caused an alteration in the expression of different ribosomal proteins leading to a reduction of total protein translation capacity and altered modes of translation, which was correlated with inhibition of chondrogenic differentiation. These differences were detected as far out as 7 days post knock-down (Caron et al., 2021). In human neuronal cell culture, it was shown that ribosomal proteins have long half-lives of 6-11 days (Dörrbaum et al., 2018). Taken together, these data strongly suggest that regulation of ribosomal subunit gene expression by Sox4 early in eye development may contribute to the later developmental phenotypes of microphthalmia and altered rod photoreceptor neurogenesis. To follow up on this hypothesis, there are some methods currently available to test ribosomal function such as the SUnSET assay (Caron et al., 2021; Goodman & Hornberger, 2013; Schmidt et al., 2009), Polysome Fractionation (Caron et al., 2021; Panda et al., 2017), and the Bicistronic Reporter Assay (Caron et al., 2021; van den Akker et al., 2021). The caveat to the aforementioned methods, is that they all examine the function of ribosomal activity overall. RIBO-seq can be used in parallel with RNA-seq to determine which mRNA transcripts are actively being transcribed versus translated and provide a sense of translational efficiency and how that varies across different transcripts (Wu et al., 2022). Given the consideration that ribosomes may not be a monolith and instead may be heterogenous according to developmental or tissue context (Genuth & Barna, 2018), mass spectrometry can be used to detect

the different subunits of the ribosome and determine if they are actually a heterogenous population (Benjamin et al., 1998; Van De Waterbeemd et al., 2018).

In summary, these findings support a role for Sox4 in specification of the eyefield and in rod photoreceptor neurogenesis and maturation. The *sox4* MZ zebrafish mutants will be a useful tool in determining the precise mechanism by which Sox4 contributes to these processes. The scRNA-seq data provides evidence that the eyefield is already a heterogenous population as early as 12 hpf. It is still unclear exactly how the different cell identities in the eyefield impact the process of ocular morphogenesis and possibly later events in neurogenesis of the retina, but it may in part be possibly mediated by ribosomal proteins.

3.5   Methods

3.5.1   Animal Husbandry

All experiments involving the use of zebrafish (*Danio rerio*) were carried out in accordance with protocols established by the University of Kentucky Institutional Animal Care and Use Committee (IACUC). The Tg(XlRho:EGFP) transgenic line (referred to as XOPS:GFP) was obtained from J.M. Fadool (Florida State University, Tallahassee, FL) and has been previously described (Fadool, 2003). The Tg(Rx3:eGFP) transgenic line was obtained from J. Famulski (University of Kentucky, Lexington, KY) and has been previously described (Cavodeassi et al., 2013; Ebert et al., 2014; Katherine E Brown et al., 2010). Zebrafish were bred, raised, and kept with a 14 h light:10 h dark cycle at 28.5°C.

3.5.2   Genotyping

Adult fish were anesthetized in 0.168 mg/mL of tricane (MS222) in fish water. To extract DNA, part of the tail was removed (Westerfield, 2007), placed in 20ml of 1x ThermolPol Buffer and incubated at 95°C for 15 min. Sample was cooled. 5ml of ProteinaseK was added to the sample and incubated at 55°C overnight.

ProteinaseK was inactivated the next morning at 95°C for 15 min. DNA was used in a PCR of *sox4a* and/or *sox4b* and run on an agarose gel to screen for the presence of a large deletion. Primer details can be found in table 3.1.

3.5.3   RNA Extraction, RT-PCR, and Real-Time Quantitative PCR (qPCR)

Samples were homogenized in TRIzol (Invitrogen, Grand Island, NY) and then treated with DNAse I (Roche, Indianapolis, IN), according to the respective manufacture's protocols. The sample was then purified by a phenol/chloroform extraction. cDNA was synthesized from 500ng of RNA using the GoScript Reverse Transcriptase System (Promera, Madison, WI). qPCR primers were then used in combination with Faststart Essential DNA Green Master mix (Roche) to amplify a specific region on the genes of interest on the Lightcycler 96 Real-Time PCR System (Roche). Biological and technical replicates? Primer details can be found in table 3.1. The relative transcript abundance was normalized to a geometric mean of two housekeeping genes, *atp5h* and *elfa* to determine the Dct. The Dct was then used to determine the log fold change between genotypes.

3.5.4   Tissue Sectioning

Samples were fixed in 4% paraformaldehyde (PFA) overnight and then cryoprotected in 10% sucrose for 8 hours followed by 30% sucrose overnight. The samples were then arranged in OTC Medium (Ted Pella, Redding, CA) and frozen at -80°C overnight. Tissue samples were sectioned in 10-micron thick sections on a cryostat (Leica CM 1850, Leica Biosystems, Buffalo Grove, IL). The sections were then adhered to Superfrost Plus (VWR, Randor, PA) or gelatin-coated slides and air-dried at room temperature overnight.

3.5.5 Immunohistochemistry

Immunohistochemistry was performed on retinal sections, whole zebrafish embryos, or whole mount zebrafish retinas as previously described (Forbes-Osborne et al., 2013). Primary antibodies used can be found in Table 3.2. Secondary antibodies used were Alex Fluor conjugated antibodies (Molecular Probes, Invirtogen) and Cy5-conjugated antibodies (Jackson Immunoresearch) at a 1:200 dilution. DAPI (1:10,000 dultion) was used to counterstain and visualize nuclei. Slides were mounted in 40% glycerol in 1xPBS. Whole zebrafish embryos, or whole mount zebrafish retinas were mounted in 1% low-melting temperature (LMT) agarose. Samples were imaged at 20x and 40x on an inverted fluorescent microscope (Eclipse Ti-U, Nikon Instruments), a fluorescent scanning laser confocal microscope (Nikon C2 plus), or at 20x on a lightsheet microscope (Zeiss LightSheet Z.1 Dual Illumination Microscope System).

3.5.6 TUNEL Staining

The ApopTag Fluorescein Direct In Situ Apoptosis Detection Kit (Millipore, Billerica, MA) was used to perform Teminal deoxynucleotide transferase (TdT)-mediated dUTP nick end labeling (TUNEL) on retinal cryosections. Slides were mounted in 40% glycerol in 1xPBS and imaged at 20x and 40x on an inverted fluorescent microscope (Eclipse Ti-U, Nikon Instruments).

3.5.7 EdU labeling

Zebrafish embryos were incubated in fish water containing 1.5mM EdU (made from 10mM EdU in DMSO stock) for 1 hour at room temperature. Samples were then fixed, cryoprotected and sectioned as described in 3.11.4 or whole embryos were fixed in 4% overnight and stored in 1xPBS. Samples were post-fixed with

1% PFA, washed in PBS, rinsed in TBS, incubated in the Click-iT reaction cocktail (Invitrogen), washed in TBS, and then washed in PBS. DAPI (1:10,000 dultion) was used to counterstain and visualize nuclei. Slides were mounted in 40% glycerol in 1xPBS and imaged at 20x and 40x on an inverted fluorescent microscope (Eclipse Ti-U, Nikon Instruments).

3.5.8   Acridine Orange staining

24 hpf embryos were incubated in 5ug/mL acridine orange (Sigma) for 10 minutes in the dark and then rinsed in fish water for 30 seconds. Embryos were mounted in 1% low-melting temperature (LMT) agarose on a glass bottomed petri dish and imaged using a fluorescent scanning laser confocal microscope (Leica TCS SP8 DLS) using the 10x objective. Acridine orange positive cells were counted in FIJI (Schindelin et al., 2012) from between the otic vesicle and the anterior most end of the embryos.

3.5.9   Hybridization chain reaction (HCR)

Tg(Rx3:eGFP) fish were collected in 4% PFA at 12 hpf from both Wildtype and *sox4b* MZ mutants. After an 8-hour fixation, the samples were washed in 1x PBS for 5 min. 4 times followed by being washing in MeOH for 5 min 4 times. The samples were then stored in MeOH at -20°C until ready for use. Next, the samples were rehydrated in a MeOH:1xPBST gradient (3:1, 1:1, 1:3) until in 1xPBST. Samples were washed in 1xPBST 2 times, post-foxed with 1mL of 4% PFA for 20 min, and washed in 1xPBST 5 times for 5 min. each. Samples were pre-hybridized with probe hybridization buffer (Molecular Instruments, Inc) for 30 min at 37 °C and then incubated in the probe solution (Molecular Instruments, Inc) overnight at 37 °C. Then the samples were washed 4 times for 15 min in probe wash buffer at 37 °C, then 2 times for 5 min with 5× SSCT at room

temperature. Samples were pre-amplified in amplification buffer (Molecular Instruments, Inc) for 30 min at room temperature and then incubated in the hairpin solution (Molecular Instruments, Inc) overnight in the dark at room temperature. Samples were washed in 5× SSCT at room temperature 2 times for 30 min. Samples were imaged on a lightsheet microscope (Zeiss LightSheet Z.1 Dual Illumination Microscope System).

3.5.10 Eye size measurements

Zebrafish embryos were anesthetized in 0.168 mg/mL of tricane (MS222) in fish water, placed in 3% Methyl Cellulose, and imaged at 24, 48, and 72 hpf using a stereo microscope (Digital Sight Ds-Fi2, Nikon instruments). Area of the eye and length of the embryos were measured using FIJI (Schindelin et al., 2012).

3.5.11 Live Imaging

Live imaging and analysis of Tg(Rx3:eGFP) fish was performed as previously described (Petersen & Morris, 2021) on Wildtype and *sox4b* MZ embryos from 10-24 hpf using a Zeiss Z.1 Lightsheet microscope. Analysis of live imaging datasets was performed using arivis Vision4D software to detect the volume of the eye as it evaginates and splits into the optic vesicles and prethalamus.

3.5.12 Cell counts and statistics

All retinal cell counts and retinal measurements were performed blindly. Cell counts taken from sections containing the optic nerve and were normalized to the measured perimeter of the retina. A minimum of 15 transverse retinal sections were imaged per genotype, 5 retinas for each of 3 biological replicates. Analysis

pipelines were built in arivisVison4D to analyze static images of Tg(Rx3:eGFP) fish, HCR samples, and IHC of whole zebrafish embryos.

Cell counts, retinal measurements, eyefield and optic vesicle measurements, qPCR results were compared across the various genotypes using either a student t-test or a one-way ANOVA followed by a Tukey Test to determine any significant differences. Statistical analyses were run through the open-source software R, using the program stats. The open-source software R was used to generate boxplots of quantitative measurements using the program ggplot2.

3.5.13 Single cell RNA-seq

Fluorescent Activated Cell Sorting (FACS) was performed on GFP positive cells from Tg(Rx3:eGFP) fish at 12, 18, and 24 hpf on 2 biological replicates from both Wildtype and *sox4b* MZ mutants.   The GFP positive cells were processed through 10x genomics to isolate and extract RNA from individual cells, label the RNA from each cell it originated from, and generate a cDNA library from that RNA. The cDNA library was then sent for sequencing at Novogene. Sequencing results were then run through Cell Ranger to align and count the reads. Cell Ranger output a filtered feature matrix for each sample that was subsequently imported to Partek (*Partek® Genomics Suite®*, 2022). Cell counts, ribosomal counts, and mitochondrial counts were used to set quality control thresholds. Cells with total counts between 600 and 50,000 were accepted to eliminate any data from cell duplicates. Cells with mitochondrial transcripts accounting for greater than 10% of the cells total counts were eliminated from analysis (Fig. 3.13). The cell population was acquired during an active developmental process therefore, variation due to cell cycle transcripts was not regressed from the data set (Luecken 2019). PCA, UMAP, graph-based clustering, and trajectory analyses were performed. Specific cell markers were used to classify different cell types in the dataset and can be found in table 3.3.

Video 3.1 Time-lapse video of Tg(rx3:GFP) WT zebrafish embryo from 1ss-24hpf

Video 3.2 Time-lapse video of Tg(rx3:GFP) *sox4b* **MZ zebrafish embryo from 1ss-24hpf**

Table 3.1 PCR Primer List

Target	Forward Primer	Reverse Primer	Product	Purpose
sox4a	TAGTGCATGGG CACAGACC	GCTGTCCTTTCATAACT AGCGC	1120 bp	Genotyping
sox4b	GAAGGATATGC AGAAGGAGTCG	AACGTGCAAAAATCAA TCACAG	1513 bp	Genotyping
sox4a	CAGAGCATGAA AAAGTGCAGTC	TTTGGTCAATGTGGAA ACAAAG	279 bp	qPCR
sox4b	GAAGGATATGC AGAAGGAGTCG	ACTCAGTCTGATTGCA GCACA	209 bp	qPCR
sox11 a	TCTAGGTCCGT TTCCACGTC	GCTCAGGCGTGCAATA GTCT	217 bp	qPCR
sox11 b	AGTGCGCCAAA CTCAAGC	CGTCGTCTTCGTCGTC AGTA	205 bp	qPCR
elfa	CTTCTCAGGCT GACTGTGC	CCGCTAGCATTACCCT CC	358 bp	qPCR
atp5h	TGCCATCTCAG CAAAACTTG	CACAGGCTCAGGAACA GTCA	200 bp	qPCR

Table 3.2 Primary Antibody List

Antibody	Labels	Raised in	Dilution	Vendor
HuC/D	Ganglion & Amacrine Cells	Mouse	1:40	Invitrogen
PKC-(A-3)	Bipolar Cells	Mouse	1:100	Santa Cruz Biotechnology
Prox-1	Horizontal Cells	Rabbit	1:2000	Milliopore
Zpr-1	Red/Green Cones Photoreceptors	Mouse	1:20	ZIRC
GS	Müller Glia	Mouse	1:500	BD Biosciences
α-GPF	GFP	Rabbit	1:1000	abcam
PH3	Mitotic Cells (G2/M)	Rabbit	1:500	Milliopore

Table 3.3 Cell Markers for scRNA-seq

Prethalamus	Optic Vesicle/Cup
crlfa	bsx
emx3	hmx4
emx2	rx1
fezf1	rx2
vamp2	thbx5a
gng3	vsx2
mllt11	
sncb	
stmn1b	
stxbp1a	
dlx1a	
dlx2a	
dlx2b	
dlx5a	
dlx6a	
gad1	
otpa	
nkx2.2b	

Table 3.4 Pathway Report for 12 hpf WT Supercluster 1 vs. 2 Cells – Top 25 Results

Gene set	Description	Enrichment score	P-value	Genes in list	Genes not in list
path:dre04330	Notch signaling pathway	12.8371	2.66E-06	13	51
path:dre04210	Apoptosis	9.35112	8.69E-05	20	159
path:dre04068	FoxO signaling pathway	8.86781	0.00014085	19	152
path:dre04350	TGF-beta signaling pathway	8.63168	0.000178365	15	104
path:dre04310	Wnt signaling pathway	8.03895	0.000322648	20	177
path:dre04218	Cellular senescence	6.91371	0.00099406	18	166
path:dre04110	Cell cycle	6.37366	0.0017059	15	132
path:dre04140	Autophagy - animal	5.3666	0.00467	16	163
path:dre04115	p53 signaling pathway	4.73115	0.00881637	9	73
path:dre04150	mTOR signaling pathway	4.56088	0.0104529	16	179

Table 3.4 Continued.

path:dre04625	C-type lectin receptor signaling pathway	4.09666	0.0166282	11	111
path:dre03460	Fanconi anemia pathway	4.08058	0.0168977	6	42
path:dre04012	ErbB signaling pathway	3.42237	0.032635	9	93
path:dre04217	Necroptosis	3.05621	0.0470658	12	149
path:dre00440	Phosphonate and phosphinate metabolism	2.89321	0.0553983	2	7
path:dre00565	Ether lipid metabolism	2.73941	0.0646082	5	45
path:dre03320	PPAR signaling pathway	2.73697	0.0647661	7	75
path:dre03018	RNA degradation	2.73697	0.0647661	7	75
path:dre04137	Mitophagy - animal	2.43898	0.0872501	7	81
path:dre04920	Adipocytokine signaling pathway	2.39272	0.0913805	7	82
path:dre04010	MAPK signaling pathway	2.33183	0.0971182	22	356

Table 3.4 Continued.

path:dre04 340	Hedgehog signaling pathway	2.134	0.118363	5	55
path:dre04 810	Regulation of actin cytoskeleton	2.03767	0.130332	16	255
path:dre04 620	Toll-like receptor signaling pathway	2.01498	0.133323	7	91

Table 3.5 Pathway Report for 12 hpf WT vs. *sox4b* MZ Cells – Top 25 Results

Gene set	Description	Enrichment score	P-value	Genes in list	Genes not in list
path:dre04 142	Lysosome	14.7379	3.98E-07	66	91
path:dre04 141	Protein processing in endoplasmic reticulum	13.8528	9.63E-07	76	116
path:dre00 970	Aminoacyl-tRNA biosynthesis	11.4067	1.11E-05	21	15
path:dre00 513	Various types of N-glycan biosynthesis	9.8184	5.44E-05	24	23
path:dre04 330	Notch signaling pathway	9.81585	5.46E-05	30	34
path:dre04 340	Hedgehog signaling pathway	9.15194	0.000106014	28	32

Table 3.5 Continued.

path:dre03010	Ribosome	8.94807	0.000129988	50	79
path:dre04310	Wnt signaling pathway	8.10835	0.000301015	69	128
path:dre00510	N-Glycan biosynthesis	7.1474	0.000786911	25	32
path:dre04210	Apoptosis	7.08999	0.000833408	62	117
path:dre04350	TGF-beta signaling pathway	6.8653	0.00104337	44	75
path:dre00280	Valine, leucine and isoleucine degradation	6.51878	0.00147546	24	32
path:dre00900	Terpenoid backbone biosynthesis	6.20658	0.00201613	12	10
path:dre00071	Fatty acid degradation	6.17804	0.00207449	22	29
path:dre04068	FoxO signaling pathway	6.15682	0.00211899	58	113
path:dre00310	Lysine degradation	5.98386	0.00251908	30	47
path:dre04115	p53 signaling pathway	5.59603	0.00371258	31	51

Table 3.5 Continued.

path:dre01 212	Fatty acid metabolism	5.525	0.00398 587	26	40
path:dre00 531	Glycosaminoglyca n degradation	5.26452	0.00517 185	12	12
path:dre04 110	Cell cycle	5.02066	0.00660 019	49	98
path:dre00 514	Other types of O-glycan biosynthesis	4.76583	0.00851 581	21	32
path:dre04 145	Phagosome	4.69722	0.00912 058	52	108
path:dre04 012	ErbB signaling pathway	4.39433	0.01234 71	35	67
path:dre00 534	Glycosaminoglyca n biosynthesis - heparan sulfate / heparin	4.14942	0.01577 36	13	17

3.6   Acknowledgements

Digital Sight Ds-Fi2, and to Lucas Vieira Francisco, Evelyn M. Turnbaugh, and Brandi Bolton for expert zebrafish care.

CHAPTER 4. DISCUSSION

There are many conditions that result in visual impairment, only a portion of which are able to be treated. Understanding the mechanisms behind eye development is an essential step prior to preventing these conditions or developing therapies to treat them. Eye development is a complex process that is tightly regulated by a vast network of genes and signaling pathways. Our understanding of this network and how it operates is rapidly expanding with the advent of new techniques, but there is still much to be learned.

SOXC transcription factors have been implicated in having an important role in eye development in model organisms and in humans. Several congenital disorders with ocular complications have been attributed to mutations in *SOX4* or *SOX11*, like MAC, CSS, CHARGE syndrome, and SOX4-Related Neurodevelopmental Syndrome (Al-Jawahiri et al., 2022; Marco Angelozzi et al., 2022; Ghaffar et al., 2021; Pillai-Kastoori et al., 2014; Sperry et al., 2016; Tsurusaki et al., 2014; Zawerton et al., 2019). However, the specifics of how SOXC transcription factors lead to those ocular complications are not fully understood. Furthering our understanding of the mechanisms in this process will build a base of information that can be used to derive future therapeutic and preventative measures for patients with ocular complications due to mutations in *SOX4* or *SOX11.* Some studies have already been done on the role of Sox4, implicating it as an important factor in both ocular morphogenesis and retinal development by studies in mice, zebrafish, and Xenopus (Bhattaram et al., 2010; Cizelsky et al., 2013; Jiang et al., 2013; Usui, Iwagawa, et al., 2013; Usui, Mochizuki, et al., 2013; Wen, 2016; Wen et al., 2015). The goal of this dissertation was to further elucidate the role of Sox4 in both ocular morphogenesis and retinal neurogenesis.

The *sox4* MZ mutants display microphthalmia, suggesting a role for Sox4 in ocular morphogenesis. Visualizing ovular morphogenesis in vivo by time lapse imaging increases the temporal resolution at which events like ocular morphogenesis can be observed. This makes it an ideal tool to determine how

the process of ocular morphogenesis is altered in the *sox4* MZ mutants. In Chapter 2, I established a protocol, using Lightsheet microscopy, to perform time-lapse imaging of eye development using the Rx3:GFP transgenic reporter line. The resulting dataset from this approach can provide valuable insights into the process of ocular morphogenesis, as well as perturbations to this process as a result of genetic mutation, exposure to pharmacological agents, or other experimental parameters. There are additional modifications that can be made to this protocol that would allow for multiple embryos to be sequentially imaged at each time interval or by quantifying the eye field by other parameters. A pipeline could be made to quantify and track individual cells or determine the rate of optic vesicle evagination. This information could be used to inform on different dynamic aspects that impact ocular morphogenesis and how they might be altered under experimental conditions. Additionally, this protocol provides instructions for image acquisition analysis specifically using the Lightsheet Z.1 Dual Illumination Microscope System and arivis Vision4D analysis software. There are other commercially available Lightsheet microscopes made by Leica, Olympus, and Luxendo, as well as image analysis software by Imaris, that could be used to achieve similar results. The selection of equipment and software for this protocol was determined by availability at our institution, and therefore some steps may be specific to the type of imaging equipment being used. Nevertheless, this protocol provides a starting point for conducting time-lapse imaging using Lightsheet microscopy and for image quantification of early eye development in zebrafish, which I was able to utilize in Chapter 3 to compare wildtype and *sox4b* MZ embryos. This technique was particularly useful for demonstrating that the timing of key events in the process of ocular morphogenesis, such as evagination of the optic vesicles, was not altered in the *sox4b* MZ embryos. However, given the challenge in acquiring a high number of replicates, static imaging of the RX3:eGFP transgenic line proved more useful for volume analysis at individual time points. Additionally, if the relationship between RX3:eGFP positive cells and another marker of interest is to be observed, it

needs to be paired with another transgenic line for live experiments or fixed to stain at a static point in time.

In Chapter 3, I characterized novel zebrafish mutants for the genes *sox4a* and *sox4b*. Interestingly, *sox4a* -/- and *sox4b* -/- zygotic mutant zebrafish had no detectable phenotype. *Sox4* mRNA transcripts are maternally deposited, so homozygous *sox4a* -/- and *sox4b* -/- zebrafish were incrossed to generate embryos lacking any wildtype copy of *sox4*, maternal or zygotic. The *sox4* MZ mutants displayed microphthalmia and delayed choroid fissure closure. This was similar to the phenotype described in the *sox4* morphants, which also displayed microphthalmia and coloboma, although the mutants displayed reduced penetrance and severity of these phenotypes compared to the *sox4* morphants (Wen, 2016; Wen et al., 2015). The *sox4* morphants were generated with translation blocking morpholinos injected at the single-cell stage. This prevented the translation of both maternal and zygotic sox4 mRNAs. Therefore, it is unsurprising that the *sox4* MZ mutants have a more similar phenotype to the morphants than the *sox4* zygotic mutants. Additionally, both the *sox4* morphants and mutants showed a reduction in rod photoreceptors, which was similar in severity in the mutants when compared to the *sox4* morphants without coloboma. The *sox4* morphants with coloboma had a much more severe reduction in rods but this may have been secondary to the coloboma phenotype (Wen, 2016). One advantage of generating the *sox4* mutants is the ability to examine phenotypes at much later stages of development, at timepoints when morpholinos would no longer be effective. When the *sox4* MZ mutants were examined at later timepoints (5, 7, and 14 dpf), there was still a reduction in rods compared to wild type retinas of the same age. The magnitude of this reduction initially seems to start catching up at 5 dpf but then fails to increase in density at the same rate as the wildtype retinas. This suggests that although rods are able to be generated, this process is occurring at a slower rate in the absence of Sox4 and thus indicates that Sox4 is involved in the differentiation of rod photoreceptors beyond the initial wave of neurogenesis.

Although the *sox4* mutants had microphthalmia, delayed choroid fissure closure and reduced rods, similar to the *sox4* morphants, overall, the mutant phenotype was less severe than what was observed in the *sox4* morphants. This phenomenon has been previously observed when comparing morphant and mutant phenotypes in zebrafish (El-Brolosy et al., 2018; Rossi et al., 2015). Evidence suggests it is due to non-sense mediated decay of the mutant transcript which triggers transcriptional adaptation from genes with similar function and sequence (El-Brolosy et al., 2018). Indeed, I detected an upregulation of other SoxC family members in individual *sox4* mutants by qPCR. We were able to show that the severity and penetrance of the mutant phenotypes increased when zebrafish lacked both *sox4a* and *sox4b.* However, these double mutants showed an increase in *sox11b* expression. To fully appreciate the effect SoxC transcription factors have on zebrafish eye development, quadruple mutants for *sox4a*, *sox4b*, *sox11a*, and *sox11b* will need to be generated.

To further characterize the microphthalmia phenotype, I used the RX3:eGFP transgenic line to observe the process of ocular morphogenesis. I found that the *sox4* MZ mutant eyefield was reduced in volume and displayed lower transgene expression starting at 1 SS. This was observed in response to the loss of *sox4a* and *sox4b* both individually. Loss of both *sox4a* and *sox4b* together further reduced the size of the eyefield, suggesting a role for both *sox4a* and *sox4b* in eyefield induction. Live imaging of the *sox4b* MZ eyefield did not show a significant difference in the timing of separation between the optic vesicles and prethalamus, indicating that the eyefield is not reduced due to a developmental delay. The *sox4* MZ mutant eyefield did not display a significant difference in apoptosis or cell proliferation at 1 SS. This suggests that the reduction in eyefield upon loss of Sox4 is a result of improper specification or induction of this domain. As discussed in the Introduction, formation of the vertebrate eyefield requires the expression of the transcription factor Rx (Rx3 in zebrafish*),* which is regulated by Wnt and b-Catenin signaling (Cavodeassi et al., 2005). It is possible that loss of Sox4 disrupts either or both of these signaling pathways, which would place *rx3* expression downstream of Sox4. However, *rx3*

expression is still detectable in the *sox4* MZ mutants which indicates that *rx3* expression is not fully dependent on Sox4. The *sox4* morphants have a reduction in Bmp signaling and an expansion of Hh signaling (Wen, 2016; Wen et al., 2015). Hh signaling along the ventral midline has been shown to play a role in ocular morphogenesis through regulation of the *pax2/6* gradient of expression (Ekker et al., 1995; Macdonald et al., 1995). Similarly, Bmp ligand expression was reduced in the *sox4b* MZ mutant RX3:eGFP positive cells at 12 and 18 hpf by scRNA-seq. This supports a model whereby Sox4 upregulates Bmp signaling, which in turn downregulates Hh signaling to promote proper ocular morphogenesis in zebrafish. In addition to *rx3,* the expression pattern of other known eyefield markers like *pax6*, *six3*, and *otx2,* which are known to partially overlap but are also expressed in distinct regions of the eyefield (Zaghloul & Moody, 2007), was reduced in *sox4b* MZ RX3:eGFP positive cells at 12 hpf by scRNA-seq. This suggests that loss of Sox4 causes a reduction of eyefield through a reduction but not a complete loss of several genes necessary for proper specification of the eyefield.

Sox4 was originally identified as having a potential role in rod photoreceptor neurogenesis in a microarray analysis of the adult XOPS:mCFP zebrafish retina (Ann C. Morris et al., 2011) In *sox4* morphants, there was a decrease in the number of rod photoreceptors present at larval stages. (Wen, 2016). Taken together, these data suggested that Sox4 is important for the genesis of rod photoreceptors, both during embryonic development and in adult retinal regeneration. In the *sox4* MZ mutants, the loss of Sox4 leads to a reduction of the number of rod photoreceptors and delays their maturation, adding another piece of evidence to support a role for Sox4 in rod photoreceptor neurogenesis. This reduction in rod photoreceptors is not due to apoptosis of the rods or their progenitors. There was a reduction in proliferating cells the CMZ of *sox4* mutants at 72 hpf, suggesting that abnormal rod progenitor proliferation might account for the rod phenotype of sox4 mutants. However, the rod photoreceptor progenitors are derived from proliferating cells in the ONL and not the CMZ. Therefore, cell proliferation in this region needs to be assessed at 48

hpf to determine if there are any alterations of proliferation in the ONL contributing to the phenotype. Additionally, the reduction in rod photoreceptors could be due to a failure to terminally differentiate. This can be assessed by doing in situ hybridization to look for the presence and density of markers of rod photoreceptor specification and differentiation, such as *crx*, *nrl*, and *nr2e3* in the *sox4* MZ mutants. Data from *sox4* morphants showed no reduction in the number of *nr2e3* positive rod progenitors through fluorescent *in situ* hybridization, suggesting the reduction in rod photoreceptors is due to a delay or arrest of terminal differentiation, rather than specification, of rod precursors (Wen, 2016).

Given the reduction of rod photoreceptors and the delay in maturation at 14 dpf, it is possible that this impacts the vision of the *sox4* MZ mutants. Rod photoreceptors in wildtype zebrafish reach full maturity and begin to contribute to zebrafish dark-adapted vision at 20 dpf (Branchek & Bremiller, 1984). At this age two different methods could provide more insight to rod photoreceptor function, the Optokinetic Reflex (OKR) and electroretinogram (ERG). OKR uses the phenomena of fish tracking the movement of a rotating grating with their eyes. The movement of their eyes can be tracked to provide information regarding how well they are able to see (Easter, Jr. & Nicola, 1996; Easter & Gregory Nicola, 1997; Zou et al., 2010). ERGs can be done on zebrafish larvae and adults (Brockerhoff et al., 1998). The ERG response consists of three major components, an a-wave that measures photoreceptor cell activity, a b- wave that measures activity of second order neurons, and the c-wave that measures RPE activity (Chrispell et al., 2015). To ensure rod function is being measured rather than cone function, the zebrafish would need to be dark adapted prior to being tested (Bilotta et al., 2001).

As mentioned above, Sox4 was originally identified as having a potential role in rod photoreceptor neurogenesis in a microarray analysis of the adult XOPS:mCFP zebrafish retina (Ann C. Morris et al., 2011). Studying neurogenesis from the context of regeneration also provides valuable information on the genetic pathways required to regenerate rod photoreceptors. Damage can be specifically induced to the photoreceptors by the use high intensity light

(Vihtelic & Hyde, 2000), through use of the nitroreductase-metronidazole system to chemically ablate rods expressing the appropriate transgene (Mathias et al., 2014; Montgomery et al., 2010), or through the XOPS:mCFP transgenic line (Ann C. Morris et al., 2011). These methods could be applied to adult *sox4* mutants to determine the role Sox4 plays in the regeneration of rod photoreceptors. It would be of interest to compare rod regeneration in zygotic vs. MZ *sox4* mutants. It may be that loss of early Sox4 in retinal development may affect retinal regenerative capabilities later and may exacerbate any potential affect the loss of zygotic Sox4 has on the regeneration of rod photoreceptors.

It is interesting that only the reduction in the rod photoreceptors was only apparent in the *sox4* mutants lacking both maternal and zygotic copies of *sox4*. Eyefield specification begins early in development with the expression of *rx3* in the forebrain at the end of gastrulation (Chow & Lang, 2001; Chuang et al., 1999; Fuhrmann, 2010; Katherine E Brown et al., 2010; Loosli et al., 2003; Rojas-Muñoz et al., 2005; Stigloher et al., 2006); therefore, it is possible that loss of maternal *sox4* alters this population in a way that leads to the reduction of rods several days later in development.

This is the earliest stage in eye development that has been analyzed by scRNA-seq thus far. Our data from scRNA-seq of the eyefield at the 12 hpf suggests that the eyefield is already a heterogenous population of cells primarily divided by the presence or absence of strong expression of canonical eyefield markers like *lhx2b*, *otx2*, *pax6*, *rx3*, and *six3*. These genes are strongly expressed in supercluster 1 and are still present supercluster 2 but they are downregulated and expressed in fewer cells (Fig. 3.14 K). Supercluster 2 is primarily distinguished by the downregulation or absence of the genes highly expressed in supercluster 1 rather than by any upregulated gene signature of its own. A pathway analysis revealed that the top pathways differentially regulated between superclusters 1 and 2 were Notch signaling, FoxO signaling, TGF-beta signaling, and Wnt signaling, all of which were downregulated in supercluster 2 (Table 3.4). These signaling pathways all have established roles in eye

development (Bernardos et al., 2005; Cavodeassi et al., 2005; Eckert et al., 2019; Moose et al., 2003; Saika, 2005). At 12 hpf, the eyefield is preparing to evaginate into the optic vesicles. The differences in these signaling pathways could correlate to cells within the eyefield preparing for this event. They may indicate the onset of structural changes, polarity within the tissue, or both. While we did find evidence for cell type heterogeneity in the eyefield, there is no overt evidence of individual subpopulations being skewed towards a later neuronal fate; rather, the evidence points towards the source of heterogeneity being the strength of eyefield identity.

One gene of interest that was differentially expressed between the two superclusters was *her9,* which was upregulated in supercluster 1. Previous research in our lab has shown a role for Her9 in photoreceptor fate specification and rod and red/green cone photoreceptor survival (Coomer et al., 2020). In the wildtype eyefield, 68.87% of 12 hpf RX3:eGFP positive cells express *her9.* This expression was confirmed by HCR performed on wild type Rx3:eGFP transgenic fish at 12 hpf to detect *her9* RNA expression, which showed that *her9* expression is restricted the lateral and posterior edges outside of the eyefield and posterior region within the eyefield, colocalizing with 69.05% of eyefield (Fig. 3.14 E,J). Given that the labeling of *her9* is restricted to the edges of the eyefield it could be possible that these cells are preparing to evaginate and give rise to the optic vesicle. This could be tested by using the rx3:Kaede transgenic line (Samuel et al., 2016) to label cells on the periphery of the eyefield and track their movement though optic morphogenesis and later fates in retinal differentiation, providing evidence towards whether these specific cells are skewed towards a later neuronal fate.

In the *sox4b* MZ mutants the majority of eyefield cells clustered independently from their wildtype counterparts due to transcriptomic differences. This separate cluster of *sox4b* MZ cells was distinct from the wildtype superclusters 1 and 2 and was therefore labeled as supercluster 3. This suggests that the loss of *sox4b* transcriptomically alters the identity of cells within

the eyefield at 12 hpf. A pathway analysis on the DEGs between the wildtype and *sox4b* MZ cells revealed that the top pathways were for ribosomal proteins in addition to other post-transcriptional modification pathways, Notch signaling, Hh signaling, and Wnt signaling. Notch, Hh, and Wnt signaling have all been shown to have roles in eye development (Bernardos et al., 2005; Cavodeassi et al., 2005; Eckert et al., 2019; Ekker et al., 1995; Macdonald et al., 1995). Therefore, the alteration in expression of these pathways could be contributing to the *sox4b* MZ phenotype of microphthalmia and possibly the later retinal phenotype of reduced rod photoreceptors.

In addition to being differentially expressed across the two superclusters, *her9* was also downregulated in the *sox4b* MZ mutant cells that made up supercluster 3 and the number of cells expressing *her9* was 19.22% (Fig. 3.14 E,J). HCR of *her9* was repeated under the same conditions on *sox4b* MZ mutants and the amount of *her9* expression colocalizing to RX3:eGFP signal was compared to the wildtype. In contrast to the scRNA-Seq data, quantification of Rx3:GFP+ and *her9* positive cells indicated that *sox4b* MZ mutants had a higher percentage of their eyefield expressing her9 compared to wildtype with 97.8% colocalizing with the eyefield. Based on the expression pattern of her9 in the wildtype eyefield, it could be possible that these cells are preparing to evaginate and give rise to the optic vesicle. With the expansion of her9 expression it could indicated that it might alter evagination of the eyefield into the optic vesicles. Live imaging of ocular morphogenesis in the sox4b MZ mutants did not indicate any difference in the timing of events during optic vesicle evagination. Therefore, the change in her9 expression may be acting differently to affect later neurogenic fates. This could also be tested by using the rx3:Kaede transgenic line (Samuel et al., 2016) to label cells on the periphery versus the center of the eyefield and track their movement though optic morphogenesis and later fates in retinal differentiation in the *sox4b* MZ mutants.

The conflicting results between the scRNA-seq dataset and HCR of *her9* expression in the sox4b MZ mutants was surprising given the reproducibility

found in the wildtype dataset at this same timepoint. The scRNA-Seq was obtained from cells that were collected by FACS; therefore, cells must have a threshold level of GFP to be collected by this method. We have observed that expression of the Rx3:eGFP transgene is reduced in the *sox4b* MZ mutants. Therefore, it is possible that a portion of low-expressing Rx3:GFP+ cells that also express *her9* were detected by the more sensitive imaging methods but were not detected by scRNA-Seq due to not meeting the threshold of fluorescence for FACs sorting, thus skewing the ultimate RNA-Seq data.

Despite the discrepancies between scRNA-seq dataset and HCR of *her9* expression, the HCR of *her9* does show a different expression pattern in the *sox4b* MZ mutants compared to the wildtype. Expression of *her9* is expanded along the lateral edges, reduced at the midline posterior to the eyefield, and expanded within the eyefield (Fig. 3.14 H-I). Given that Her9 has a known role in photoreceptor differentiation and survival (Coomer et al., 2020), the expanded *her9* expression in the *sox4b* MZ eyefield may indicate a pathway through which the later retinal phenotypes are explained. *Her9* has been shown to be downregulated of Bmp signaling in inter-pro-neural domains during embryonic development (Bae et al., 2006). Expression data from *sox4* morphants (Wen, 2016; Wen et al., 2015) and scRNA-seq data from *sox4b* MZ mutants, show downregulation of Bmp signaling in response to the loss of Sox4. Therefore, Sox4 may be mediating *her9* expression through Bmp signaling. This could be tested by microinjecting a small dose of *her9* morpholino at the single cell stage to see if reduction of the expansion of her9 expression rescues the phenotypes of microphthalmia and reduction of rod photoreceptors.

A pathway analysis was done on the DRGs and one of the top pathways was for ribosomal proteins. 40 ribosomal proteins were upregulated and 7 were downregulated by at least a 2-fold change in the *sox4b* MZ cells. One in particular that was differentially expressed in the eyefield of *sox4b* MZ mutants compared to wild type was *rpl26,* which encodes 60S Ribosomal Protein L26. *Rpl26* was upregulated in the *sox4b* MZ mutants by 9.37-fold compared to wild

type. This difference will need to be validated in vivo, especially given the discrepancy noted between *her9* expression in the scRNA-seq versus by HCR. Given that *rpl26* is upregulated rather than downregulated like *her9* in the sox4b MZ cells, I would expect this upregulation to potentially be even more expanded in the eyefield in vivo. Ribosomal Protein L26 (Rpl26) contributes to part of the large (60S) subunit of the ribosome. Mutations in Rpl26 are associated with the condition Diamond-Blackfan anemia (DBA). DBA is characterized by the presence of mild-to-severe macrocytic anemia, a normocellular bone marrow, selective erythroid hypoplasia, and occasional neutropenia and/or thrombocytosis. It also presents with growth retardation and congenital anomalies of the head, neck, upper limbs, and urinary system in approximately 30-50% of patients (Gazda et al., 2012). DBA is also associated with ocular complications like cataracts and glaucoma (Tsilou et al., 2010). Other mutations in various ribosomal proteins, *RPL3, RPL7, RPL8, RPL10, RPL14, RPL17, RPL19, RPL23A, RPL26, RPL27,RPL35, RPL36A, RPL39, RPS4X, RPS4Y1,* and *RPS21* been described to cause DBA (Gazda et al., 2012). Out of these ribosomal proteins *rpl7, rpl10, rpl14, rpl23a, rpl26, rpl27, rpl35,* and *rpl36a* were upregulated in the *sox4b* MZ mutant eyefield at 12 hpf. Other mutations in ribosomal proteins are also associated with ocular complications. Mutations in *Rps7* and *Rpl38* in mice are associated with microphthalmia (Kondrashov et al., 2011; Watkins-Chow et al., 2013). Treacher Collins Syndrome is also associated with coloboma and primarily occurs in response to mutations in *TCOF1*, which is involved in ribosome biogenesis(Chang & Steinbacher, 2012). Taken together, these data suggest that the ribosome has an important role in eye development. It is interesting that changes in ribosomal proteins result in deficits in specific tissues rather than causing global complications since translation is an essential process in all cells. This sparks the consideration that there may be heterogeneity among ribosomes that influences their function (Genuth & Barna, 2018). This has interesting implications for an additional layer of complexity in the control of gene expression. The upregulation of *rpl26* along with the differential

expression of 46 other ribosomal proteins strongly implicates that proper ribosomal function, translation could be compromised in the *sox4b* MZ mutants.

Sox4 has predominantly been shown to be a transcriptional activator (Dy et al., 2008; Hoser et al., 2008; Penzo-Méndez, 2010; Van De Wetering et al., 1993; Wiebe et al., 2003) with a single study suggesting a possible role in transcriptional repression *in vitro* (Zhao et al., 2017). This suggests that any direct targets of Sox4 would likely be decreased in expression upon the loss of Sox4. The majority of ribosomal proteins differentially expressed in the *sox4b* MZ mutants are upregulated and therefore unlikely direct targets of Sox4. However, since Sox4 may have a potential ability to repress transcription, the 5' UTR of the upregulated ribosomal protein sequences should be checked for Sox4's binding motif.

The mTOR signaling pathway has been established with the ability to upregulate ribosome biogenesis through the promotion of ribosomal protein s6 kinase (S6K) activity. S6K has been shown to promote ribosome biosynthesis through rRNA synthesis and is predicted to be the rate limiting step of ribosome biogenesis (Jastrzebski et al., 2009; Lempiäinen & Shore, 2009). The mTOR signaling pathway and *rps6kb1a* (a zebrafish *S6K* orthologue) are downregulated in the *sox4b* MZ Cells at 12 hpf. This is surprising given the upregulation of ribosomal protein transcripts in the dataset at this timepoint. The mTOR signaling pathway and S6K may be upregulated in the sox4b MZ cells prior to this point in time, leading to the increase in ribosomal protein transcripts observed. This could be tested by doing an *in situ* for *s6k* at the onset of eyefield specification in wildtype and *sox4b* MZ embryos.

Alteration in translation in *sox4b* MZ mutants may be a pathway through which the loss of maternal *sox4* leads to ocular morphogenesis defects and a reduction of rod photoreceptors. To follow up on this hypothesis, there are some methods currently available to test ribosomal function. The SUnSET assay measures protein synthesis rates by incorporating 3H-puromycin to label newly synthesized proteins *in vivo* (Caron et al., 2021; Goodman & Hornberger, 2013;

Schmidt et al., 2009). Polysome Fractionation observes the presence of the size of polysomes attached to a specific mRNA at one time. It is believed, that the larger amount of polysomes attached to a mRNA correlates to the likelihood it will be translated (Caron et al., 2021; Panda et al., 2017). The Bicistronic Reporter Assay can be used to determine whether ribosome the Internal ribosomal entry site (IRES) is able to recognizes the 5' cap of a specific mRNA transcript and initiates translation *in vitro* (Caron et al., 2021; van den Akker et al., 2021). The caveat to the aforementioned methods, is that they all examine the function of ribosomal activity overall. RIBO-seq can be used in parallel with RNA-seq to determine which mRNA transcripts are actively being transcribed versus translated and provide a sense of translational efficiency and how that varies across different transcripts (Wu et al., 2022). Given the consideration that ribosomes may not be a monolith and instead may be heterogenous according to developmental or tissue context (Genuth & Barna, 2018), mass spec can be used to detect the different subunits of the ribosome and determine if they are actually a heterogenous population (Benjamin et al., 1998; Van De Waterbeemd et al., 2018). Using all of these tools would provide insight into whether ribosomal function is compromised overall in *sox4* MZ mutants, and if that deficit preferentially affects specific transcripts over others.

A recent study in mice showed that loss of *fbl*, a rRNA methyltransferase, specifically reduced translation of specific chromatin remodelers in neural stem cells of the cerebral cortex. H3K27me3 is a repressive marker for gene expression that primarily acts on genes specific to later timepoints in neuronal specification. This suggests that regulation of chromatin remodelers by translation may be a mechanism by which the neurogenic timer is regulated (Wu et al., 2022). Assessing translation efficiency in the *sox4b* MZ mutants could provide clues if a similar mechanism may be driving the retinal neurogenic timer.

Another impact this area of study would have, would be to potentially explain how maternal contributions can lead to effects much later in development. In human neuronal cell culture, it was shown that ribosomal

proteins have long half-lives of 6-11 days (Dörrbaum et al., 2018). It was shown that chondrocytes that experienced an early loss of Sox9 displayed an inhibition of chondrogenic differentiation. These effects were linked to alterations in ribosomal proteins that could be detected as far out as 7 days post knock-down (Caron et al., 2021). This indicates that any alterations to ribosomal subunits can lead to effects that occur many days beyond that initial occurrence.

In summary, in this dissertation I demonstrate a protocol to visualize the process of ocular morphogenesis with high temporal and spatial resolution and provide an initial characterization of the retinal phenotypes found *sox4* zebrafish mutants. My findings support a role for Sox4 in specification of the eyefield and in rod photoreceptor neurogenesis and maturation (Fig. 4.1). Additionally, my scRNA-seq data provides evidence that the eyefield is already a heterogenous population as early as 12 hpf. This information can be expanded upon to determine how the different cell identities in the eyefield impact the process of ocular morphogenesis and possibly later events in neurogenesis of the retina.

Going forward, the *sox4* MZ zebrafish mutants will be a useful tool in determining the precise mechanism by which Sox4 contributes to specification of the eyefield and in rod photoreceptor neurogenesis and maturation. The *sox4* MZ zebrafish mutants also provide us the opportunity to further study how maternal contributions lead to long term developmental effects which may in part be possibly mediated by ribosomal proteins (Fig 4.1B).
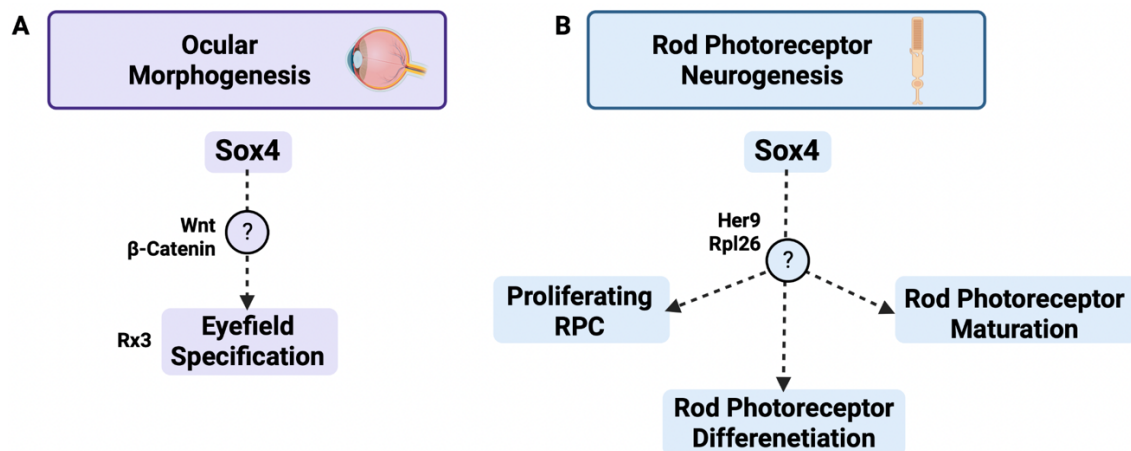
Figure 4.1 Model of the role Sox4 has in ocular morphogenesis and rod photoreceptor neurogenesis.

APPENDIX

APPENDIX 1. A POSSIBLE ROLE FOR SOX4 IN NEURAL CREST DEVELOPMENT

4.1   Abstract

Many tissues are partially derived from neural crest cells. Neural crest cells are a unique, migratory cell type that originates during formation of the neural tube. CHARGE syndrome has phenotypes of choanal atresia, coloboma, cardiovascular malformation, choanal atresia, slowed development, genital hypoplasia, and ear anomalies. These phenotypes have overlap with cell types that are known derivatives of the neural crest. CHARGE syndrome is primarily due to mutations in *CHD7.* However, CHD7 functions upstream of *SOX4* and *SOX11* in the nervous system, suggesting that some CHD7-associated CHARGE syndrome phenotypes may be due to dysregulated expression of SOX4 and SOX11. Zebrafish *sox4* MZ mutants show some similar phenotypes to those associated with CHARGE syndrome; these might be mediated through defects in the neural crest cell population upon loss of Sox4.

4.2   Introduction

Neural crest cells are derived from the neural plate border during embryogenesis. Near the end of gastrulation, the neural plate folds and closes to form a neural tube. The dorsal neural folds give rise to the neural crest cells with the onset of expression of *foxd3, snai1/2, sox8, sox9,* and *sox10.* The specified neural crest cells then undergo an epithelial-to-mesenchymal transition (EMT), delaminate from the neural tube, and migrate to a variety of developing tissues, giving rise to a diverse set of derivatives (Rocha et al., 2020; Simoes-Costa & Bronner, 2015). Chondrocytes, osteocytes, fibroblasts, odontoblasts, cardiac mesenchyme, myoblasts, adipocytes, sensory neurons, cholinergic neurons, adrenergic neurons, satellite cells, Schwann cells, glial cells, chromaffin cells, parafollicular cells, calcitonin-producing cells, and melanocytes are all known

derivatives of neural crest cells (Cordero et al., 2011; Kwak et al., 2013; Phillips et al., 2006; Rocha et al., 2020; Simoes-Costa & Bronner, 2015; Stoller & Epstein, 2005; Thomas & Erickson, 2008) Defects in neural crest cells have the potential to impact many different developmental systems.

CHARGE Syndrome is primarily characterized by the presence of choanal atresia, heart defects, coloboma, characteristic ear malformations and cranial nerve anomalies. The additional phenotypes of genital hypoplasia, cleft lip/palate, tracheoesophageal fistula, distinctive CHARGE facies, and delayed growth and development occur with varying frequencies across patients. CHARGE Syndrome is primarily due to mutations in the chromatin remodeling factor *CHD7* (Blake & Prasad, 2006; George et al., 2020; Lalani et al., 2006; Patten et al., 2012). Many of the systems affected in CHARGE patients require neural crest cells to properly develop; thus, CHARGE syndrome has been characterized as a neurocristopathy. In a zebrafish CHARGE model, *chd7* morphants exhibit defects in pigmentation, peripheral neurons, and craniofacial cartilage, which are all known derivatives of the neural crest. It was shown that there was a dysregulation of *sox10* expression in *chd7* morphants, that suggested a delay in neural crest cell development. Interestingly, knockdown of *sox10* rescued the defects in craniofacial cartilage but not the peripheral neuron and pigmentation defects, indicating that Chd7 influences these independently of *sox10* expression. (Asad et al., 2016). In another study, neural crest cells were differentiated *in vitro* from induced pluripotent stem cells (iPSC) generated from two CHARGE patients. These iPSC neural crest cells showed deficits in migratory abilities (Okuno et al., 2017).

Additional evidence for a connection between Chd7, SoxC factors, and neural crest cells comes from a CHARGE patient who was identified to have a duplication of *SOX11* instead of a mutation of *CHD7* (Sperry et al., 2016). CHD7 is a chromatin remodeler and has been shown to directly target *SOX4* and *SOX11.* This suggests that dysregulation of *SOXC* transcription factors upon loss of CHD7 may contribute to the phenotypes observed in CHARGE syndrome,

including in tissues derived from neural crest cells (Feng et al., 2013). There is also some direct evidence that SoxC transcription factors influence neural crest development. Conditional knockout of *Sox4* and *Sox11* in the neural crest did not affect delamination from the neural tube or migratory behaviors. However, some SoxC-deficient cells underwent cell death upon reaching their destination in the brachial arches (Bhattaram et al., 2010). Moreover, in lamprey and *Xenopus*, *soxC* genes are expressed in the pharyngeal arches, heart, and ganglia similar to in chicken and mouse. Knockdown of *soxC* genes in both lamprey and *Xenopus* led to down-regulation of neural crest specifier genes and defects in neural crest derived ganglia (Uy et al., 2015).

Sox4 has been shown to play a role in ocular morphogenesis, which may include a role for neural-crest derived periocular mesenchymal (POM) cells (Bhattaram et al., 2010; Jiang et al., 2013; Usui, Iwagawa, et al., 2013; Usui, Mochizuki, et al., 2013; Wen, 2016; Wen et al., 2015)*.* In zebrafish, *sox4* expression co-localizes with sox10:GFP positive cells in the POM at 24 hpf (Wen et al., 2015). There is a growing body of evidence suggesting neural crest cells in the periocular mesenchyme (POM) are critical for ocular morphogenesis (Bryan et al., 2018, 2020; Williams & Bohnsack, 2015). To determine whether Sox4 has a function in neural crest cell development, zebrafish *sox4* MZ mutants were characterized for additional phenotypes outside the eye, that would suggest defects in neural crest derived tissues.

4.3 Sox4 MZ Mutants Display Phenotypes Reminiscent of Neural Crest Defects

The *sox4a* MZ, *sox4b* MZ, and *sox4ab* MZ mutants were characterized using stereo microscopy. Zero% of *sox4a* MZ, 14% of *sox4b* MZ, and 19% of *sox4ab* MZ embryos displayed hypopigmentation at 48 hpf (Fig. A.1). Since pigment cells are derived from the neural crest (Thomas & Erickson, 2008), this suggests that Sox4 may have a role in neural crest development.
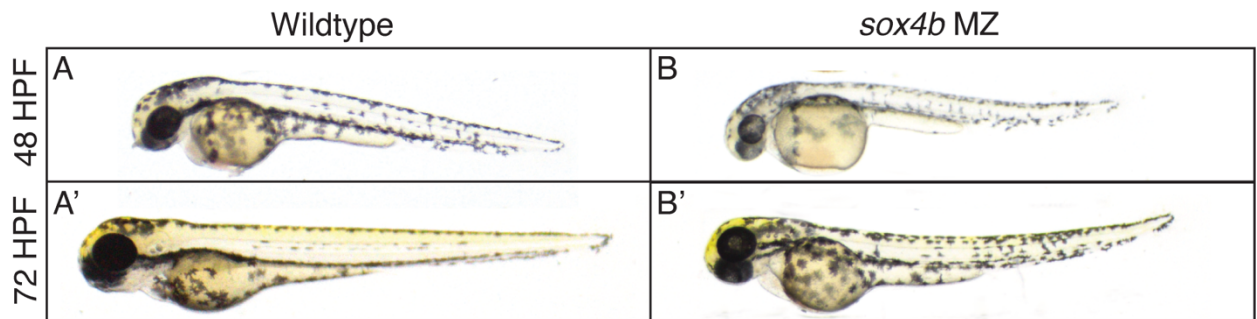
Figure A.1 *sox4b* MZ mutants are hypopigmented at 48 hpf (A-B) and 72 hpf (A'-B'). (A-A') WT (B-B') *sox4b* MZ mutant.

Neural crest cells contribute to the developing cardiovascular system (Stoller & Epstein, 2005). SOX4 is known to play a role in cardiac development as the *Sox4* knockout in mice is embryonic lethal due to heart defects in the form of a common trunk at E14 (Wurm et al., 2008; Ya et al., 1998). A proportion of the *sox4* MZ mutants do show heart abnormalities in the form of a heart edema. 30.2% of *sox4a* MZ, 34.7% of *sox4b* MZ, and 37.8% of *sox4ab* MZ have heart edema (Fig. A.3). Heart edema is a relatively non-specific finding but it is suggestive of heart failure (Narumanchi et al., 2021).
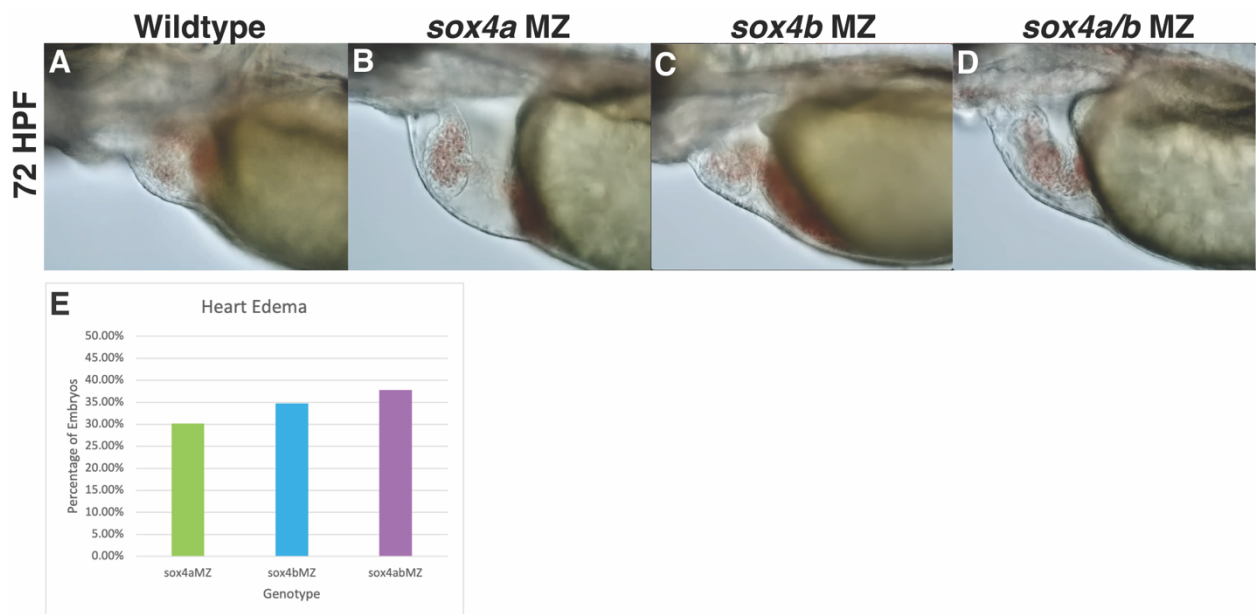
Figure A.2 *sox4* MZ mutants have heart edema at 72 hpf.

(A) WT (B) *sox4a* MZ mutant (C) *sox4b* MZ mutant (D) *sox4ab* MZ mutant (E) Percentage of *sox4* MZ mutants with heart edema.

The zebrafish auditory system consists of an otic placode which resembles the mammalian inner ear (Bever & Fekete, 2002; Haddon & Lewis, 1996). The otic placode is in part, derived from neural crest cells (Kwak et al., 2013; Phillips et al., 2006). Imaging of the otic placode by DIC microscopy showed that 20% of *sox4a* MZ, 28% of *sox4b* MZ, and 35% of *sox4ab* MZ of displayed delayed otic placode development at 48 hpf (Fig. A.3). Delayed otic placode development was determined by the presence of undersized otoliths within the otic placode as notated by the arrows in (Fig. A.3).
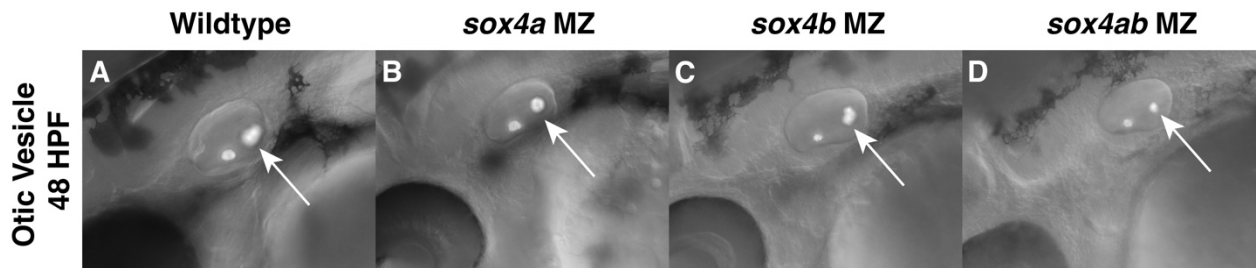
Figure A.3 *sox4* MZ mutants have delayed otic development at 48 hpf.

(A) WT (B) *sox4a* MZ mutant (C) *sox4b* MZ mutant (D) *sox4ab* MZ mutant. (A-D) Arrows point to the posterior otolith.

Chondrocytes in craniofacial cartilage are another derivative of neural crest cells (Cordero et al., 2011). Alcian blue was used to observe the craniofacial cartilage of 6dpf zebrafish larvae. 28% of *sox4a* MZ, 26% of *sox4b* MZ, and 31% of *sox4ab* MZ of displayed craniofacial defects (Fig. A.5). Out of those that displayed craniofacial defects, the ceratohyal:palatoquadrate angle and the ceratohyal angle were both increased in the *sox4* MZ mutants.
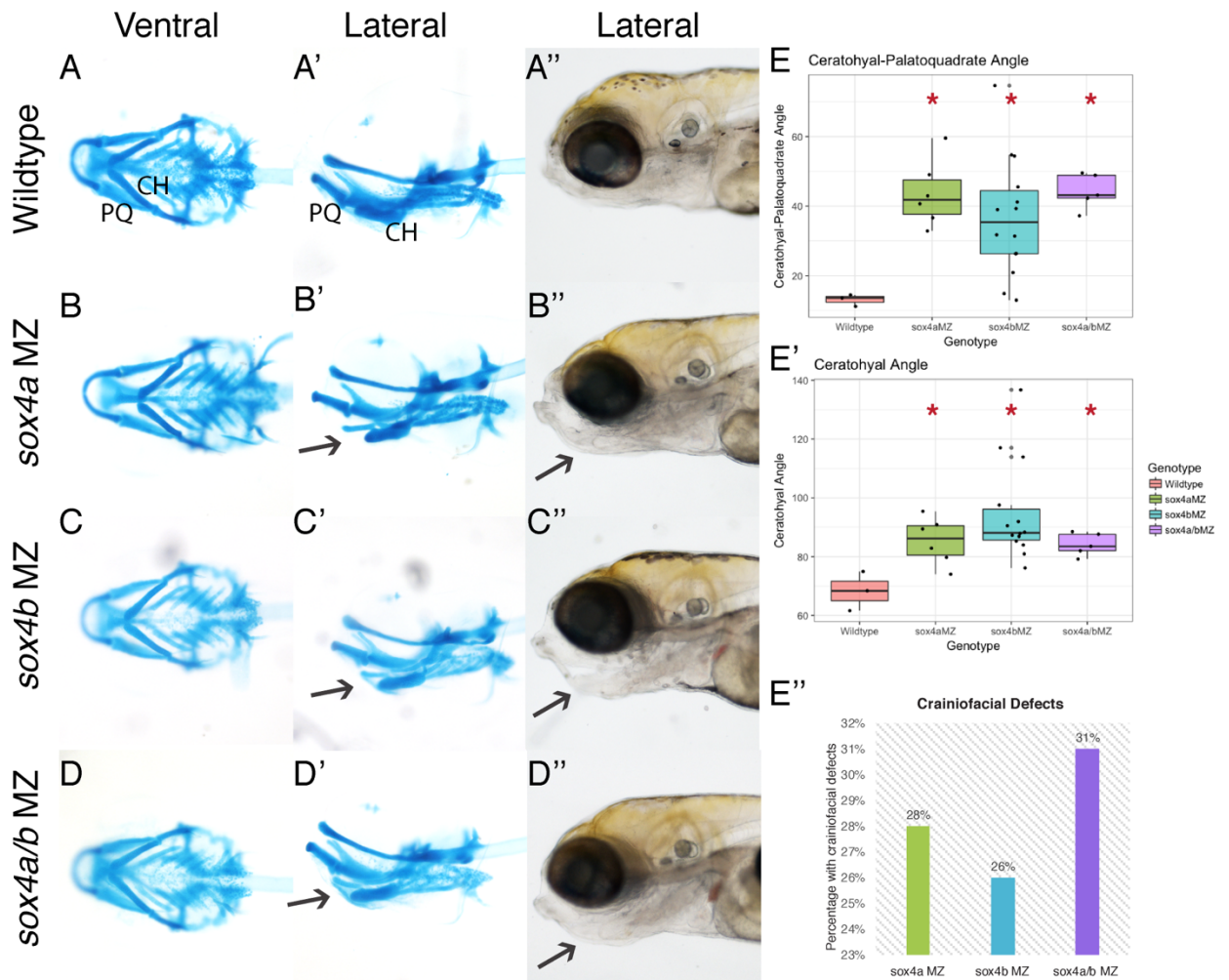
Figure A.4 *sox4* MZ mutants have craniofacial defects at 6 dpf.

(A) WT (B) *sox4a* MZ mutant (C) *sox4b* MZ mutant (D) *sox4ab* MZ mutant (E) Box plot of ceratohyal:palatoquadrate angle (E') Box plot of ceratohyal angle (E") Bar graph of *sox4* MZ mutants with craniofacial defects.

4.4   Discussion

The *sox4* MZ mutant zebrafish display phenotypes of hypopigmentation, heart edema, delay of otic development, and altered craniofacial cartilage that resemble some of the defects associated with CHARGE syndrome. These phenotypes all belong to tissues that require neural crest derived cells (Kwak et al., 2013; Phillips et al., 2006; Stoller & Epstein, 2005; Thomas & Erickson, 2008). Given that Chd7 influences neural crest development (Asad et al., 2016; Okuno et al., 2017) and *sox4* is downstream of Chd7 (Feng et al., 2013), Sox4

may be playing a role in neural crest development. The *sox4* MZ mutant zebrafish may be able to act as a model for understanding how developmental disorders caused by *sox4* mutations affect multiple developmental systems.

Taken together these data strongly indicate the need to further characterize the role of Sox4 in the neural crest cell population. This can be achieved by crossing the *sox4* mutants onto different transgenic lines that label neural crest cells, for example sox10:RFP (Kucenas et al., 2008) or foxd3:GFP (Gilmour et al., 2002) to analyze any potential changes in the neural crest cell population.

4.5   Methods

4.5.1   Animal Husbandry

All experiments involving the use of zebrafish (*Danio rerio*) were carried out in accordance with protocols established by the University of Kentucky Institutional Animal Care and Use Committee (IACUC). Zebrafish were bred, raised, and kept with a 14 h light:10 h dark cycle at 28.5°C.

4.5.2   Genotyping

Adult fish were anesthetized in 0.168 mg/mL of tricane (MS222) in fish water. To extract DNA, part of the tail was removed (Westerfield, 2007), placed in 20ml of 1x ThermolPol Buffer and incubated at 95°C for 15 min. Sample was cooled. 5ml of ProteinaseK was added to the sample and incubated at 55°C overnight. ProteinaseK was inactivated the next morning at 95°C for 15 min. DNA was used in a PCR of *sox4a* and/or *sox4b* and run on an agarose gel to screen for the presence of a large deletion. Primers details can be found in table 3.1.

4.5.3 Microscopy of Live Zebrafish Embryos/Larvae

Zebrafish embryos were anesthetized in 0.168 mg/mL of tricane (MS222) in fish water, placed in 3% Methyl Cellulose. The pigmentation of 48 hpf embryos and

the craniofacial defects of 6 dpf larvae was imaged using a stereo microscope (Digital Sight Ds-Fi2, Nikon instruments). The otic vesicles of 48 hpf embryos were imaged at 40x using DIC on an inverted fluorescent microscope (Eclipse Ti-U, Nikon Instruments).

The hearts of 72 hpf embryos were imaged at 20x on an inverted fluorescent microscope (Eclipse Ti-U, Nikon Instruments).

4.5.4 Alcian Blue

Zebrafish were treated with 1x 1-phenyl 2-thiourea (PTU) in fish water from 1dpf to 6dpf to prevent pigmentation. 6 dpf zebrafish larvae were fixed in 4% PFA overnight and then washed in 1xPBST. The samples were dehydrated in a EtOH:1xPBST gradient series (50%, 70%, 90%) and incubated in Alcian blue solution (Alcian blue cationic dye, Abcam) for 5 hours. The samples were rehydrated in a EtOH:1xPBST gradient series (70%, 50%, 30%) to 1xPBST. The samples were run through a glycerol gradient series (25%, 50%, 75%) and stored in 75%glycerol, 2% KOH. Samples were imaged using a stereo microscope (Digital Sight Ds-Fi2, Nikon instruments). Measurements were taken of the ceratohyal:palatoquadrate angle and the ceratohyal angle.

4.5.5 Statistics

All quantitative measurements were compared across the various genotypes using either a student t-test or a one-way ANOVA followed by a Tukey Test to determine any significant differences. Statistical analyses were run through the open-source software R, using the programs stats. The open-source software R was used to generate boxplots of quantitative measurements using the program ggplot2.

4.6 Acknowledgements

REFERENCES

Aanes, H., Winata, C. L., Lin, C. H., Chen, J. P., Srinivasan, K. G., Lee, S. G. P., Lim, A. Y. M., Hajan, H. S., Collas, P., Bourque, G., Gong, Z., Korzh, V., Aleström, P., & Mathavan, S. (2011). Zebrafish mRNA sequencing deciphers novelties in transcriptome dynamics during maternal to zygotic transition. *Genome Research*, *21*(8), 1328–1338. https://doi.org/10.1101/GR.116012.110

Agathocleous, M., & Harris, W. A. (2009). From Progenitors to Differentiated Cells in the Vertebrate Retina. *Http://Dx.Doi.Org/10.1146/Annurev.Cellbio.042308.113259*, *25*, 45–69. https://doi.org/10.1146/ANNUREV.CELLBIO.042308.113259

Aki, E., Atasavun, S., Turan, A., & Kayihan, H. (2007). Training motor skills of children with low vision. *Perceptual and Motor Skills*, *104*(3 II), 1328–1336. https://doi.org/10.2466/PMS.104.4.1328-1336

Al-Jawahiri, R., Foroutan, A., Kerkhof, J., McConkey, H., Levy, M., Haghshenas, S., Rooney, K., Turner, J., Shears, D., Holder, M., Lefroy, H., Castle, B., Reis, L. M., Semina, E. V., Lachlan, K., Chandler, K., Wright, T., Clayton-Smith, J., Hug, F. P., … Wood, S. M. (2022). SOX11 variants cause a neurodevelopmental disorder with infrequent ocular malformations and hypogonadotropic hypogonadism and with distinct DNA methylation profile. *Genetics in Medicine*. https://doi.org/10.1016/J.GIM.2022.02.013

Angelozzi, M., & Lefebvre, V. (2019). SOXopathies: Growing Family of Developmental Disorders Due to SOX Mutations. *Trends in Genetics*, *35*(9), 658–671. https://doi.org/10.1016/J.TIG.2019.06.003

Angelozzi, Marco, Karvande, A., Molin, A. N., Ritter, A. L., Leonard, J. M. M., Savatt, J. M., Douglass, K., Myers, S. M., Grippa, M., Tolchin, D., Zackai, E., Donoghue, S., Hurst, A. C. E., Descartes, M., Smith, K., Velasco, D., Schmanski, A., Crunk, A., Tokita, M. J., … Lefebvre, V. (2022). Consolidation of the clinical and genetic definition of a SOX4-related neurodevelopmental syndrome. *Journal of Medical Genetics*, *0*, jmedgenet-2021-108375. https://doi.org/10.1136/JMEDGENET-2021-108375

Asad, Z., Pandey, A., Babu, A., Sun, Y., Shevade, K., Kapoor, S., Ullah, I., Ranjan, S., Scaria, V., Bajpai, R., & Sachidanandan, C. (2016). Rescue of neural crest-derived phenotypes in a zebrafish CHARGE model by Sox10 downregulation. *Human Molecular Genetics*, *25*(16), 3539–3554. https://doi.org/10.1093/hmg/ddw198

Avdesh, A., Chen, M., Martin-Iverson, M. T., Mondal, A., Ong, D., Rainey-Smith, S., Taddei, K., Lardelli, M., Groth, D. M., Verdile, G., & Martins, R. N. (2012). Regular care and maintenance of a Zebrafish (Danio rerio) laboratory: An introduction. *Journal of Visualized Experiments*, *69*. https://doi.org/10.3791/4196

Bae, Y.-K., Shimizu, T., & Hibi, M. (2006). Patterning of proneuronal and inter-proneuronal domains by hairy-and enhancer of split-related genes in zebrafish neuroectoderm. *Development*, *133*, 1609. https://doi.org/10.1242/dev.02360

Baylor, D. (1996). How photons start vision. *Proceedings of the National Academy of Sciences of the United States of America*, *93*(2), 560. https://doi.org/10.1073/PNAS.93.2.560

Benjamin, D. R., Robinson, C. V., Hendrick, J. P., Hartl, F. U., & Dobson, C. M. (1998). Mass spectrometry of ribosomes and ribosomal subunits. *Proceedings of the National Academy of Sciences of the United States of America*, *95*(13), 7391–7395. https://doi.org/10.1073/PNAS.95.13.7391/ASSET/559A0CBA-AE4E-4B52-9E4B-8670828C8547/ASSETS/GRAPHIC/PQ1080999003.JPEG

Bergsland, M., Ramsköld, D., Zaouter, C., Klum, S., Sandberg, R., & Muhr, J. (2011). Sequentially acting Sox transcription factors in neural lineage development. *Genes and Development*. https://doi.org/10.1101/gad.176008.111

Bergsland, M., Werme, M., Malewicz, M., Perlmann, T., & Muhr, J. (2006). The establishment of neuronal properties is controlled by Sox4 and Sox11. *Genes and Development*. https://doi.org/10.1101/gad.403406

Bernardos, R. L., Lentz, S. I., Wolfe, M. S., & Raymond, P. A. (2005). Notch–Delta signaling is required for spatial patterning and Müller glia differentiation in the zebrafish retina. *Developmental Biology*, *278*(2), 381–395. https://doi.org/10.1016/J.YDBIO.2004.11.018

Bever, M. M., & Fekete, D. M. (2002). Atlas of the developing inner ear in zebrafish. *Developmental Dynamics*. https://doi.org/10.1002/dvdy.10062

Bhattaram, P., Penzo-Méndez, A., Sock, E., Colmenares, C., Kaneko, K. J., Vassilev, A., DePamphilis, M. L., Wegner, M., & Lefebvre, V. (2010). Organogenesis relies on SoxC transcription factors for the survival of neural and mesenchymal progenitors. *Nature Communications*. https://doi.org/10.1038/ncomms1008

Bill, B. R., Petzold, A. M., Clark, K. J., Schimmenti, L. A., & Ekker, S. C. (2009). A Primer for Morpholino Use in Zebrafish. *Zebrafish*. https://doi.org/10.1089/zeb.2008.0555

Bilotta, J., Saszik, S., & Sutherland, S. E. (2001). Rod contributions to the electroretinogram of the dark-adapted developing zebrafish. *Developmental Dynamics*. https://doi.org/10.1002/dvdy.1188

Blake, K. D., & Prasad, C. (2006). CHARGE syndrome. *Orphanet Journal of Rare Diseases*, *1*(1). https://doi.org/10.1186/1750-1172-1-34

Boulton, M., & Dayhaw-Barker, P. (2001). The role of the retinal pigment

epithelium: Topographical variation and ageing changes. *Eye 2001 15:3*, *15*(3), 384–389. https://doi.org/10.1038/eye.2001.141

Bowles, J., Schepers, G., & Koopman, P. (2000). Phylogeny of the SOX family of developmental transcription factors based on sequence and structural indicators. *Developmental Biology, 227*(2), 239–255. https://doi.org/10.1006/DBIO.2000.9883

Branchek, T., & Bremiller, R. (1984). The Development of Photoreceptors in the Zebrafish, Brachydanio rerio. I. Structure. In *THE JOURNAL OF COMPARATIVE NEUROLOGY*.

Brockerhoff, S. E., Dowling, J. E., & Hurley, J. B. (1998). Zebrafish retinal mutants. In *Vision Research* (Vol. 38).

Bryan, C. D., Casey, M. A., Pfeiffer, R. L., Jones, B. W., & Kwan, K. M. (2020). Optic cup morphogenesis requires neural crest-mediated basement membrane assembly. *Development (Cambridge), 147*(4). https://doi.org/10.1242/dev.181420

Bryan, C. D., Pfeiffer, R. L., Jones, B. W., & Kwan, K. M. (2018). *Neural crest cells regulate optic cup morphogenesis by promoting extracellular matrix assembly*. https://doi.org/10.1101/374470

Buono, L., Corbacho, J., Naranjo, S., Almuedo-Castillo, M., Moreno-Marmol, T., de la Cerda, B., Sanbria-Reinoso, E., Polvillo, R., Díaz-Corrales, F.-J., Bogdanovic, O., Bovolenta, P., & Martínez-Morales, J.-R. (2021). Analysis of gene network bifurcation during optic cup morphogenesis in zebrafish. *Nature Communications, 12*(1), 3866. https://doi.org/10.1038/s41467-021-24169-7

Burmedi, D., Becker, S., Heyl, V., Wahl, H. W., & Himmelsbach, I. (2009). Emotional and social consequences of age-related low vision. *Http://Dx.Doi.Org/10.1076/Vimr.4.1.47.15634, 4*(1), 47–71. https://doi.org/10.1076/VIMR.4.1.47.15634

Caron, M. M. J., Eveque, M., Cillero-Pastor, B., Heeren, R. M. A., Housmans, B., Derks, K., Cremers, A., Peffers, M. J., van Rhijn, L. W., van den Akker, G., & Welting, T. J. M. (2021). Sox9 Determines Translational Capacity During Early Chondrogenic Differentiation of ATDC5 Cells by Regulating Expression of Ribosome Biogenesis Factors and Ribosomal Proteins. *Frontiers in Cell and Developmental Biology, 9*, 1489. https://doi.org/10.3389/FCELL.2021.686096/BIBTEX

Catalanotto, C., Cogoni, C., & Zardo, G. (2016). Molecular Sciences MicroRNA in Control of Gene Expression: An Overview of Nuclear Functions. *Int. J. Mol. Sci., 17*, 1–17. https://doi.org/10.3390/ijms17101712

Cavodeassi, F., Carreira-Barbosa, F., Young, R. M., Concha, M. L., Allende, M. L., Houart, C., Tada, M., & Wilson, S. W. (2005). Early stages of zebrafish eye formation require the coordinated activity of Wnt11, Fz5, and the Wnt/β-

catenin pathway. *Neuron*, *47*(1), 43–56.
https://doi.org/10.1016/j.neuron.2005.05.026

Cavodeassi, F., Ivanovitch, K., & Wilson, S. W. (2013). Eph/Ephrin signalling maintains eye field segregation from adjacent neural plate territories during forebrain morphogenesis. *Development (Cambridge)*, *140*(20), 4193–4202. https://doi.org/10.1242/dev.097048

Cepko, C. L., Austin, C. P., Yang, X., Alexiades, M., & Ezzeddine, D. (1996). *Cell fate determination in the vertebrate retina*. *93*, 589–595. https://www.pnas.org

Chang, C. C., & Steinbacher, D. M. (2012). Treacher Collins Syndrome. *Seminars in Plastic Surgery*, *26*(2), 83. https://doi.org/10.1055/S-0032-1320066

Charpentier, E., & Doudna, J. A. (2013). Biotechnology: Rewriting a genome. *Nature*. https://doi.org/10.1038/495050a

Chen, S., Wang, Q. L., Nie, Z., Sun, H., Lennon, G., Copeland, N. G., Gilbert, D. J., Jenkins, N. A., & Zack, D. J. (1997). Crx, a novel Otx-like paired-homeodomain protein, binds to and transactivates photoreceptor cell-specific genes. *Neuron*. https://doi.org/10.1016/S0896-6273(00)80394-3

Chenn, A., & McConnell, S. K. (1995). Cleavage orientation and the asymmetric inheritance of notchl immunoreactivity in mammalian neurogenesis. *Cell*, *82*(4), 631–641. https://doi.org/10.1016/0092-8674(95)90035-7

Chow, R. L., & Lang, R. A. (2001). Early Eye Development in Vertebrates. *Annual Review of Cell and Developmental Biology*. https://doi.org/10.1146/annurev.cellbio.17.1.255

Choy, S. W., & Cheng, S. H. (2012). Hedgehog Signaling. *Vitamins and Hormones*. https://doi.org/10.1016/B978-0-12-394622-5.00001-8

Chrispell, J. D., Rebrik, T. I., & Weiss, E. R. (2015). Electroretinogram Analysis of the Visual Response in Zebrafish Larvae. *Journal of Visualized Experiments*. https://doi.org/10.3791/52662

Chuang, J. C., Mathers, P. H., & Raymond, P. A. (1999). Expression of three Rx homeobox genes in embryonic and adult zebrafish. *Mechanisms of Development*. https://doi.org/10.1016/S0925-4773(99)00077-5

Cizelsky, W., Hempel, A., Metzig, M., Tao, S., Hollemann, T., Kühl, M., & Kühl, S. J. (2013). Sox4 And sox11 Function during Xenopus laevis Eye Development. *PLoS ONE*. https://doi.org/10.1371/journal.pone.0069372

Clark, B. S., Stein-O'Brien, G. L., Shiau, F., Cannon, G. H., Davis-Marcisak, E., Sherman, T., Santiago, C. P., Hoang, T. V., Rajaii, F., James-Esposito, R. E., Gronostajski, R. M., Fertig, E. J., Goff, L. A., & Blackshaw, S. (2019). Single-Cell RNA-Seq Analysis of Retinal Development Identifies NFI Factors as Regulating Mitotic Exit and Late-Born Cell Specification. *Neuron*, *102*(6),

1111-1126.e5. https://doi.org/10.1016/j.neuron.2019.04.010

Coomer, C. E., Wilson, S. G., Titialii-Torres, K. F., Bills, J. D., Krueger, L. A., Petersen, R. A., Turnbaugh, E. M., Janesch, E. L., & Morris, A. C. (2020). Her9/Hes4 is required for retinal photoreceptor development, maintenance, and survival. *Scientific Reports*, *10*(1). https://doi.org/10.1038/s41598-020-68172-2

Cordero, D. R., Brugmann, S., Chu, Y., Bajpai, R., Jame, M., & Helms, J. A. (2011). Cranial neural crest cells on the move: Their roles in craniofacial development. *American Journal of Medical Genetics, Part A*. https://doi.org/10.1002/ajmg.a.33702

Cowan, C. S., Renner, M., De Gennaro, M., Gross-Scherf, B., Goldblum, D., Hou, Y., Munz, M., Rodrigues, T. M., Krol, J., Szikra, T., Cuttat, R., Waldt, A., Papasaikas, P., Diggelmann, R., Patino-Alvarez, C. P., Galliker, P., Spirig, S. E., Pavlinic, D., Gerber-Hollbach, N., … Roska, B. (2020). Cell Types of the Human Retina and Its Organoids at Single-Cell Resolution. *Cell*, *182*(6), 1623-1640.e34. https://doi.org/10.1016/j.cell.2020.08.013

Crick, F. (1970). Central Dogma of Molecular Biology. *Nature 1970 227:5258*, *227*(5258), 561–563. https://doi.org/10.1038/227561a0

Cvekl, A., & Tamm, E. R. (2004). Anterior eye development and ocular mesenchyme: New insights from mouse models and human diseases. *Bioessays*, *26*(4), 374–386.

Daugherty, K. M., & Moran, M. F. (1982). Neuropsychological, Learning and Developmental Characteristics of the Low Vision Child: *Https://Doi.Org/10.1177/0145482X8207601002*, *76*(10), 398–406. https://doi.org/10.1177/0145482X8207601002

Demb, J. B., & Singer, J. H. (2015). Functional Circuitry of the Retina. *Annual Review of Vision Science*, *1*, 263. https://doi.org/10.1146/ANNUREV-VISION-082114-035334

Dörrbaum, A. R., Kochen, L., Langer, J. D., & Schuman, E. M. (2018). Local and global influences on protein turnover in neurons and glia. *ELife*, *7*. https://doi.org/10.7554/ELIFE.34202

Doudna, J. A., & Charpentier, E. (2014). The new frontier of genome engineering with CRISPR-Cas9. *Science*, *346*(6213). https://doi.org/10.1126/SCIENCE.1258096

Dy, P., Penzo-Méndez, A., Wang, H., Pedraza, C. E., Macklin, W. B., & Lefebvre, V. (2008). The three SoxC proteins - Sox4, Sox11 and Sox12 - Exhibit overlapping expression patterns and molecular properties. *Nucleic Acids Research*. https://doi.org/10.1093/nar/gkn162

Dyer, M. A., Livesey, F. J., Cepko, C. L., & Oliver, G. (2003). Prox1 function controls progenitor cell proliferation and horizontal cell genesis in the

mammalian retina. *Nature Genetics 2003 34:1*, *34*(1), 53–58. https://doi.org/10.1038/ng1144

Easter, Jr., S. S., & Nicola, G. N. (1996). The Development of Vision in the Zebrafish (Danio rerio). *Developmental Biology*. https://doi.org/10.1006/dbio.1996.0335

Easter, S. S., & Gregory Nicola, J. N. (1997). The Development of Eye Movements in the Zebrafish (Danio rerio). *Dev Psychobiol*, *31*, 267–276.

Ebert, A. M., Childs, S. J., Hehr, C. L., Cechmanek, P. B., & McFarlane, S. (2014). Sema6a and Plxna2 mediate spatially regulated repulsion within the developing eye to promote eye vesicle cohesion. *Development (Cambridge)*, *141*(12), 2473–2482. https://doi.org/10.1242/dev.103499

Eckert, P., Knickmeyer, M. D., Schütz, L., Wittbrodt, J., & Heermann, S. (2019). Morphogenesis and axis specification occur in parallel during optic cup and optic fissure formation, differentially modulated by BMP and Wnt. *Open Biology*, *9*(2). https://doi.org/10.1098/rsob.180179

Edlund, T., & Jessell, T. M. (1999). Progression from extrinsic to intrinsic signaling in cell fate specification: A view from the nervous system. *Cell*, *96*(2), 211–224. https://doi.org/10.1016/S0092-8674(00)80561-9

Ekker, S. C., Ungar, A. R., Greenstein, P., von Kessler, D. P., Porter, J. A., Moon, R. T., & Beachy, P. A. (1995). Patterning activities of vertebrate hedgehog proteins in the developing eye and brain. *Current Biology : CB*, *5*(8), 944–955. https://doi.org/10.1016/S0960-9822(95)00185-0

El-Brolosy, M. A., Rossi, A., Kontarakis, Z., Kuenne, C., Günther, S., Fukuda, N., Takacs, C., Lai, S.-L., Fukuda, R., Gerri, C., Kikhi, K., Giraldez, A. J., & Stainier, D. Y. R. (2018). *Genetic compensation is triggered by mutant mRNA degradation*. https://doi.org/10.1101/328153

Emerson, S. E., St Clair, R. M., Waldron, A. L., Bruno, S. R., Duong, A., Driscoll, H. E., Ballif, B. A., McFarlane, S., & Ebert, A. M. (2017). Identification of Target Genes Downstream of Semaphorin6A/PlexinA2 Signaling in Zebrafish. *Developmental Dnamics*, *246*(7), 539–549. https://doi.org/10.1002/dvdy

Engerer, P., Suzuki, S. C., Yoshimatsu, T., Chapouton, P., Obeng, N., Odermatt, B., Williams, P. R., Misgeld, T., & Godinho, L. (2017). Uncoupling of neurogenesis and differentiation during retinal development. *The EMBO Journal*, *36*, 1134–1146. https://doi.org/10.15252/embj

England, S. J., Blanchard, G. B., Mahadevan, L., & Adams, R. J. (2006). A dynamic fate map of the forebrain shows how vertebrate eyes form and explains two causes of cyclopia. *Development*, *133*(23), 4613–4617. https://doi.org/10.1242/DEV.02678

Fadool, J. M. (2003). Development of a rod photoreceptor mosaic revealed in

transgenic zebrafish. *Developmental Biology*, *258*(2), 277–290. https://doi.org/10.1016/S0012-1606(03)00125-8

Fahnehjelm, C., Dafgård Kopp, E., Wincent, J., Güven, E., Nilsson, M., Olsson, M., & Teär Fahnehjelm, K. (2022). Anophthalmia and microphthalmia in children: associated ocular, somatic and genetic morbidities and quality of life. *Https://Doi.Org/10.1080/13816810.2021.1989600*, *43*(2), 172–183. https://doi.org/10.1080/13816810.2021.1989600

Fausett, B. V., & Goldman, D. (2006). A role for alpha1 tubulin-expressing Müller glia in regeneration of the injured zebrafish retina. *The Journal of Neuroscience : The Official Journal of the Society for Neuroscience*, *26*(23), 6303–6313. https://doi.org/10.1523/JNEUROSCI.0332-06.2006

Feng, W., Khan, M. A., Bellvis, P., Zhu, Z., Bernhardt, O., Herold-Mende, C., & Liu, H. K. (2013). The chromatin remodeler CHD7 regulates adult neurogenesis via activation of soxc transcription factors. *Cell Stem Cell*. https://doi.org/10.1016/j.stem.2013.05.002

Flaxman, A. D., Wittenborn, J. S., Robalik, T., Gulia, R., Gerzoff, R. B., Lundeen, E. A., Saaddine, J., & Rein, D. B. (2017). National Health and Nutrition Examination Survey. *JAMA Ophthalmology*, *139*(7), 717–723. https://doi.org/10.1001/jamaophthalmol.2021.0527

Flomerfelt, F. A., & Gress, R. E. (2016). Analysis of Cell Proliferation and Homeostasis Using EdU Labeling. *Methods in Molecular Biology (Clifton, N.J.)*, *1323*, 211. https://doi.org/10.1007/978-1-4939-2809-5_18

Forbes-Osborne, M. A., Wilson, S. G., & Morris, A. C. (2013). Insulinoma-associated 1a (Insm1a) is required for photoreceptor differentiation in the zebrafish retina. *Developmental Biology*, *380*(2), 157–171. https://doi.org/10.1016/J.YDBIO.2013.05.021

Fry, C. J., & Peterson, C. L. (2001). Chromatin remodeling enzymes: who's on first? *Current Biology*, *11*(5), R185–R197. https://doi.org/10.1016/S0960-9822(01)00090-2

Fuhrmann, S. (2010). Eye Morphogenesis and Patterning of the Optic Vesicle. *Current Topics in Developmental Biology, 93*(C), 61. https://doi.org/10.1016/B978-0-12-385044-7.00003-5

Gazda, H. T., Preti, M., Sheen, M. R., O'Donohue, M. F., Vlachos, A., Davies, S. M., Kattamis, A., Doherty, L., Landowski, M., Buros, C., Ghazvinian, R., Sieff, C. A., Newburger, P. E., Niewiadomska, E., Matysiak, M., Glader, B., Atsidaftos, E., Lipton, J. M., Gleizes, P. E., & Beggs, A. H. (2012). Frameshift mutation in p53 regulator RPL26 is associated with multiple physical abnormalities and a specific pre-rRNA processing defect in Diamond-Blackfan anemia. *Human Mutation*, *33*(7), 1037. https://doi.org/10.1002/HUMU.22081

Genuth, N. R., & Barna, M. (2018). The discovery of ribosome heterogeneity and

its implications for gene regulation and organismal life. *Molecular Cell*, *71*(3), 364. https://doi.org/10.1016/J.MOLCEL.2018.07.018

George, A., Cogliati, T., & Brooks, B. P. (2020). Genetics of syndromic ocular coloboma: CHARGE and COACH syndromes. In *Experimental Eye Research* (Vol. 193). Academic Press. https://doi.org/10.1016/j.exer.2020.107940

Ghaffar, A., Rasheed, F., Rashid, M., van Bokhoven, H., Ahmed, Z. M., Riazuddin, S., & Riazuddin, S. (2021). Biallelic in-frame deletion of SOX4 is associated with developmental delay, hypotonia and intellectual disability. *European Journal of Human Genetics 2021 30:2*, *30*(2), 243–247. https://doi.org/10.1038/s41431-021-00968-w

Gilmour, D. T., Maischein, H. M., & Nüsslein-Volhard, C. (2002). Migration and function of a glial subtype in the vertebrate peripheral nervous system. *Neuron*, *34*(4), 577–588. https://doi.org/10.1016/S0896-6273(02)00683-9

Godinho, L., Williams, P. R., Claassen, Y., Provost, E., Leach, S. D., Kamermans, M., & Wong, R. O. L. (2007). Nonapical Symmetric Divisions Underlie Horizontal Cell Layer Formation in the Developing Retina In Vivo. *Neuron*, *56*(4), 597–603. https://doi.org/10.1016/J.NEURON.2007.09.036

Goodman, C. A., & Hornberger, T. A. (2013). Measuring protein synthesis with SUnSET: a valid alternative to traditional techniques? *Exerc Sport Sci Rev.*, *41*(2). https://doi.org/10.1097/JES.0b013e3182798a95

Goslik E. Schepers, Rohan D. Teasdale, & Peter Koopman. (2002). Twenty Pairs of Sox: Extent, Homology, and Nomenclature of the Mouse and Human Sox Transcription Factor Gene Families. *Developmental Cell*, *3*, 167–170. http://www.celera.

Haddon, C., & Lewis, J. (1996). Early ear development in the embryo of the zebrafish, Danio rerio. *Journal of Comparative Neurology*. https://doi.org/10.1002/(SICI)1096-9861(19960129)365:1<113::AID-CNE9>3.0.CO;2-6

Heermann, S., Schütz, L., Lemke, S., Krieglstein, K., & Wittbrodt, J. (2015). Eye morphogenesis driven by epithelial flow into the optic cup facilitated by modulation of bone morphogenetic protein. *ELife*, *2015*(4). https://doi.org/10.7554/eLife.05216

Hehr, C. L., Halabi, R., & McFarlane, S. (2018). Polarity and morphogenesis of the eye epithelium requires the adhesion junction associated adaptor protein Traf4. *Cell Adhesion and Migration*, *12*(5), 489–502. https://doi.org/10.1080/19336918.2018.1477900

Hirsinger, E., & Steventon, B. (2017). A versatile mounting method for long term imaging of zebrafish development. *Journal of Visualized Experiments*, *2017*(119), 55210. https://doi.org/10.3791/55210

Holt, C. E., Bertsch, T. W., Ellis, H. M., & Harris, W. A. (1988). Cellular determination in the xenopus retina is independent of lineage and birth date. *Neuron*. https://doi.org/10.1016/0896-6273(88)90205-X

Hoser, M., Potzner, M. R., Koch, J. M. C., Bösl, M. R., Wegner, M., & Sock, E. (2008). Sox12 Deletion in the Mouse Reveals Nonreciprocal Redundancy with the Related Sox4 and Sox11 Transcription Factors. *Molecular and Cellular Biology*. https://doi.org/10.1128/mcb.00338-08

Hu, Y., Wang, X., Hu, B., Mao, Y., Chen, Y., Yan, L., Yong, J., Dong, J., Wei, Y., Wang, W., Wen, L., Qiao, J., & Tang, F. (2019). Dissecting the transcriptome landscape of the human fetal neural retina and retinal pigment epithelium by single-cell RNA-seq analysis. *PLoS Biology*, *17*(7). https://doi.org/10.1371/journal.pbio.3000365

Huang, J., Arsenault, M., Kann, M., Lopez-Mendez, C., Saleh, M., Wadowska, D., Taglienti, M., Ho, J., Miao, Y., Sims, D., Spears, J., Lopez, A., Wright, G., & Hartwig, S. (2013). The transcription factor sry-related HMG box-4 (SOX4) is required for normal renal development in vivo. *Developmental Dynamics*. https://doi.org/10.1002/dvdy.23971

Huisken, J., Swoger, J., Del Bene, F., Wittbrodt, J., & Stelzer, E. H. K. (2004). Optical sectioning deep inside live embryos by selective plane illumination microscopy. *Science*, *305*(5686), 1007–1009. https://doi.org/10.1126/science.1100035

Icha, J., Schmied, C., Sidhaye, J., Tomancak, P., Preibisch, S., & Norden, C. (2016). Using light sheet fluorescence microscopy to image zebrafish eye development. *Journal of Visualized Experiments*, *2016*(110). https://doi.org/10.3791/53966

Ivanovitch, K., Cavodeassi, F., & Wilson, S. W. (2013). Precocious Acquisition of Neuroepithelial Character in the Eye Field Underlies the Onset of Eye Morphogenesis. *Developmental Cell*, *27*(3), 293–305. https://doi.org/10.1016/j.devcel.2013.09.023

Jacob, A., Wüst, H. M., Thalhammer, J. M., Fröb, F., Küspert, M., Reiprich, S., Balta, E.-A. D., Lie, C., Wegner, M., & Sock, E. (2018). The transcription factor prospero homeobox protein 1 is a direct target of SoxC proteins during developmental vertebrate neurogenesis. *Journal of Neurochemistry*, *146*, 251–268. https://doi.org/10.1111/jnc.14456

James, A., Lee, C., Williams, A. M., Angileri, K., Lathrop, K. L., & Gross, J. M. (2016). The hyaloid vasculature facilitates basement membrane breakdown during choroid fissure closure in the zebrafish eye. *Developmental Biology*. https://doi.org/10.1016/j.ydbio.2016.09.008

Jastrzebski, K., Hannan, K. M., Tchoubrieva, E. B., Hannan, R. D., & Pearson, R. B. (2009). Coordinate regulation of ribosome biogenesis and function by the ribosomal protein S6 kinase, a key mediator of mTOR function.

Http://Dx.Doi.Org/10.1080/08977190701779101, *25*(4), 209–226. https://doi.org/10.1080/08977190701779101

Jemielita, M., Taormina, M. J., Delaurier, A., Kimmel, C. B., & Parthasarathy, R. (2013). Comparing phototoxicity during the development of a zebrafish craniofacial bone using confocal and light sheet fluorescence microscopy techniques. *Journal of Biophotonics*, *6*(11–12), 920–928. https://doi.org/10.1002/jbio.201200144

Jia, L., Oh, E. C. T., Ng, L., Srinivas, M., Brooks, M., Swaroop, A., & Forrest, D. (2009). Retinoid-related orphan nuclear receptor RORβ is an early-acting factor in rod photoreceptor development. *Proceedings of the National Academy of Sciences of the United States of America*, *106*(41), 17534–17539. https://doi.org/10.1073/PNAS.0902425106/SUPPL_FILE/0902425106SI.PDF

Jiang, Y., Ding, Q., Xie, X., Libby, R. T., Lefebvre, V., & Gan, L. (2013). Transcription factors SOX4 and SOX11 function redundantly to regulate the development of mouse retinal ganglion cells. *Journal of Biological Chemistry*. https://doi.org/10.1074/jbc.M113.478503

Kalloniatis, M., & Fletcher, E. L. (2021). Retinitis pigmentosa: understanding the clinical presentation, mechanisms and treatment options. *Https://Doi.Org/10.1111/j.1444-0938.2004.Tb03152.X*, *87*(2), 65–80. https://doi.org/10.1111/J.1444-0938.2004.TB03152.X

Katherine E Brown, Philipp J Keller, Mirana Ramialison, Martina Rembold, Ernst H K Stelzer, Felix Loosli, & Joachim Wittbrodt. (2010). Nlcam modulates midline convergence during anterior neural plate morphogenesis. *Developmental Biology*, *339*(1), 14–25.

Keller, P. J., & Dodt, H. U. (2012). Light sheet microscopy of living or cleared specimens. In *Current Opinion in Neurobiology* (Vol. 22, Issue 1, pp. 138–143). https://doi.org/10.1016/j.conb.2011.08.003

Keller, P. J., Schmidt, A. D., Santella, A., Khairy, K., Bao, Z., Wittbrodt, J., & Stelzer, E. H. K. (2010). Fast, high-contrast imaging of animal development with scanned light sheet-based structured-illumination microscopy. *Nature Methods*, *7*(8), 637–642. https://doi.org/10.1038/nmeth.1476

Keller, P. J., Schmidt, A. D., Wittbrodt, J., & Stelzer, E. H. K. (2008). Reconstruction of zebrafish early embryonic development by scanned light sheet microscopy. *Science*, *322*(5904), 1065–1069. https://doi.org/10.1126/science.1162493

Kim, J. Y., Jeong, H. S., Chung, T., Kim, M., Lee, J. H., Jung, W. H., & Koo, J. S. (2017). The value of phosphohistone H3 as a proliferation marker for evaluating invasive breast cancers: A comparative study with Ki67. *Oncotarget*, *8*(39), 65064. https://doi.org/10.18632/ONCOTARGET.17775

Kimmel, C. B., Ballard, W. W., Kimmel, S. R., Ullmann, B., & Schilling, T. F. (1995). Stages of Embryonic Development of the Zebrafish. *Developmental Dynamics*, *203*(3), 253–310.

Kolovos, P., Knoch, T. A., Grosveld, F. G., Cook, P. R., & Papantonis, A. (2012). Enhancers and silencers: An integrated and simple model for their function. *Epigenetics and Chromatin*, *5*(1), 1–8. https://doi.org/10.1186/1756-8935-5-1/METRICS

Kondrashov, N., Pusic, A., Stumpf, C. R., Shimizu, K., Hsieh, A. C., Xue, S., Ishijima, J., Shiroishi, T., & Barna, M. (2011). Ribosome-mediated specificity in Hox mRNA translation and vertebrate tissue patterning. *Cell*, *145*(3), 383–397. https://doi.org/10.1016/J.CELL.2011.03.028

Kucenas, S., Takada, N., Park, H. C., Woodruff, E., Broadie, K., & Appel, B. (2008). CNS-derived glia ensheath peripheral nerves and mediate motor root development. *Nature Neuroscience 2007 11:2*, *11*(2), 143–151. https://doi.org/10.1038/nn2025

Kuhlbrodt, K., Herbarth, B., Sock, E., Enderich, J., Hermans-Borgmeyer, I., & Wegner, M. (1998). Cooperative function of POU proteins and SOX proteins in glial cells. *The Journal of Biological Chemistry*, *273*(26), 16050–16057. https://doi.org/10.1074/JBC.273.26.16050

Kurosaki, T., Popp, M. W., & Maquat, L. E. (2019). Quality and quantity control of gene expression by nonsense-mediated mRNA decay. *Nature Reviews Molecular Cell Biology 2019 20:7*, *20*(7), 406–420. https://doi.org/10.1038/s41580-019-0126-2

Kuwajima, T., Soares, C. A., Sitko, A. A., Lefebvre, V., & Mason, C. (2017). SoxC Transcription Factors Promote Contralateral Retinal Ganglion Cell Differentiation and Axon Guidance in the Mouse Visual System. *Neuron*. https://doi.org/10.1016/j.neuron.2017.01.029

Kwak, J., Park, O. K., Jung, Y. J., Hwang, B. J., Kwon, S. H., & Kee, Y. (2013). Live image profiling of neural crest lineages in zebrafish transgenic lines. *Molecules and Cells 2013 35:3*, *35*(3), 255–260. https://doi.org/10.1007/S10059-013-0001-5

Kwan, K. M., Otsuna, H., Kidokoro, H., Carney, K. R., Saijoh, Y., & Chien, C. Bin. (2012). A complex choreography of cell movements shapes the vertebrate eye. *Development*, *139*(2), 359–372. https://doi.org/10.1242/dev.071407

Lakshmi Pillai-Kastoori. (2015). *Role of Sox11 During Vertebrate Ocular Morphogenesis and Retinal Neurogenesis*.

Lalani, S. R., Safiullah, A. M., Fernbach, S. D., Harutyunyan, K. G., Thaller, C., Peterson, L. E., McPherson, J. D., Gibbs, R. A., White, L. D., Hefner, M., Davenport, S. L. H., Graham, J. M., Bacino, C. A., Glass, N. L., Towbin, J. A., Craigen, W. J., Neish, S. R., Lin, A. E., & Belmont, J. W. (2006). Spectrum of CHD7 Mutations in 110 Individuals with CHARGE Syndrome

and Genotype-Phenotype Correlation. *The American Journal of Human Genetics*. https://doi.org/10.1086/500273

Latchman, D. S. (1997). Transcription factors: An overview. *The International Journal of Biochemistry & Cell Biology*, *29*(12), 1305–1312. https://doi.org/10.1016/S1357-2725(97)00085-X

Lempiäinen, H., & Shore, D. (2009). Growth control and ribosome biogenesis. *Current Opinion in Cell Biology*, *21*(6), 855–863. https://doi.org/10.1016/J.CEB.2009.09.002

Li, X., Zhang, L., Tang, F., & Wei, X. (2021). Retinal Organoids: Cultivation, Differentiation, and Transplantation. *Frontiers in Cellular Neuroscience*, *15*. https://doi.org/10.3389/FNCEL.2021.638439

Li, Z., Joseph, N. M., & Easter, S. S. (2000). The morphogenesis of the zebrafish eye, including a fate map of the optic vesicle. *Developmental Dynamics*. https://doi.org/10.1002/(SICI)1097-0177(200005)218:1<175::AID-DVDY15>3.0.CO;2-K

Ling, K. H., Hewitt, C. A., Beissbarth, T., Hyde, L., Banerjee, K., Cheah, P. S., Cannon, P. Z., Hahn, C. N., Thomas, P. Q., Smyth, G. K., Tan, S. S., Thomas, T., & Scott, H. S. (2009). Molecular networks involved in mouse cerebral corticogenesis and spatio-temporal regulation of Sox4 and Sox11 novel antisense transcripts revealed by transcriptome profiling. *Genome Biology*, *10*(10). https://doi.org/10.1186/gb-2009-10-10-r104

Livesey, F. J., & Cepko, C. L. (2001). *Vertebrate Neural Cell-Fate Determination: Lessons From The Retina*. www.nature.com/reviews/neuro

Loosli, F., Staub, W., Finger-Baier, K. C., Ober, E. A., Verkade, H., Wittbrodt, J., & Baier, H. (2003). Loss of eyes in zebrafish caused by mutation of chokh/rx 3. *EMBO Reports*, *4*(9), 894–899. https://doi.org/10.1038/sj.embor.embor919

Lu, Y., Shiau, F., Yi, W., Lu, S., Wu, Q., Pearson, J. D., Kallman, A., Zhong, S., Hoang, T., Zuo, Z., Zhao, F., Zhang, M., Tsai, N., Zhuo, Y., He, S., Zhang, J., Stein-O'Brien, G. L., Sherman, T. D., Duan, X., … Clark, B. S. (2020). Single-Cell Analysis of Human Retina Identifies Evolutionarily Conserved and Species-Specific Mechanisms Controlling Development. *Developmental Cell*, *53*(4), 473-491.e9. https://doi.org/10.1016/j.devcel.2020.04.009

Luecken, M. D., & Theis, F. J. (2019). Current best practices in single-cell RNA-seq analysis: a tutorial. *Molecular Systems Biology*, *15*(6). https://doi.org/10.15252/msb.20188746

Lusk, S., & Kwan, K. M. (2022). Pax2a, but not pax2b, influences cell survival and periocular mesenchyme localization to facilitate zebrafish optic fissure closure. *Developmental Dynamics*, *251*(4), 625–644. https://doi.org/10.1002/DVDY.422

Macdonald, R., Barth, K. A., Xu, Q., Holder, N., Mikkola, I., & Wilson, S. W. (1995). Midline signalling is required for Pax gene regulation and patterning of the eyes. *Development (Cambridge, England)*, *121*(10), 3267–3278. https://doi.org/10.1242/DEV.121.10.3267

Masland, R. H. (2012). The Neuronal Organization of the Retina. *Neuron*, *76*(2), 266. https://doi.org/10.1016/J.NEURON.2012.10.002

Mathias, J. R., Zhang, Z., Saxena, M. T., & Mumm, J. S. (2014). Enhanced Cell-Specific Ablation in Zebrafish Using a Triple Mutant of Escherichia Coli Nitroreductase. *Zebrafish*, *11*(2), 85. https://doi.org/10.1089/ZEB.2013.0937

Mavropoulos, A., Devos, N., Biemar, F., Zecchin, E., Argenton, F., Edlund, H., Motte, P., Martial, J. A., & Peers, B. (2005). sox4b is a key player of pancreatic α cell differentiation in zebrafish. *Developmental Biology*. https://doi.org/10.1016/j.ydbio.2005.06.024

Mears, A. J., Kondo, M., Swain, P. K., Takada, Y., Bush, R. A., Saunders, T. L., Sieving, P. A., & Swaroop, A. (2001). Nrl is required for rod photoreceptor development. *Nature Genetics*. https://doi.org/10.1038/ng774

Millar, A. H., Heazlewood, J. L., Giglione, C., Holdsworth, M. J., Bachmair, A., & Schulze, W. X. (2019). The Scope, Functions, and Dynamics of Posttranslational Protein Modifications. *Https://Doi.Org/10.1146/Annurev-Arplant-050718-100211*, *70*, 119–151. https://doi.org/10.1146/ANNUREV-ARPLANT-050718-100211

Montgomery, J. E., Parsons, M. J., & Hyde, D. R. (2010). A Novel Model of Retinal Ablation Demonstrates That the Extent of Rod Cell Death Regulates the Origin of the Regenerated Zebrafish Rod Photoreceptors. *The Journal of Comparative Neurology*, *518*(6), 800. https://doi.org/10.1002/CNE.22243

Moose, H. E., Kelly, L. E., Nekkalapudi, S., & El-Hodiri, H. M. (2003). Ocular forkhead transcription factors: seeing eye to eye. *International Journal of Developmental Biology*, *53*(1), 29–36. https://doi.org/10.1387/IJDB.072505HM

Morris, A. C., & Fadool, J. M. (2005). Studying rod photoreceptor development in zebrafish. In *Physiology and Behavior*. https://doi.org/10.1016/j.physbeh.2005.08.020

Morris, Ann C., Forbes-Osborne, M. A., Pillai, L. S., & Fadool, J. M. (2011). Microarray Analysis of XOPS-mCFP Zebrafish Retina Identifies Genes Associated with Rod Photoreceptor Degeneration and Regeneration. *Investigative Opthalmology & Visual Science*. https://doi.org/10.1167/iovs.10-6022

Mount, N. M., Ward, S. J., Kefalas, P., & Hyllner, J. (2015). Cell-based therapy technology classifications and translational challenges. *Phil. Trans. R. Soc. B*, *370*, 20150017. https://doi.org/10.1098/rstb.2015.0017

Mu, L., Berti, L., Masserdotti, G., Covic, M., Michaelidis, T. M., Doberauer, K., Merz, K., Rehfeld, F., Haslinger, A., Wegner, M., Sock, E., Lefebvre, V., Couillard-Despres, S., Aigner, L., Berninger, B., & Lie, D. C. (2012). SoxC Transcription Factors Are Required for Neuronal Differentiation in Adult Hippocampal Neurogenesis. *Journal of Neuroscience*. https://doi.org/10.1523/JNEUROSCI.4679-11.2012

Muthu, V., Eachus, H., Ellis, P., Brown, S., & Placzek, M. (2016). Rx3 and Shh direct anisotropic growth and specification in the zebrafish tuberal/anterior hypothalamus. *Development (Cambridge)*, *143*(14), 2651–2663. https://doi.org/10.1242/dev.138305

Narumanchi, S., Wang, H., Perttunen, S., Tikkanen, I., Lakkisto, P., & Paavola, J. (2021). Zebrafish Heart Failure Models. *Frontiers in Cell and Developmental Biology*, *9*. https://doi.org/10.3389/FCELL.2021.662583/FULL

Nathans, J., Thomas, D., & Hogness, D. S. (1986). Molecular Genetics of Human Color Vision: The Genes Encoding Blue, Green, and Red Pigments. *Science*, *232*(4747), 196–202. https://doi.org/10.1126/SCIENCE.2937147

Neirijnck, Y., Reginensi, A., Renkema, K. Y., Massa, F., Kozlov, V. M., Dhib, H., Bongers, E. M. H. F., Feitz, W. F., van Eerde, A. M., Lefebvre, V., Knoers, N. V. A. M., Tabatabaei, M., Schulz, H., McNeill, H., Schaefer, F., Wegner, M., Sock, E., & Schedl, A. (2018). Sox11 gene disruption causes congenital anomalies of the kidney and urinary tract (CAKUT). *Kidney International*. https://doi.org/10.1016/j.kint.2017.11.026

Newport, J., & Kirschner, M. (1982). A major developmental transition in early xenopus embryos: I. characterization and timing of cellular changes at the midblastula stage. *Cell*, *30*(3), 675–686. https://doi.org/10.1016/0092-8674(82)90272-0

Newton, F., & Megaw, R. (2020). Mechanisms of Photoreceptor Death in Retinitis Pigmentosa. *Genes*, *11*(1120), 1–29. https://doi.org/10.3390/genes11101120

Ng, L., Hurley, J. B., Dierks, B., Srinivas, M., Saltó, C., Vennström, B., Reh, T. A., & Forrest, D. (2001). A thyroid hormone receptor that is required for the development of green cone photoreceptors. *Nature Genetics*, *27*(1), 94–98. https://doi.org/10.1038/83829

Niell, C. M., & Smith, S. J. (2005). Functional imaging reveals rapid development of visual response properties in the zebrafish tectum. *Neuron*, *45*(6), 941–951. https://doi.org/10.1016/j.neuron.2005.01.047

Okuno, H., Mihara, F. R., Ohta, S., Fukuda, K., Kurosawa, K., Akamatsu, W., Sanosaka, T., Kohyama, J., Hayashi, K., Nakajima, K., Takahashi, T., Wysocka, J., Kosaki, K., & Okano, H. (2017). *CHARGE syndrome modeling using patient-iPSCs reveals defective migration of neural crest cells harboring CHD7 mutations*.

Pampaloni, F., Chang, B. J., & Stelzer, E. H. K. (2015). Light sheet-based fluorescence microscopy (LSFM) for the quantitative imaging of cells and tissues. In *Cell and Tissue Research* (Vol. 360, Issue 1, pp. 129–141). Springer Verlag. https://doi.org/10.1007/s00441-015-2144-5

Panda, A. C., Martindale, J. L., & Gorospe, M. (2017). *Polysome Fractionation to Analyze mRNA Distribution Profiles*. 7. https://doi.org/10.21769/BioProtoc.2126

Pantazis, P., & Supatto, W. (2014). Advances in whole-embryo imaging: A quantitative transition is underway. In *Nature Reviews Molecular Cell Biology* (Vol. 15, Issue 5, pp. 327–339). Nature Publishing Group. https://doi.org/10.1038/nrm3786

Park, O. K., Kwak, J., Jung, Y. J., Kim, Y. H., Hong, H. S., Hwang, B. J., Kwon, S. H., & Kee, Y. (2015). 3D light-sheet fluorescence microscopy of cranial neurons and vasculature during zebrafish embryogenesis. *Molecules and Cells*, *38*(11), 975–981. https://doi.org/10.14348/molcells.2015.0160

Partek® Genomics Suite® (7.0). (2022). Partek Inc. https://www.partek.com/partek-genomics-suite/

Patla, A. E. (1997). Understanding the roles of vision in the control of human locomotion. *Gait & Posture*, *5*, 54–69.

Patten, S. A., Jacobs-McDaniels, N. L., Zaouter, C., Drapeau, P., Albertson, R. C., & Moldovan, F. (2012). Role of Chd7 in zebrafish: A model for CHARGE syndrome. *PLoS ONE*. https://doi.org/10.1371/journal.pone.0031650

Paul, M. (2014). *The role of transcription factors Sox4 and Sox11 in mouse heart development*.

Paul, M. H., Harvey, R. P., Wegner, M., & Sock, E. (2014). Cardiac outflow tract development relies on the complex function of Sox4 and Sox11 in multiple cell types. *Cellular and Molecular Life Sciences*. https://doi.org/10.1007/s00018-013-1523-x

Penzo-Méndez, A. I. (2010). Critical roles for SoxC transcription factors in development and cancer. *The International Journal of Biochemistry & Cell Biology*, *42*(3), 425–428. https://doi.org/10.1016/J.BIOCEL.2009.07.018

Petersen, R. A., & Morris, A. C. (2021). Visualizing Ocular Morphogenesis by Lightsheet Microscopy using rx3:GFP Transgenic Zebrafish. *JoVE (Journal of Visualized Experiments)*, *2021*(170), e62296. https://doi.org/10.3791/62296

Phillips, B. T., Kwon, H. J., Melton, C., Houghtaling, P., Fritz, A., & Riley, B. B. (2006). Zebrafish msxB, msxC and msxE function together to refine the neural-nonneural border and regulate cranial placodes and neural crest development. *Developmental Biology*, *294*(2), 376–390. https://doi.org/10.1016/J.YDBIO.2006.03.001

Picker, A., Cavodeassi, F., Machate, A., Bernauer, S., Hans, S., Abe, G., Kawakami, K., Wilson, S. W., & Brand, M. (2009). Dynamic coupling of pattern formation and morphogenesis in the developing vertebrate retina. *PLoS Biology*, *7*(10), 1000214. https://doi.org/10.1371/journal.pbio.1000214

Pillai-Kastoori, L., Wen, W., & Morris, A. C. (2015). Keeping an eye on SOXC proteins. In *Developmental Dynamics*. https://doi.org/10.1002/dvdy.24235

Pillai-Kastoori, L., Wen, W., Wilson, S. G., Strachan, E., Lo-Castro, A., Fichera, M., Musumeci, S. A., Lehmann, O. J., & Morris, A. C. (2014). Sox11 Is Required to Maintain Proper Levels of Hedgehog Signaling during Vertebrate Ocular Morphogenesis. *PLoS Genetics*. https://doi.org/10.1371/journal.pgen.1004491

Potzner, M. R., Tsarovina, K., Binder, E., Penzo-Mendez, A., Lefebvre, V., Rohrer, H., Wegner, M., & Sock, E. (2010). Sequential requirement of Sox4 and Sox11 during development of the sympathetic nervous system. *Development*. https://doi.org/10.1242/dev.042101

Powell, C., Grant, A. R., Cornblath, E., & Goldman, D. (2013). Analysis of DNA methylation reveals a partial reprogramming of the Müller glia genome during retina regeneration. *Proceedings of the National Academy of Sciences of the United States of America*, *110*(49), 19814–19819. https://doi.org/10.1073/PNAS.1312009110

Rainey, L., Elsman, E. B. M., van Nispen, R. M. A., van Leeuwen, L. M., & van Rens, G. H. M. B. (2016). Comprehending the impact of low vision on the lives of children and adolescents: a qualitative approach. *Quality of Life Research*, *25*(10), 2633–2643. https://doi.org/10.1007/S11136-016-1292-8/FIGURES/2

Ramachandran, R., Fausett, B. V., & Goldman, D. (2010). Ascl1a regulates Müller glia dedifferentiation and retina regeneration via a Lin-28-dependent, let-7 miRNA signaling pathway. *Nature Cell Biology*, *12*(11), 1101. https://doi.org/10.1038/NCB2115

Ramachandran, R., Reifler, A., Parent, J. M., & Goldman, D. (2010). Conditional gene expression and lineage tracing of tuba1a expressing cells during zebrafish development and retina regeneration. *The Journal of Comparative Neurology*, *518*(20), 4196–4212. https://doi.org/10.1002/CNE.22448

Reynaud, E. G., Kržič, U., Greger, K., & Stelzer, E. H. K. (2008). Light sheet-based fluorescence microscopy: More dimensions, more photons, and less photodamage. *HFSP Journal*, *2*(5), 266–275. https://doi.org/10.2976/1.2974980

Reynaud, E. G., Peychl, J., Huisken, J., & Tomancak, P. (2014). Guide to light-sheet microscopy for adventurous biologists. *Nature Methods*, *12*(1), 30–34. https://doi.org/10.1038/nmeth.3222

Riham Mohamed Aly. (2020). Current state of stem cell-based therapies: an

overview. *Stem Cell Investigation*, *7*(8). https://doi.org/10.21037/sci-2020-001

Rocha, M., Singh, N., Ahsan, K., Beiriger, A., & Prince, V. E. (2020). Neural crest development: insights from the zebrafish. *Developmental Dynamics*, *249*(1), 88–111. https://doi.org/10.1002/DVDY.122

Rojas-Muñoz, A., Dahm, R., & Nüsslein-Volhard, C. (2005). chokh/rx3 specifies the retinal pigment epithelium fate independently of eye morphogenesis. *Developmental Biology*, *288*(2), 348–362. https://doi.org/10.1016/j.ydbio.2005.08.046

Rossi, A., Kontarakis, Z., Gerri, C., Nolte, H., Hölper, S., Krüger, M., & Stainier, D. Y. R. (2015). Genetic compensation induced by deleterious mutations but not gene knockdowns. *Nature*. https://doi.org/10.1038/nature14580

Royer, L. A., Lemon, W. C., Chhetri, R. K., Wan, Y., Coleman, M., Myers, E. W., & Keller, P. J. (2016). Adaptive light-sheet microscopy for long-term, high-resolution imaging in living organisms. *Nature Biotechnology*, *34*(12), 1267–1278. https://doi.org/10.1038/nbt.3708

Saika, S. (2005). TGFβ pathobiology in the eye. *Laboratory Investigation 2006 86:2*, *86*(2), 106–115. https://doi.org/10.1038/labinvest.3700375

Saint-Amant, L., & Drapeau, P. (1998). Time course of the development of motor behaviors in the zebrafish embryo. *Journal of Neurobiology*, *37*(4), 622–632. https://doi.org/10.1002/(SICI)1097-4695(199812)37:4<622::AID-NEU10>3.0.CO;2-S

Sampath, K., Rubinstein, A. L., Cheng, A. M. S., Liang, J. O., Fekany, K., Solnica-Krezel, L., Korzh, V., Halpern, M. E., & Wright, C. V. E. (1998). Induction of the zebrafish ventral brain and floorplate requires cyclops/nodal signalling. *Nature 1998 395:6698*, *395*(6698), 185–189. https://doi.org/10.1038/26020

Sampson, T. R., & Weiss, D. S. (2014). Exploiting CRISPR/Cas systems for biotechnology. *BioEssays*. https://doi.org/10.1002/bies.201300135

Samuel, A., Rubinstein, A. M., Azar, T. T., Ben-Moshe Livne, Z., Kim, S. H., & Inbal, A. (2016). Six3 regulates optic nerve development via multiple mechanisms. *Scientific Reports 2016 6:1*, *6*(1), 1–14. https://doi.org/10.1038/srep20267

Santi, P. A. (2011). Light sheet fluorescence microscopy: A review. In *Journal of Histochemistry and Cytochemistry* (Vol. 59, Issue 2, pp. 129–138). SAGE PublicationsSage CA: Los Angeles, CA. https://doi.org/10.1369/0022155410394857

Schier, A. F., & Talbot, W. S. (2003). Nodal signaling and the zebrafish organizer. *International Journal of Developmental Biology*, *45*(1), 289–297. https://doi.org/10.1387/IJDB.11291859

Schilham, M. W., Oosterwegel, M. A., Moerer, P., Ya, J., De Boert, P. A. J., Van De Wetering, M., Verbeek, S., Lamers, W. H., Kruisbeek, A. M., Cumano, A., & Clevers, H. (1996). Defects in cardiac outflow tract formation and pro-B-lymphocyte expansion in mice lacking Sox-4. *Nature 1996 380:6576*, *380*(6576), 711–714. https://doi.org/10.1038/380711a0

Schindelin, J., Arganda-Carreras, I., Frise, E., Kaynig, V., Longair, M., Pietzsch, T., Preibisch, S., Rueden, C., Saalfeld, S., Schmid, B., Tinevez, J.-Y., White, D. J., Hartenstein, V., Eliceiri, K., Tomancak, P., & Cardona, A. (2012). Fiji: an open-source platform for biological-image analysis. *Nature Methods*, *9*(7), 676–682. https://doi.org/10.1038/nmeth.2019

Schmidt, E. K., Clavarino, G., Ceppi, M., & Pierre, P. (2009). SUnSET, a nonradioactive method to monitor protein synthesis. *Nature Methods 2009 6:4*, *6*(4), 275–277. https://doi.org/10.1038/nmeth.1314

Schmitt, E. A., & Dowling, J. E. (1996). Comparison of topographical patterns of ganglion and photoreceptor cell differentiation in the retina of the zebrafish, Danio rerio - PubMed. *The Journal of Comparative Neurology*, *371*, 222–234. https://pubmed.ncbi.nlm.nih.gov/8835728/

Schmitt, E. A., & Dowling, J. E. (1999). Early Retinal Development in the Zebrafish, Danio rerio: Light and Electron Microscopic Analyses. *J. Comp. Neurol*, *404*, 515–536.

Schrier, S. A., Bodurtha, J. N., Burton, B., Chudley, A. E., Chiong, M. A. D., Gabriella D'avanzo, M., Lynch, S. A., Musio, A., Nyazov, D. M., Sanchez-Lara, P. A., Shalev, S. A., & Deardorff, M. A. (2012). The Coffin-Siris syndrome: A Proposed Diagnostic Approach and Assessment of 15 Overlapping Cases. *American Journal of Medical Genetics Part A*, *158*(8), 1865–1876. https://doi.org/10.1002/ajmg.a.35415

Scott, A. W., Bressler, N. M., Ffolkes, S., Ba, M. ;, Wittenborn, J. S., & Jorkasky, J. (2016). Public Attitudes About Eye and Vision Health. *JAMA Ophthalmol*, *134*(10), 1111–1118. https://doi.org/10.1001/jamaophthalmol.2016.2627

Shiau, F., Ruzycki, P. A., & Clark, B. S. (2021). A single-cell guide to retinal development: Cell fate decisions of multipotent retinal progenitors in scRNA-seq. *Developmental Biology*, *478*, 41–58. https://doi.org/10.1016/J.YDBIO.2021.06.005

Shin, C., & Manley, J. L. (2004). Cell signalling and the control of pre-mRNA splicing. *Nature Reviews Molecular Cell Biology 2004 5:9*, *5*(9), 727–738. https://doi.org/10.1038/nrm1467

Sidhaye, J., & Norden, C. (2017). Concerted action of neuroepithelial basal shrinkage and active epithelial migration ensures efficient optic cup morphogenesis. *ELife*. https://doi.org/10.7554/eLife.22689

Simoes-Costa, M., & Bronner, M. E. (2015). Establishing neural crest identity: a gene regulatory recipe. *Development*. https://doi.org/10.1242/dev.105445

Sock, E., Rettig, S. D., Enderich, J., Bösl, M. R., Tamm, E. R., & Wegner, M. (2004). Gene Targeting Reveals a Widespread Role for the High-Mobility-Group Transcription Factor Sox11 in Tissue Remodeling. *Molecular and Cellular Biology*, *24*(15), 6635–6644. https://doi.org/10.1128/MCB.24.15.6635-6644.2004/ASSET/C4B0D2C4-F2FE-499C-B9EB-9D3E4DEB8CBD/ASSETS/GRAPHIC/ZMB0150442500009.JPEG

Sowden, J. C. (2007). Molecular and developmental mechanisms of anterior segment dysgenesis. *Eye*, *21*, 1310–1318. https://doi.org/10.1038/sj.eye.6702852

Sperry, E. D., Schuette, J. L., van Ravenswaaij-Arts, C. M. A., Green, G. E., & Martin, D. M. (2016). Duplication 2p25 in a child with clinical features of CHARGE syndrome. *American Journal of Medical Genetics Part A*, *170*(5), 1148–1154. https://doi.org/10.1002/AJMG.A.37592

Sridhar, A., Hoshino, A., Finkbeiner, C. R., Chitsazan, A., Dai, L., Haugan, A. K., Eschenbacher, K. M., Jackson, D. L., Trapnell, C., Bermingham-McDonogh, O., Glass, I., & Reh, T. A. (2020). Single-Cell Transcriptomic Comparison of Human Fetal Retina, hPSC-Derived Retinal Organoids, and Long-Term Retinal Cultures. *Cell Reports*, *30*(5), 1644-1659.e4. https://doi.org/10.1016/j.celrep.2020.01.007

Stenkamp, D. L. (2007). Neurogenesis in the Fish Retina. In *International Review of Cytology*. https://doi.org/10.1016/S0074-7696(06)59005-9

Stevanovic, M., Drakulic, D., Lazic, A., Ninkovic, D. S., Schwirtlich, M., & Mojsin, M. (2021). SOX Transcription Factors as Important Regulators of Neuronal and Glial Differentiation During Nervous System Development and Adult Neurogenesis. *Frontiers in Molecular Neuroscience*, *14*, 51. https://doi.org/10.3389/FNMOL.2021.654031/BIBTEX

Stigloher, C., Ninkovic, J., Laplante, M., Geling, A., Tannhäuser, B., Topp, S., Kikuta, H., Becker, T. S., Houart, C., & Bally-Cuif, L. (2006). Segregation of telencephalic and eye-field identities inside the zebrafish forebrain territory is controlled by Rx3. *Development*, *133*(15), 2925–2935. https://doi.org/10.1242/dev.02450

Stoller, J. Z., & Epstein, J. A. (2005). Cardiac neural crest. *Seminars in Cell & Developmental Biology*, *16*(6), 704–715. https://doi.org/10.1016/J.SEMCDB.2005.06.004

Swaroop, A., Kim, D., & Forrest, D. (2010). Transcriptional regulation of photoreceptor development and homeostasis in the mammalian retina. *Nature Reviews Neuroscience 2010 11:8*, *11*(8), 563–576. https://doi.org/10.1038/nrn2880

Tanaka, S., Kamachi, Y., Tanouchi, A., Hamada, H., Jing, N., & Kondoh, H. (2004). Interplay of SOX and POU Factors in Regulation of the Nestin Gene

in Neural Primordial Cells . *Molecular and Cellular Biology*, *24*(20), 8834–8846. https://doi.org/10.1128/MCB.24.20.8834-8846.2004/ASSET/2E154360-2905-4CC1-84C0-868DB352D7A2/ASSETS/GRAPHIC/ZMB0200444580009.JPEG

Thein, D. C., Thalhammer, J. M., Hartwig, A. C., Bryan Crenshaw, E., Lefebvre, V., Wegner, M., & Sock, E. (2010). The closely related transcription factors Sox4 and Sox11 function as survival factors during spinal cord development. *Journal of Neurochemistry*. https://doi.org/10.1111/j.1471-4159.2010.06910.x

Thill, S., Spence, C., Tas, C., & Hutmacher, F. (2019). Why Is There So Much More Research on Vision Than on Any Other Sensory Modality? *Front. Psychol*, *10*, 2246. https://doi.org/10.3389/fpsyg.2019.02246

Thomas, A. J., & Erickson, C. A. (2008). The making of a melanocyte: The specification of melanoblasts from the neural crest. In *Pigment Cell and Melanoma Research*. https://doi.org/10.1111/j.1755-148X.2008.00506.x

Thorleifsson, G., Magnusson, K. P., Sulem, P., Walters, G. B., Gudbjartsson, D. F., Stefansson, H., Jonsson, T., Jonasdottir, A., Jonasdottir, A., Stefansdottir, G., Masson, G., Hardarson, G. A., Petursson, H., Arnarsson, A., Motallebipour, M., Wallerman, O., Wadelius, C., Gulcher, J. R., Thorsteinsdottir, U., … Stefansson, K. (2007). Common sequence variants in the LOXL1 gene confer susceptibility to exfoliation glaucoma. *Science*, *317*(5843), 1397–1400. https://doi.org/10.1126/SCIENCE.1146554/SUPPL_FILE/THORLEIFSSON.SOM.PDF

Tomita, K., Moriyoshi, K., Nakanishi, S., Guillemot, F., & Kageyama, R. (2000). Mammalian achaete-scute and atonal homologs regulate neuronal versus glial fate determination in the central nervous system. *EMBO Journal*, *19*(20), 5460–5472. https://doi.org/10.1093/EMBOJ/19.20.5460

Trapnell, C. (2015). Defining cell types and states with single-cell genomics. In *Genome Research* (Vol. 25, Issue 10, pp. 1491–1498). Cold Spring Harbor Laboratory Press. https://doi.org/10.1101/gr.190595.115

Tsilou, E. T., Giri, N., Weinstein, S., Mueller, C., Savage, S. A., & Alter, B. P. (2010). OCULAR AND ORBITAL MANIFESTATIONS OF THE INHERITED BONE MARROW FAILURE SYNDROMES: FANCONI ANEMIA AND DYSKERATOSIS CONGENITA. *Ophthalmology*, *117*(3), 615. https://doi.org/10.1016/J.OPHTHA.2009.08.023

Tsurusaki, Y., Koshimizu, E., Ohashi, H., Phadke, S., Kou, I., Shiina, M., Suzuki, T., Okamoto, N., Imamura, S., Yamashita, M., Watanabe, S., Yoshiura, K. I., Kodera, H., Miyatake, S., Nakashima, M., Saitsu, H., Ogata, K., Ikegawa, S., Miyake, N., & Matsumoto, N. (2014). De novo SOX11 mutations cause Coffin-Siris syndrome. *Nature Communications*, *5*. https://doi.org/10.1038/ncomms5011

Turner, D. L., & Cepko, C. L. (1987). A common progenitor for neurons and glia persists in rat retina late in development. *Nature*. https://doi.org/10.1038/328131a0

Turner, D. L., Snyder, E. Y., & Cepko, C. L. (1990). Lineage-independent determination of cell type in the embryonic mouse retina. *Neuron*, *4*(6), 833–845. https://doi.org/10.1016/0896-6273(90)90136-4

Usui, A., Iwagawa, T., Mochizuki, Y., Iida, A., Wegner, M., Murakami, A., & Watanabe, S. (2013). Expression of Sox4 and Sox11 is regulated by multiple mechanisms during retinal development. *FEBS Letters*. https://doi.org/10.1016/j.febslet.2012.12.017

Usui, A., Mochizuki, Y., Iida, A., Miyauchi, E., Satoh, S., Sock, E., Nakauchi, H., Aburatani, H., Murakami, A., Wegner, M., & Watanabe, S. (2013). The early retinal progenitor-expressed gene Sox11 regulates the timing of the differentiation of retinal cells. *Development (Cambridge)*, *140*(4), 740–750. https://doi.org/10.1242/DEV.090274

Uy, B. R., Simoes-Costa, M., Koo, D. E. S., Sauka-Spengler, T., & Bronner, M. E. (2015). Evolutionarily conserved role for SoxC genes in neural crest specification and neuronal differentiation. *Developmental Biology*, *397*(2), 282–292. https://doi.org/10.1016/J.YDBIO.2014.09.022

Van De Waterbeemd, M., Tamara, S., Fort, K. L., Damoc, E., Franc, V., Bieri, P., Itten, M., Makarov, A., Ban, N., & Heck, A. J. R. (2018). Dissecting ribosomal particles throughout the kingdoms of life using advanced hybrid mass spectrometry methods. *Nature Communications 2018 9:1*, *9*(1), 1–12. https://doi.org/10.1038/s41467-018-04853-x

Van De Wetering, M., Oosterwegel, M., Van Norren, K., & Clevers1, H. (1993). Sox-4, an Sry-like HMG box protein, is a transcriptional activator in lymphocytes. In *The EMBO Journal vol* (Vol. 12, Issue 10).

van den Akker, G. G. H., Zacchini, F., Housmans, B. A. C., van der Vloet, L., Caron, M. M. J., Montanaro, L., & Welting, T. J. M. (2021). Current practice in bicistronic ires reporter use: A systematic review. *International Journal of Molecular Sciences*, *22*(10), 5193. https://doi.org/10.3390/IJMS22105193/S1

Varga, Z. M., Wegner, J., & Westerfield, M. (1999). Anterior movement of ventral diencephalic precursors separates the primordial eye field in the neural plate and requires cyclops. *Development*, *126*(24), 5533–5546. https://doi.org/10.1242/DEV.126.24.5533

Vihtelic, T. S., & Hyde, D. R. (2000). Light-induced rod and cone cell death and regeneration in the adult albino zebrafish (Danio rerio) retina. *Journal of Neurobiology*. https://doi.org/10.1002/1097-4695(20000905)44:3<289::AID-NEU1>3.0.CO;2-H

Von Wittgenstein, J., Zheng, F., Wittmann, M. T., Balta, E. A., Ferrazzi, F., Schäffner, I., Häberle, B. M., Valero-Aracama, M. J., Koehl, M., Miranda, C.

J., Kaspar, B. K., Ekici, A. B., Reis, A., Abrous, D. N., Alzheimer, C., & Lie, D. C. (2020). Sox11 is an Activity-Regulated Gene with Dentate-Gyrus-Specific Expression Upon General Neural Activation. *Cerebral Cortex (New York, N.Y. : 1991)*, *30*(6), 3731–3743. https://doi.org/10.1093/CERCOR/BHZ338

Wan, J., & Goldman, D. (2016). Retina regeneration in zebrafish. *Current Opinion in Genetics & Development*, *40*, 41. https://doi.org/10.1016/J.GDE.2016.05.009

Wang, P., Wei, L., Rafei, M., Shammaa, R., El, A., & El-Kadiry, H. (2021). Cell Therapy: Types, Regulation, and Clinical Benefits. *Frontiers in Medicine | Www.Frontiersin.Org*, *8*, 756029. https://doi.org/10.3389/fmed.2021.756029

Watkins-Chow, D. E., Cooke, J., Pidsley, R., Edwards, A., Slotkin, R., Leeds, K. E., Mullen, R., Baxter, L. L., Campbell, T. G., Salzer, M. C., Biondini, L., Gibney, G., Phan Dinh Tuy, F., Chelly, J., Morris, H. D., Riegler, J., Lythgoe, M. F., Arkell, R. M., Loreni, F., … Keays, D. A. (2013). Mutation of the Diamond-Blackfan Anemia Gene Rps7 in Mouse Results in Morphological and Neuroanatomical Phenotypes. *PLOS Genetics*, *9*(1), e1003094. https://doi.org/10.1371/JOURNAL.PGEN.1003094

Wen, W. (2016). *The Role of Sox4 in Regulating Choroid Fissure Closure and Retinal Neurogenesis*. https://doi.org/10.13023/ETD.2016.180

Wen, W., Pillai-Kastoori, L., Wilson, S. G., & Morris, A. C. (2015). Sox4 regulates choroid fissure closure by limiting Hedgehog signaling during ocular morphogenesis. *Developmental Biology*. https://doi.org/10.1016/j.ydbio.2014.12.026

Westerfield, M. (2007). The Zebrafish Book. A Guide for the Laboratory Use of Zebrafish (Danio rerio), 5th Edition. *University of Oregon Press, Eugene (Book)*.

Wetts, R., & Fraser, S. E. (1988). Multipotent Precursors Can Give Rise to All Major Cell Types of the Frog Retina. *Science*, *239*, 1142–1145.

Weysse, A. W., & Burgess, W. S. (1906). Histogenesis of the Retina. *The American Naturalist*, *XL*(477), 611–637. https://www.journals.uchicago.edu/doi/pdf/10.1086/278664

Wiebe, M. S., Nowling, T. K., & Rizzino, A. (2003). Identification of Novel Domains within Sox-2 and Sox-11 Involved in Autoinhibition of DNA Binding and Partnership Specificity. *Journal of Biological Chemistry*, *278*(20), 17901–17911. https://doi.org/10.1074/JBC.M212211200

Williams, A. L., & Bohnsack, B. L. (2015). Neural crest derivatives in ocular development: Discerning the eye of the storm. In *Birth Defects Research Part C - Embryo Today: Reviews*. https://doi.org/10.1002/bdrc.21095

Wilson, M. E., Yang, K. Y., Kalousova, A., Lau, J., Kosaka, Y., Lynn, F. C.,

Wang, J., Mrejen, C., Episkopou, V., Clevers, H. C., & German, M. S. (2005). The HMG box transcription factor Sox4 contributes to the development of the endocrine pancreas. *Diabetes*. https://doi.org/10.2337/diabetes.54.12.3402

Wilson, S. W., & Houart, C. (2004). Early Steps in the Development of the Forebrain. *Developmental Cell*, *6*(2), 167–181. https://doi.org/10.1016/S1534-5807(04)00027-9

Wu, Q., Shichino, Y., Abe, T., Suetsugu, T., Omori, A., Kiyonari, H., Iwasaki, S., & Matsuzaki, F. (2022). Selective translation of epigenetic modifiers affects the temporal pattern and differentiation of neural stem cells. *Nature Communications 2022 13:1*, *13*(1), 1–18. https://doi.org/10.1038/s41467-022-28097-y

Wurm, A., Sock, E., Fuchshofer, R., Wegner, M., & Tamm, E. R. (2008). Anterior segment dysgenesis in the eyes of mice deficient for the high-mobility-group transcription factor Sox11. *Experimental Eye Research*. https://doi.org/10.1016/j.exer.2008.03.004

Xie, S., Han, S., Qu, Z., Liu, F., Li, J., Yu, S., Reilly, J., Tu, J., Liu, X., Lu, Z., Hu, X., Yimer, T. A., Qin, Y., Huang, Y., Lv, Y., Jiang, T., Shu, X., Tang, Z., Jia, H., … Liu, M. (2019). Knockout of Nr2e3 prevents rod photoreceptor differentiation and leads to selective L-/M-cone photoreceptor degeneration in zebrafish. *Biochimica et Biophysica Acta. Molecular Basis of Disease*, *1865*(6), 1273–1283. https://doi.org/10.1016/J.BBADIS.2019.01.022

Xu, B., Tang, X., Jin, M., Zhang, H., Du, L., Yu, S., & He, J. (2020). Unifying developmental programs for embryonic and postembryonic neurogenesis in the zebrafish retina. *Development (Cambridge)*, *147*(12). https://doi.org/10.1242/DEV.185660/266906/AM/UNIFYING-DEVELOPMENTAL-PROGRAMS-FOR-EMBRYONIC-AND

Xu, E. E., Krentz, N. A. J., Tan, S., Chow, S. Z., Tang, M., Nian, C., & Lynn, F. C. (2015). SOX4 cooperates with neurogenin 3 to regulate endocrine pancreas formation in mouse models. *Diabetologia*, *58*, 1013–1023. https://doi.org/10.1007/s00125-015-3507-x

Ya, J., Schilham, M. W., De Boer, P. A. J., Moorman, A. F. M., Clevers, H., & Lamers, W. H. (1998). Sox4-Deficiency Syndrome in Mice Is an Animal Model for Common Trunk. *Circulation Research*, *83*(10), 986–994. https://doi.org/10.1161/01.RES.83.10.986

Yamada, R., Oguri, A., Fujiki, K., Shirahige, K., Takezoe, H., Takahashi, N., & Kanai, Y. (2021). Single-cell transcriptional analysis reveals developmental stage-dependent changes in retinal progenitors in the murine early optic vesicle. *Biochemical and Biophysical Research Communications*, *543*, 80–86. https://doi.org/10.1016/j.bbrc.2021.01.043

Yang, S., Zhou, J., & Li, D. (2021). Functions and Diseases of the Retinal

Pigment Epithelium. *Frontiers in Pharmacology*, *12*. https://doi.org/10.3389/fphar.2021.727870

Yasuda, G. K., & Schubiger, G. (1992). Temporal regulation in the early embryo: is MBT too good to be true? *Trends in Genetics*, *8*(4), 124–127. https://doi.org/10.1016/0168-9525(92)90369-F

Yoon, K. H., Fox, S. C., Dicipulo, R., Lehmann, O. J., & Waskiewicz, A. J. (2020). Ocular coloboma: Genetic variants reveal a dynamic model of eye development. *American Journal of Medical Genetics Part C: Seminars in Medical Genetics*, *184*(3), 590–610. https://doi.org/10.1002/ajmg.c.31831

Zaghloul, N. A., & Moody, S. A. (2007). Alterations of rx1 and pax6 expression levels at neural plate stages differentially affect the production of retinal cell types and maintenance of retinal stem cell qualities. *Developmental Biology*, *306*(1), 222–240. https://doi.org/10.1016/J.YDBIO.2007.03.017

Zawerton, A., Yao, B., Yeager, J. P., Pippucci, T., Haseeb, A., Smith, J. D., Wischmann, L., Kühl, S. J., Dean, J. C. S., Pilz, D. T., Holder, S. E., McNeill, A., Graziano, C., & Lefebvre, V. (2019). De Novo SOX4 Variants Cause a Neurodevelopmental Disease Associated with Mild Dysmorphism. *American Journal of Human Genetics*, *104*(2), 246–259. https://doi.org/10.1016/J.AJHG.2018.12.014

Zhao, L., Arsenault, M., Ng, E. T., Longmuss, E., Chau, T. C. Y., Hartwig, S., & Koopman, P. (2017). SOX4 regulates gonad morphogenesis and promotes male germ cell differentiation in mice. *Developmental Biology*. https://doi.org/10.1016/j.ydbio.2017.01.013

Zhou, X., Liao, W. J., Liao, J. M., Liao, P., & Lu, H. (2015). Ribosomal proteins: functions beyond the ribosome. *Journal of Molecular Cell Biology*, *7*(2), 92–104. https://doi.org/10.1093/JMCB/MJV014

Zou, S.-Q., Yin, W., Zhang, M.-J., Hu, C.-R., Huang, Y.-B., & Hu, B. (2010). Using the optokinetic response to study visual function of zebrafish. *Journal of Visualized Experiments*. https://doi.org/10.3791/1742

Vita

Education

B.S. Biology – Bellarmine University – 2015

Professional Publications

Petersen, R. A., & Morris, A. C. (2021). Visualizing Ocular Morphogenesis by Lightsheet Microscopy using rx3:GFP Transgenic Zebrafish. *JoVE (Journal of Visualized Experiments)*, *2021*(170), e62296. https://doi.org/10.3791/62296

Hentig J, Cloghessy K, Lahne M, Jung YJ, Petersen RA, Morris AC, Hyde DR. Zebrafish Blunt-Force TBI Induces Heterogenous Injury Pathologies That Mimic Human TBI and Responds with Sonic Hedgehog-Dependent Cell Proliferation across the Neuroaxis. Biomedicines. 2021 Jul 22;9(8):861. doi: 10.3390/biomedicines9080861. PMID: 34440066; PMCID: PMC8389629.

Coomer, C. E., Wilson, S. G., Titialii-Torres, K. F., Bills, J. D., Krueger, L. A., Petersen, R. A., Turnbaugh, E. M., Janesch, E. L., & Morris, A. C. (2020). Her9/Hes4 is required for retinal photoreceptor development, maintenance, and survival. *Scientific Reports*, *10*(1). https://doi.org/10.1038/s41598-020-68172-2